

GROWTH AND SURVIVAL DURING DROUGHT: THE LINK BETWEEN HYDRAULIC
ARCHITECTURE AND DROUGHT TOLERANCE IN GRASSES

by

TROY W. OCHELTREE

B.S., University of Minnesota-Morris, 1997
M.S., University of Idaho, 2002

AN ABSTRACT OF A DISSERTATION

submitted in partial fulfillment of the requirements for the degree

DOCTOR OF PHILOSOPHY

Department of Agronomy
College of Agriculture

KANSAS STATE UNIVERSITY
Manhattan, Kansas

2012

Abstract

The pathway for the movement of water through plants, from the soil matrix to the atmosphere, constitutes the hydraulic architecture of a plant. The linkage between the hydraulic architecture of woody plants and drought tolerance has received considerable attention, but much less work has been done on grasses. I investigated the linkage between the hydraulic architecture of grasses to physiological patterns of water use across a range of species and conditions. The rate of stomatal conductance (g_s) and photosynthesis (A) increased acropetally along the leaves of 5 grass species, which is a unique feature of this growth form. The internal structure of leaves also changed acropetally in order to minimize the pressure gradient across the mesophyll that would otherwise occur as a result of increasing g_s . The resistance to water movement through the mesophyll represented 80-90% of leaf resistance in six genotypes of *Sorghum bicolor* L. (Moench). This resistance was most important in controlling g_s and A when water was readily available, but as soil-moisture decreased it was the efficient transport of water through the xylem that was most important in maintaining plant function. I also investigated the relationship between hydraulic architecture and stomatal responses of grasses to increasing Vapor Pressure Deficit (D). Grasses with a larger proportion of their hydraulic resistance within the xylem were less sensitive to increasing D and plants with high root conductance maintained higher rates of gas exchange D increased. Finally, I investigated the tolerance of grasses to extreme drought events to test if there was a trade-off between drought tolerance and growth in grasses. Plants with drought tolerant leaf traits typically sacrificed the ability to move water efficiently through their leaves. Having drought tolerant leaves did not limit the plants ability to have high rates of gas exchange, and, in fact, the most drought tolerant plants had the high rates of g_s when expressed on a mass basis. Leaf-level drought tolerance did contribute to species' occurrence, as the drought intolerant species I studied are not commonly found in low precipitation systems. The results presented here highlight the importance of studying the hydraulic architecture of plants to provide a better understanding of what controls plant function across a range of environmental conditions.

GROWTH AND SURVIVAL DURING DROUGHT: THE LINK BETWEEN HYDRAULIC
ARCHITECTURE AND DROUGHT TOLERANCE IN GRASSES

by

TROY W. OCHELTREE

B.S., University of Minnesota-Morris, 1997
M.S., University of Idaho, 2002

A DISSERTATION

submitted in partial fulfillment of the requirements for the degree

DOCTOR OF PHILOSOPHY

Department of Agronomy
College of Agriculture

KANSAS STATE UNIVERSITY
Manhattan, Kansas

2012

Approved by:

Major Professor
P.V. Vara Prasad

Abstract

The pathway for the movement of water through plants, from the soil matrix to the atmosphere, constitutes the hydraulic architecture of a plant. The linkage between the hydraulic architecture of woody plants and drought tolerance has received considerable attention, but much less work has been done on grasses. I investigated the linkage between the hydraulic architecture of grasses to physiological patterns of water use across a range of species and conditions. The rate of stomatal conductance (g_s) and photosynthesis (A) increased acropetally along the leaves of 5 grass species, which is a unique feature of this growth form. The internal structure of leaves also changed acropetally in order to minimize the pressure gradient across the mesophyll that would otherwise occur as a result of increasing g_s . The resistance to water movement through the mesophyll represented 80-90% of leaf resistance in six genotypes of *Sorghum bicolor* L. (Moench). This resistance was most important in controlling g_s and A when water was readily available, but as soil-moisture decreased it was the efficient transport of water through the xylem that was most important in maintaining plant function. I also investigated the relationship between hydraulic architecture and stomatal responses of grasses to increasing Vapor Pressure Deficit (D). Grasses with a larger proportion of their hydraulic resistance within the xylem were less sensitive to increasing D and plants with high root conductance maintained higher rates of gas exchange D increased. Finally, I investigated the tolerance of grasses to extreme drought events to test if there was a trade-off between drought tolerance and growth in grasses. Plants with drought tolerant leaf traits typically sacrificed the ability to move water efficiently through their leaves. Having drought tolerant leaves did not limit the plants ability to have high rates of gas exchange, and, in fact, the most drought tolerant plants had the high rates of g_s when expressed on a mass basis. Leaf-level drought tolerance did contribute to species' occurrence, as the drought intolerant species I studied are not commonly found in low precipitation systems. The results presented here highlight the importance of studying the hydraulic architecture of plants to provide a better understanding of what controls plant function across a range of environmental conditions.

Table of Contents

List of Figures	viii
List of Tables	xiii
Acknowledgements	xv
Dedication	xvi
Chapter 1 - Introduction	1
Literature Cited	3
Chapter 2 - Changes in stomatal conductance along grass blades reflects changes in leaf structure	5
Abstract	5
Introduction	6
Materials and Methods	8
Plant Tissue	8
Gas Exchange	9
Hydraulic Conductivity	9
Leaf Anatomy	11
Results	12
Gas Exchange	12
Hydraulic Conductivity	13
Leaf Anatomy	14
Discussion	14
Functional Changes Along Grass Leaves	14
Structural Changes Along Grass Leaves	17
Implications	18
Conclusions	19
Acknowledgements	19
Literature Cited	19
Tables and Figures	23

Chapter 3 - Partitioning hydraulic resistances in grass leaves reveals unique correlations	
with stomatal conductance during drought	32
Abstract	32
Introduction	33
Materials and Methods	35
Plant Material	35
Hydraulic Conductivity	36
Gas Exchange	38
Biomass Production	38
Leaf Water Potential	39
Results	39
Hydraulic Conductivity	39
Gas Exchange	40
Leaf Water Potential	40
Biomass Production	40
Discussion	41
Implications for Plant Strategies	43
Conclusions	44
Acknowledgements	44
Literature Cited	45
Tables and Figures	48
Chapter 4 - Stomatal responses to changes in vapor pressure deficit reflect tissue-specific	
differences in hydraulic resistance	54
Abstract	54
Introduction	55
Materials and Methods	57
Plant Material	57
D Response Curves	58
Hydraulic Conductivity	59
Statistical Analyses	60
Results	61

Discussion	62
Conclusions	65
Literature Cited	66
Tables and Figures	68
Chapter 5 - A trade-off between drought tolerance and growth characteristics at the leaf-	
level in grasses	76
Abstract	76
Introduction	77
Materials and Methods	78
Results	81
Discussion	83
Conclusions	86
Literature Cited	86
Tables and Figures	90
Chapter 6 - Conclusions	97
General Discussion	97
Specific Conclusions	97
Future Directions	99
Literature Cited	101

List of Figures

- Figure 2.1 Cross section of an *Elymus canadensis* blade double stained with Safranin-O and Fast Green taken on a light microscope at 40X magnification. Key anatomical characteristics are labeled as well as the measurements used to calculate D_m (Eqn. 2.1). D_v was measured from the top of the vascular bundle to the outer edge of the epidermis, and D_h was measured as the transverse distance from the edge of the vascular bundle to the center of the stomatal pore. 25
- Figure 2.2 Relationship between stomatal conductance (g_{wv} , panels A and B), leaf temperature (T_{Leaf} , panels C and D) and leaf blade position, reported as the percentage of leaf length measured from the ligule. Black symbols are measurements made on leaf sections with an angle $>0^\circ$ from horizontal, red symbols are measurements made where the leaf tip was drooping and leaf angle was $< 0^\circ$ from horizontal. g_{wv} increased acropetally for all species when leaf angle was $>0^\circ$ 26
- Figure 2.3 Relationship between Transpiration (E , panels A and B), Photosynthetic rate (A , panels C and D) and leaf blade position reported as the percentage of leaf length measured from the ligule. Black symbols are measurements made on leaf sections with an angle $>0^\circ$ from horizontal, red symbols are measurements made where the leaf tip was drooping and leaf angle was $< 0^\circ$ from horizontal. Data represented by the red symbols were not included in the regression analyses. 27
- Figure 2.4 Leaf specific hydraulic conductivity (K_{x*leaf}) as a function of leaf blade position. K_{x*leaf} remained relatively constant for all species measured as the linear regression between K_{x*leaf} and leaf position was not significant at the $p < 0.05$ level within a functional group or for any individual species. When K_{x*leaf} of all leaf segments were pooled, *Sonu* (*Sorghastrum nutans* Nash) had the highest K_{x*leaf} (1.19) followed by *Ange* (*Andropogon gerardii* Vitman; 0.90) and no significant differences between the other species. 28
- Figure 2.5 Changes in structural characteristics along grass blades. Inter-veinal distance (panels A and B) and diffusional path from vascular bundle to stomatal pore (D_m , panels C and D) decreased acropetally for all species in this study. *Ange* (*Andropogon*

<i>gerardii</i> Vitman) and <i>Sonu</i> (<i>Sorghastrum nutans</i> Nash) had the smallest change along their blades compared to the other species measured.	29
Figure 2.6 Structure-function relationship within grass leaves. D_m is the distance of the diffusional path from vascular bundle to stomatal pore within grass blades. For well-watered plants, g_{wv} is closely related to D_m within individual leaf blades. Analysis was performed using mixed-effects modeling and were significant at the $p < 0.001$ level for pooled C_3 species and <i>Scsc</i> (<i>Schizachyrium scoparium</i> Nash), but only significant at the $p < 0.1$ level for <i>Ange</i> (<i>Andropogon gerardii</i> Vitman) and <i>Sonu</i> (<i>Sorghastrum nutans</i> Nash).....	30
Figure 2.7 The modeled change in water potential gradient between the vascular bundle to epidermis ($\Delta\Psi_{vb-e}$) for a C_3 grass blade. The solid line represents the increase in $\Delta\Psi_{vb-e}$ assuming no acropetal change in D_m . When D_m decreased, as observed for C_3 grass blades in this study, the increase in $\Delta\Psi_{vb-e}$ was 63% less than when D_m remained constant along the blade.	31
Figure 3.1 Hydraulic resistance of different leaf components for six genotypes of <i>Sorghum bicolor</i> L. (Moench). Eight replicates of each genotype were measured. The resistance in the xylem (r_x , panel A) and outside the xylem (r_{ox} , panel B) are presented normalized by leaf area. The proportion of leaf resistance in the xylem (panel C) was calculated based on direct measurements of both r_{leaf} and r_x . Lowercase levels indicate significant differences at $p < 0.05$ significance level of pair wise comparisons using a ‘Holm’ correction for multiple comparisons.	49
Figure 3.2 Relationship between the stomatal conductance (g_s) and hydraulic resistance in the xylem (r_x) and outside the xylem (r_{ox}) at different levels of Soil Water Content (SWC_{mass}). Panels A, C, and E show r_{ox} values and panels B, D, and F show r_x . The level of soil moisture is shown on the right hand side of the figure for each pair of panels. The equation for the linear regression is given in each panel and its’ corresponding r^2 value. The different symbols represent each genotype tested; BTx623 (open circles), B35 (diamonds), SC1019 (triangles), SC1205 (inverted triangles), SC15 (closed circles), and Tx7078 (squares).....	50

Figure 3.3 Relationship between whole leaf hydraulic resistance and root characteristics of the six genotypes. High water use in the leaves, which correlated to low hydraulic resistance resulted in greater root biomass (panel A) and greater allocation of biomass belowground (panel B) for water acquisition. The equation for the linear regression is given in each panel and its' corresponding r^2 value. The different symbols represent each genotype tested; BTx623 (open circles), B35 (diamonds), SC1019 (triangles), SC1205 (inverted triangles), SC15 (closed circles), and Tx7078 (squares)..... 51

Figure 3.4 Relationship between leaf structure and hydraulic resistance in leaves of *Sorghum bicolor* L. (Moench). There was a significant relationship ($p < 0.05$) between major vein density and axial hydraulic resistance in the xylem (panel A). The relationship between the distance water travels from vascular bundle to stomata (D_m) and resistance outside the xylem was non-significant at the $p < 0.05$ level (panel B). The equation for the linear regression is given in each panel and its' corresponding r^2 value. The different symbols represent each genotype tested; BTx623 (open circles), B35 (diamonds), SC1019 (triangles), SC1205 (inverted triangles), SC15 (closed circles), and Tx7078 (squares)..... 52

Figure 3.5 Temporal trend in photosynthesis for two contrasting genotypes as soil moisture was depleted from evapotranspiration from the pots. The lines are cubic fit to the mean (SE bars) for each sampling period. Genotype SC15 (black line) had high hydraulic resistance outside the xylem (r_{ox}) compared to SC1019 (red line). Although the initial rates of photosynthesis were lower in genotype SC15, this genotype conserved water for prolonged growth into the drought and results in greater aboveground biomass (insert). 53

Figure 4.1 Vapor pressure response curve of *Panicum virgatum* shown as an example. Measurements were started with a low vapor pressure deficit (D) and then increased in discrete increments, waiting for transpiration (E) and photosynthesis (A) to stabilize at each level of D . The breakpoint for E and A were calculated using a segmented regression analysis in R. 71

Figure 4.2 The resistance of the xylem (r_x) and extra-xylery (r_{ox}) components scale with whole-leaf resistance (r_{leaf}). r_x scaled most closely with r_{leaf} (panel A). r_{ox} did not scale as closely with r_{leaf} (panel B) but was still significantly correlated ($p = 0.02$). Finally,

resistance of the root system was not significantly correlated with r_{leaf} (panel C, $p = 0.262$).....	72
Figure 4.3 The sensitivity of stomatal conductance in response to changing D was related to the magnitude of g_s at $D = 1.0$ kPa (g_{ref} , panel A). g_{ref} was calculated from the regression of g_s and $\ln(D)$. g_s of the different species converged to similar values as D was increased to the point that transpiration rate stabilized (g_{min} , panel B). At a vapor pressure deficit of 1.0 kPa the coefficient of variation was 0.59, but decreased to 0.47 at high values of D	73
Figure 4.4 The minimum g_s calculated from a non-linear regression were related to the proportion of plant resistance that occurred in the xylem. When a greater proportion of resistance occurred in the xylem, g_s did not decrease as much from g_{ref} compared to when xylem resistance was a small proportion of whole plant resistance.....	74
Figure 4.5 Relationship between the hydraulic conductance of the root system and and D_{break} . The breakpoint between D and E was tightly correlated with the hydraulic conductivity of the root system such that plants with lower K_{root} reached the asymptote of E at lower values of D	75
Figure 5.1 An example of vulnerability curves constructed for leaf level hydraulic conductance. K_{leaf} declined as leaf water potential decreased in all species, but the rate of decline varied greatly. A general logistic curve was fit to the data (Eqn. 5.1) and the point at which K_{leaf} decreased by 80% from K_{sat} was calculated and reported as Ψ_{80K} . Two contrasting species are shown; <i>Sorghastrum nutans</i> (red symbols) maintained higher rates of K_{leaf} compared to <i>Spartina pectinata</i> (black symbols). Ψ_{80K} for all species are shown in Table 5.1.....	91
Figure 5.2 The relationship between Ψ_{80} for K_{leaf} and g_s . The dotted line is a 1:1 reference line and the solid line is the linear regression between the two variables with the intercept set to zero. Ψ_{80g} was always lower than Ψ_{80K} indicating that the plants studied close their stomata to prevent catastrophic cavitation. The slope of the line was less than one, indicating that plants with greater resistance to cavitation also operated with a larger safety margin.	92

Figure 5.3 The trade-off between hydraulic conductance and drought tolerance. The relationship between K_{leaf} and Ψ_{80K} was not significant unless (panel A) or the point at which 80% leaf mortality after re-watering (Ψ_{80mort} , panel B). Finally, there was a negative correlation between K_{leaf} and g_s (panel C). 'ns' indicates relationships that were non-significant at the $p < 0.05$ level. The dotted line in panel C is a linear regression of the 90% quantile suggesting the relationship between K_{leaf} and g_s has a threshold such that drought intolerant species do not have high stomatal conductance.

..... 93

Figure 5.4 The relationship between leaf hydraulic conductance normalized by leaf mass) and leaf-level drought tolerance. Grasses that had an ability to transport water efficiently (high K_{mass}) were not able to maintain K_{leaf} at low leaf water potentials. Normalizing leaf hydraulic conductance by leaf mass accounts for total leaf material that must be supplied with water rather than just the surface area of the leaf. 94

Figure 5.5 Relationship between leaf level drought tolerance (Ψ_{80K}) and plant growth rate calculated on the whole plant level (including both above and below ground growth). There was a strong correlation between Ψ_{80K} and stomatal conductance calculated on mass basis (panel A), but only a weak non-linear relationship between drought tolerance and whole plant growth (panel B). 95

Figure 5.6 The Mean Annual Precipitation for all occurrences of each species correlates with leaf-level drought tolerance. Although the regression analysis was not significant, none of the grasses that were drought intolerant were commonly found in dry ecosystems, (lower left section of the figure). 96

List of Tables

Table 2.1 Leaf characteristics for the 5 species used in this study. Mean (sd) values for 5 replicates are shown for grass blade length and the blade width at 50% of the blade length..... 23

Table 2.2 Relationship between leaf position and anatomical characteristics within grass leaves. Mean \pm SD values of each leaf segments for all species are reported. Large interspecies differences were still apparent despite the acropetal variability that was the focus of this study. The slope and p-value of the regression between the anatomical variable and leaf position are also shown. The slope of leaf position and inter-veinal distance is the most consistently significant relationship. 24

Table 3.1 Mean (SE) values for aboveground biomass, root biomass, and Ψ_{leaf} for the six genotypes of *Sorghum bicolor* L. (Moench). Lowercase letters indicate significant differences at the $p < 0.05$ level. Aboveground biomass is shown for a ‘control’ group that was grown under well-watered conditions and the ‘drought’ treatment group. Root biomass and Ψ_{leaf} are shown only for the ‘drought’ treatment group. The p-value for the sampling date in a mixed-effects model is shown for each genotype, indicating that there was no significant difference in Ψ_{leaf} throughout the drought treatment experiment. 48

Table 4.1 The 20 species selected for our study are shown, grouped by their photosynthetic pathway. The vapor pressure deficit breakpoint (D_{break}) for each species is listed, multiple values are listed if replicates were measured. The hydraulic conductance of the whole plant along with the partitioning of plant resistances by plant component are also shown. A two sample t-test was carried out between C₃ and C₄ species and significant differences at the $p < 0.05$ and $p < 0.1$ level are indicated with ‘*’ and ‘**’, respectively. ‘nd’ indicates these values could not be determined for that species. 68

Table 4.2 Results from multiple linear regression analyses and the percentage of the Sums of Squares (SS) explained by the significant variables. ‘ns’ indicates non-significant variables at the $p < 0.1$ level, and ‘nd’ indicates these values could not be determined. K_{root} , g_s , and K_{xylem} are all significant in predicting the vapor pressure deficit breakpoint

(D_{break}). K_{root} was not correlated with any of the root system characteristics measured in this study..... 70

Table 5.1 Grass species used to test drought tolerance. All plants except *Andropogon gerardii* were grown from seeds obtained through the Germplasm Resources Information Network (GRIN). An insufficient number of *A. gerardii* seeds germinated and so plants were grown from rhizomes collected at Konza Prairie Biological Station, Kansas, USA. The median of the Mean Annual Precipitation (MAP) is also shown for all occurrences of each species in the GBIF database. Leaf-level drought tolerance quantified as the point at which there was an 80% loss in K_{leaf} , g_s , and A (Ψ_{80K} , Ψ_{80g} , and Ψ_{80A} , respectively) are listed as well as K_{leaf} when the soils were at pot-holding capacity (K_{sat})..... 90

Acknowledgements

I would like to acknowledge the help and support of many people throughout my PhD experience. I would like to thank my committee members (Drs. Vara Prasad, Jesse Nippert, Mary Beth Kirkham and John Blair) for being helpful, supportive, and patient as I attempted to balance family, work, and school. I would also like to thank Dr. Kendra McLauchlan and Dr. Joseph Craine for stimulating discussions, career perspectives, and help in motivating me along the way. I would like to thank my fellow graduate student Zak Ratajczak (aka 'standing man') for always being willing to help and discuss ideas and for just being an all-around swell guy. I would especially like to thank Jesse Nippert, my friend and committee member for being so extremely helpful and supportive during this process, without his help I would most definitely not have made it to this point. I would like to thank my family (Sonny, Quinn and Syri) for being willing to make this journey with me. Their patience, support, and interest in things other than plants helped make life fun during my PhD and helped me maintain balance and some level of sanity. And finally I would like that thank the K-State Center for Sorghum Improvement, the Konza Prairie Long-Term Ecological Research site, and the Schrader-Massie Fellowship (KSU, Department of Agronomy) for their financial support.

Dedication

I would like to dedicate my dissertation to my family: my perpetually supportive parents, my amazingly patient and understanding wife, and my two inspiring daughters.

Chapter 1 - Introduction

Since Stephen Hales discovered that water moved through plants and evaporates from the leaf surface people have been fascinated with the hydraulic system of plants. The pathway by which water moves through the plant is considered the hydraulic architecture of plants and comprises root morphology and anatomy, the structure of vessel elements, as well as the vascular arrangement within leaves. These structural characteristics of plants play a role in: water and nutrient acquisition from the soil, drought and freezing tolerance, competition for light, and maximum rates of gas exchange in leaves. Although there are a host of biochemical reactions that contribute to plant function in relation to water use and drought tolerance, the hydraulic architecture of plants provides the framework within which these biochemical processes occur, and as such, understanding the boundaries of the hydraulic system provides insight into the constraints on plant growth under different environmental conditions.

As water travels through the Soil-Plant-Atmosphere-Continuum, plants experience water deficits at both ends of the spectrum. Atmospheric air is extremely dry compared to the internal air spaces of a plant leaf, and this dry air provides the driving gradient for transpiration. As water evaporates from the leaf, tension is generated on the water column, essentially pulling water up through the plant from the soil to the atmosphere. The vascular tissue provides the pathway for water movement from the roots to the leaf and affects the efficiency by which water moves between these organs. Finally, the roots provide the interface for the extraction of water from the soil matrix. If the supply of water from the soil matrix to leaves does not meet the demand of the atmosphere, plants must regulate the loss of water or else face turgor loss and desiccation of cells, which disrupts optimal plant function. Plants regulate the loss of water by adjusting their stomatal aperture to minimize the danger of turgor loss resulting from low pressure potentials acting on cell membranes within the leaf. As such, stomatal regulation acts to alter both leaf hydration status and an overall reduction in total water lost. Typically, the water status of leaves is measured as the water potential of the bulk leaf tissue (Ψ_{leaf}). Although it is unlikely that plants themselves can detect critical thresholds in Ψ_{leaf} , stomatal regulation

effectively maintains a constant Ψ_{leaf} under different soil and atmospheric conditions. As the water deficit of the atmosphere or soil increases, plants close their stomata in order to maintain Ψ_{leaf} at optimal (or near optimal) levels.

Due to the friction of moving water along cell walls and through small pore spaces, the hydraulic system in plants acts as a resistor, which causes a reduction in the water potential along a plant, from root surface to leaf cells. The lower the resistance, the lower the pressure gradient from soil to leaf. Since plants regulate stomatal conductance to keep Ψ_{leaf} above a specific threshold, minimizing the resistance from root to leaf would help maintain Ψ_{leaf} as high as possible at a given level of soil moisture. The flow through a xylem vessel is proportional to the radius of the vessel raised to the fourth power, so constructing wide diameter vessels is one mechanism plants can utilize to minimize resistance to water flow. As water moves through the vascular system it crosses the cell walls of vessel elements via bordered pits (in angiosperms), and the easier water can move through these pits the more efficiently it can be moved to the leaf. Large pore spaces within the bordered-pit membrane allow water to pass easily from one vessel element to another.

It would seem logical then for plants to produce large diameter vessels with large-pored bordered pits to facilitate water transport with minimal resistance. However, efficient water transport is not the only constraint on the plant hydraulic system; plants must also maintain the integrity of the water column so that the supply of water to the leaves will not be disrupted (referred to as the safety vs. efficiency trade-off, discussed by Meinzer *et al.* 2010). If tension on the water column becomes great enough, air can enter the water column, expand, and cause cavitation (disruption of the water column) thus stopping the flow of water (called the air-seeding hypothesis, Zimmerman 1983). Two characteristics increase the tendency for air-seeding to occur: large diameter vessels and bordered-pits with large pores (Hacke *et al.* 2006). These are the same two characteristics that provide efficient transport of water through the plant. These constraints on the hydraulic architecture of plants have played a major role in the evolution and distribution of plants around the globe.

As plants adjust stomatal conductance in order to maintain turgor in their cells and prevent cavitation, the change in stomatal aperture also affects photosynthetic rates. The

rate of photosynthesis is affected by the internal CO₂ concentration in the leaf (c_i), as the efficiency of carboxylation decreases in proportion to c_i (Taiz and Ziegler 2010). When stomatal conductance decreases (resulting in decreased water loss from the leaf), the consequence is a subsequent reduction in the rate of CO₂ diffusion from the atmosphere into the internal leaf spaces thereby reducing photosynthetic rates. Although C₄ plants reach maximum photosynthetic rates at lower c_i values due to the CO₂ concentrating mechanism of this functional group (Sage and Monson 1999), reduced stomatal conductance will negatively impact carbon assimilation in both C₃ and C₄ plants. Therefore, in order to understand the spatial and temporal variability in plant growth, it is imperative to have a greater understanding of the controls on stomatal conductance and role of hydraulic architecture as a structural constraint on stomatal responses to environmental conditions.

Scientists have investigated the safety vs. efficiency trade-off in the woody tissue of many species, and related the functional characteristics of these species to distributions across the regional and global landscapes. In contrast, very little is known about the hydraulic architecture of grasses, a growth-form that covers ~40% of the global biosphere and comprise nearly all of the globally important agriculturally species (for direct consumption and forage). Do the same principles that govern woody plants apply to grasses? Does the unique parallel-veined structure of grasses provide similar physiological responses as species with dichotomous vasculature? Are some plant organs more capable of maintaining a constant supply of water to cells? Answering these questions will help us better understand the growth and distribution of grasses. The objective of this dissertation was to develop a better understanding of how the hydraulic architecture of grasses affects their physiology across a range of environmental conditions. I did this by measuring both anatomical and physiological traits of grasses. I investigated the variability in traits from within individual leaves, between genotypes, and finally across a wide range of species.

Literature Cited

Hacke U.G., Sperry J.S., Wheeler J.K., and Castro L. 2006. Scaling of angiosperm xylem structure with safety and efficiency. *Tree Physiology* 26, 689–701.

- Meinzer F.C., McCulloh K.A., Lachenbruch B., Woodruff D.R., and Johnson D.M. 2010. The blind men and the elephant: the impact of context and scale in evaluating conflicts between plant hydraulic safety and efficiency. *Oecologia* 164, 287–296.
- Sage R.F., and Monson R.K. 1999. *C4 Plant Biology*, Academic Press. San Diego, CA, USA.
- Taiz L., and Zeiger E. 2010. *Plant Physiology, Fifth Edition*, Sinauer Associates, Inc., Sunderland, MA, USA.
- Zimmermann M.H. 1983. *Xylem structure and the ascent of sap*. Springer-Verlag. Berlin, Germany.

Chapter 2 - Changes in stomatal conductance along grass blades reflects changes in leaf structure

Abstract

Identifying the consequences of grass blade morphology (long, narrow leaves) on the heterogeneity of gas exchange is fundamental to an understanding of the physiology of this growth form. I examined acropetal changes in anatomy, hydraulic conductivity, and rates of gas exchange in 5 grass species (including C₃ and C₄ functional types). Both stomatal conductance and photosynthesis increased along all grass blades despite constant light availability. Hydraulic efficiency within the xylem remained constant along the leaf, but structural changes outside the xylem changed in concert with stomatal conductance. Stomatal density and stomatal pore index remained constant along grass blades but interveinal distance decreased acropetally resulting in a decreased path length for water movement from vascular bundle to stomate. The increase in stomatal conductance was correlated with the decreased pathlength through the leaf mesophyll. A strong correlation between the distance from vascular bundles to stomatal pores and stomatal conductance has been identified across species; our results suggest this relationship also exists within individual leaves.

Introduction

Identifying the relationship between leaf structure and function across species has received considerable attention (Sack and Frole 2006, Brodribb, Field and Jordan 2007), and has elucidated many trade-offs between water use and carbon gain. However, the relationship between structure and function within individual leaves has received less attention. Water potential gradients within individual eudicot leaves suggest that the balance between water supply and demand changes within individual leaves. In the elongate leaves of *Laurel nobilis* L., water potential decreased from the base to tip of individual leaves (Zwienecki *et al.* 2002, Cochard, Nardini and Coll 2004), which would result in acropetal changes in cell water status. These acropetal water potential gradients would be exacerbated in long, narrow leaves (such as monocot leaves) and would likely correspond to large changes in plant behavior across a single leaf. A better understanding of the structure and function of monocot leaves is necessary to understand changes in the balance between water loss and carbon assimilation as water is transported through the vasculature to the site of evaporation.

The heterogeneity of stomatal conductance to water vapor (g_{wv}) within individual eudicot leaves has been the focus of recent studies (Buckley and Mott 2000, Marengo *et al.* 2006, Nardini *et al.* 2008). 'Patchy' adjustments in g_{wv} appear to respond to local changes in hydraulic conductance in eudicot leaves, as xylem conduits cavitate and refill on diurnal timescales (Marengo *et al.* 2006). Localized dynamic control of g_{wv} in eudicots leads to seemingly random heterogeneity as the plant maximizes gas exchange across the entire leaf surface as the environment changes (Buckley, Farquhar and Mott 1999). Preliminary data on the heterogeneity of stomatal conductance in monocot leaves suggests a more systematic pattern; measurements made along grass blades found photosynthesis (A) increased acropetally for *Saccharum officinarum* L. (Meinzer and Saliendra 1997) and *Zea mays* L. (Miranda *et al.* 1981a, Long *et al.* 1989). Systematic changes in transpiration (E) along grass blades have been shown in research modeling the enrichment of ^{18}O in leaf water of grasses (Helliker and Ehleringer 2000, Affek, Krisch and Yakir 2006, Ogee *et al.* 2007). Model accuracy of ^{18}O enrichment is high only when E increased acropetally. Furthermore, Ogee *et al.* (2007) showed that all published data of ^{18}O enrichment along

leaves could be accurately described assuming increases in E . Thus, while acropetal increases in E have been reported in monocots previously, most research has been limited to either *Zea mays* L. or *Saccharum officinarum* L. and the implications of increased water demand along grass blades has not been investigated.

Broadly, the structure of the hydraulic system within leaves constrains whole plant water use and correlates with maximum rates of leaf-level gas exchange. For example, the conductance to water flow through leaves has been shown to correlate positively with photosynthetic capacity (Brodribb *et al.* 2002, Brodribb *et al.* 2005, Brodribb *et al.* 2007). Furthermore, the resistance within leaves correlated strongly with the pathlength from vascular bundle to stomatal pore (Brodribb *et al.* 2007), suggesting that vein placement within leaves may be the limiting factor to maximum rates of gas exchange. In tropical rainforest leaves, the structure of the mesophyll exerted strong controls on the movement of water through leaves; both xylem density and palisade: spongy mesophyll ratio correlated with leaf resistance to water flow (Sack and Frole 2006). These results emphasize the importance of extra-vascular resistances to the movement of water through leaves and maximum rates of gas exchange, at least under well-watered conditions.

Monocot leaf blades are typically long and tapering, and this shape influences the internal structure of the hydraulic pathway. As blades taper, the distance between vascular bundles decreases (Colbert and Evert 1982, Russell and Evert 1995, Dannenhoffer, Ebert and Evert 1990, Martre and Durand 2001) as fewer bundles terminate compared to the degree of tapering. The mean diameter of xylem vessels decreases, resulting in decreasing hydraulic conductivity within the xylem (K_x), but when normalized by leaf area, leaf specific K_x remains relatively constant along grass blades (Martre and Durand 2001). This is consistent with plant scaling theory for trees (West, Brown and Enquist 1999) and would minimize the pressure drop along the blade. In contrast to the changes in inter-veinal distances, the density of stomatal pores often remains constant along the grass blades (*Zea mays* L. - Miranda, Baker and Long 1989b). If stomatal densities remain constant and inter-veinal distances decrease, it then follows that the diffusional pathlength from vascular bundle to stomate should also change along the length of monocot leaf blades, and these changes in pathlength would provide a structural mechanism to facilitate corresponding changes in g_{ww} .

The objective of this study was to investigate the correlation between hydraulic architecture and rates of gas exchange within individual grass blades. I measured the hydraulic conductance, gas exchange rates, and anatomical characteristics from corresponding positions within leaves of 5 common tallgrass prairie species. I hypothesized that: 1) A , E and g_{wv} will increase along the leaf even in the presence of constant light intensity along the leaf; 2) Leaf specific K_x will remain constant along the leaf; and 3) The distance from vascular bundle to stomatal pore will decrease acropetally and will correlate with g_{wv} within individual grass blades.

Materials and Methods

Plant Tissue

Five common grass species native to the tallgrass prairie were selected for this study; *Andropogon gerardii* Vitman (*Ange*, C₄ NADP-ME), *Sorghastrum nutans* Nash (*Sonu*, C₄ NADP-ME), *Schizachyrium scoparium* Nash (*Scsc*, C₄ NADP-ME), *Elymus canadensis* L. (*Elca*, C₃), and *Bromus inermis* Leyss. (*Brin*, C₃). C₃ and C₄ species were included in this study to investigate the generality of the patterns across a range of grass species rather than an attempt to characterize differences between these functional groups. Leaf characteristics of the measured species are shown in Table 1. Seeds were collected from Konza Prairie Biological Station, Kansas, USA (KPBS) and stored at 4°C until the initiation of the study. Seeds of each species were germinated on wet filter paper and then 5 individuals were transplanted into 1.65 L pots (“Short One” Treepots, Stuewe and Sons, Inc., Tangent, OR 97389) filled with soil taken from KPBS. This resulted in five replicates per species, which were then randomly distributed within a growth chamber (Convion PGV 36, Convion Environments Limited, Winnipeg, Manitoba, Canada). Air temperature in the growth chamber was maintained at 30°C with a 16 hr photoperiod. The light intensity at the top of the canopy was maintained at ~1000 $\mu\text{mol m}^{-2} \text{s}^{-1}$ by adjusting the height of the lights as the canopy grew. Plants were watered daily to ensure that soil moisture remained near pot-holding capacity. Plants were grown until they had 4-6 mature leaves before beginning measurements. On day 1 of a measurement cycle three plants were randomly selected across all species and gas exchange measurements were made on one

leaf per plant. After the photoperiod ended on that same day, plants were covered with a plastic bag and placed in a dark enclosure to allow leaves to fully hydrate for hydraulic conductance measurements, which were made on day 2 of the measurement cycle. Immediately after hydraulic conductance measurements were completed plant tissue was placed in a chemical fixative and stored until further processing for microscopic analysis. This 3-day measurement cycle was continued until all plants had been measured.

Gas Exchange

The most recently mature leaf blade of each plant was identified and divided into five equal longitudinal sections. The middle of each section was marked (using a black marker) and all subsequent measurements were centered on this mid-point. The distance from the ligule to the center of each blade section (d_L) was measured for leaf position. A , E , g_{wv} , and leaf temperature (T_{Leaf}) were measured using an Infrared Gas Exchange System (Li-6400, Li-Cor, Inc., Lincoln, Nebraska, USA) with the fluorometer cuvette, which has a smaller chamber size (2 cm²), to maximize the proportion of the cuvette occupied by the leaf section. Conditions inside the cuvette were maintained to match the condition of the growth chamber (~400 ppm CO₂, 30°C, 50±5% relative humidity, 1000 μmol m⁻² s⁻¹ PAR). Gas exchange measurements were first made on the basal section and then sequentially along the length of the blade toward the apex. Data from the Li-6400 was logged every 5 seconds until both A and g_{wv} were stable for >1 min (typically ~5-10 minutes of logged data). Data was imported into Matlab (Mathworks, Inc., Natick, Massachusetts, USA), visually inspected to ensure stability and then the mean of the last minute of data (12 logged points) was calculated and corrected for the amount of leaf area in the chamber during the measurement.

Hydraulic Conductivity

Axial Hydraulic conductivity within the xylem (K_X) was determined by measuring the flow rate through a blade segment when exposed to a hydrostatic pressure gradient as described by Sperry, Donnelly and Tyree (1988) for woody stems and modified by Martre,

Durand and Cochard (2000) for grass blades. The selected blade from each plant was cut under water and transported to the water reservoir for K_x measurements. A ~40 mm leaf segment was cut under water and wrapped longitudinally around a ½-inch silicone rubber rod and each end secured with Teflon tape taking care to leave the cut end of the leaf segment exposed and extending beyond the end of the silicone rod. Each end of the blade section was trimmed with a razor blade immediately prior to placement in a 5/8" ID vinyl tube. The basal end of the leaf was connected to a reservoir of degassed deionized water filtered (0.2 micron) and pressurized to ~ 10 kPa. The apical end of the leaf was connected to a reservoir of degassed de-ionized water on a micro-balance (± 0.1 mg, Ohaus Pioneer, Ohaus Corporation, Parsippany, New Jersey, USA.) to measure the flow rate of pressurized water through the leaf. Data from the balance was captured via a laptop computer at 1 sec intervals and flow rate was calculated as the change in water mass per unit time. Flow was measured on each segment until the rate stabilized (typically ~ 5-10 min), and then 5 min of data were collected to calculate K_x . The temperature of the water bath was also monitored during measurements and K_x of each section was normalized to the viscosity of water at 20°C.

The background flow rate was also determined before and after measuring K_x of each blade segment. The pressure on each side of the leaf was equilibrated to eliminate any pressure gradient across the leaf segment and the background flow was measured for 10 min. The average of the two measurements was used in calculations of hydraulic conductivity, and was typically less than 5% of the measured flow rate through the leaf section. Background flow was subtracted from pressurized flow and the result divided by the pressure gradient to yield K_x ($\text{mmol mm MPa}^{-1} \text{s}^{-1}$).

Following K_x measurements of all sections of an individual leaf blade, the entire blade (including the sections not used for K_x and gas exchange measurements) was scanned (at 600 dpi, Epson Perfection V500, Epson America Inc., Long Beach, California, USA) for determination of leaf area (Rasband, 1997-2011, Image J, U. S. National Institutes of Health, Bethesda, Maryland, USA, <http://rsb.info.nih.gov/ij/>). K_x was divided by the amount of leaf area distal to each blade section to yield leaf specific hydraulic conductivity K_{x*leaf} ($\text{mmol mm}^{-1} \text{MPa}^{-1} \text{s}^{-1}$).

Leaf Anatomy

Immediately following hydraulic measurements, leaf blade tissue was vacuum infiltrated with a fixative (Formalin-acetic acid-alcohol) and placed in 4°C storage for further processing. Each blade section was divided in half; the basal half was used for determination of stomatal density and the apical half was embedded with paraffin, stained and used for characterization of internal leaf structure. Stomatal density images were taken directly on the leaf blade tissue to avoid errors associated with any stretching that can result during casting. This maximized our potential to identify small differences along individual leaves. Leaf blade tissue was illuminated with 543 nm wavelength (Zeiss lsm5 Pascal confocal microscope, Carl Zeiss MicroImaging, LLC, Peabody, Massachusetts, USA) and fluoresced images were taken using a digital camera (Zeiss Axiocam, Carl Zeiss MicroImaging, LLC, Peabody, Massachusetts, USA). Each image consisted of 8 slices taken at 5 µm increments, which effectively changed the focal length in order to capture all stomata on the undulating surface of the grass blades. Stomatal density was determined on four images per surface (abaxial and adaxial) of each blade section and averaged. The image area was 1.5 mm² and stomatal densities are reported in stomata mm⁻². Guard cell length was also measured on these same images; the guard cell length of 10 stomata per image were measured (80 guard cells per section) and averaged for each blade section. Stomatal Pore Index (SPI) was calculated as guard cell length² multiplied by stomatal density as a unitless index of maximum stomatal pore area per lamina area (Sack *et al.* 2003).

Blade sections were embedded with paraffin to determine inter-veinal distance and diffusional pathlength. Blade segments were embedded with paraffin at the K-State Histology Lab and then double stained with safranin-O and Fast Green (Ruzin 1999). Images were taken with a digital camera (Leica DFC 290, Leica Microsystems GmbH, Wetzlar, Germany) coupled to a light microscope (Leica DM1000, Leica Microsystems GmbH, Wetzlar, Germany) and analyzed using ImageJ (Rasband 1997-2011). Inter-veinal distance was determined by measuring the distance between the centroid's of two neighboring vascular bundles, and the mean distance of all measurements per blade segment determined. I calculated an index of the diffusional pathlength of water movement through the mesophyll (D_m) to estimate the change in extra-xylery resistance

along grass blades. As the exact pathway water moves through the mesophyll is still the subject of debate (Westgate and Steudle 1985, Ye, Holbrook and Zwieniecki 2008). I calculated an index of this pathlength rather than try to estimate the exact distance water must travel from vascular bundle to evaporating site, which I assumed to be near the stomatal pore (Pickard 1981). D_m was determined by measuring the vertical distance (D_v) from each vascular bundle to the epidermis, and the horizontal distance (D_h) to the nearest stomatal pore (Figure 2.1) then D_m was calculated as:

$$D_m = \sqrt{D_v^2 + D_h^2} \quad (\text{Eqn. 2.1}).$$

For the grass blades measured, stomata were typically arranged in rows associated with each vascular bundle. Due to this structural arrangement, I assumed that the water supplying the cells around the stomatal complex was from the nearest bundle, and so D_h was only measured for the closest stomate.

All statistical analyses were performed using the R open source statistical software package (R Development Core Team, 2008). Data were first checked for normality and any outliers removed. Linear regression was used for all analyses of variables with leaf blade position. For comparisons of anatomical features between species paired t-tests were made using the ‘Holm’ correction for multiple comparisons. To determine the relationship between D_m and g_{wv} , linear mixed-effects model analysis (from the ‘nlme’ library – Pinheiro *et al.* 2008) was used to minimize variability attributed to individuals (individual was the random variable).

Results

Gas Exchange

Stomatal conductance increased acropetally for all species measured. Species within functional groups had similar values and were grouped together for regression analyses (Figure 2.2A and 2.2B). g_{wv} was generally lower for C₄ species (range: 0.05-0.22 mol m⁻² s⁻¹) compared to C₃ species (0.1-0.45 mol m⁻² s⁻¹), which is expected due to differences in photosynthetic pathways. The acropetal increase in g_{wv} was greater per unit length for the selected C₃ species than for the C₄ species as determined by the slope of the line between d_L and g_{wv} (Figure 2.2A and 2.2B), but the relative increase was similar

between the two functional groups (C₃-105%, C₄-140%). T_{Leaf} decreased acropetally for C₃ blades as would be expected with increasing g_{wv} (Figure 2.2C) but showed no consistent pattern for C₄ blades (Figure 2.2D). Smaller increases in g_{wv} for the C₄ species may have been too small to generate temperature differences detectable by the sensor. While g_{wv} always increased acropetally when the angle of the leaf blade was greater than 0° from horizontal, g_{wv} decreased toward the tip when the blade angle was < 0° (Figure 2.2, red symbols). Data represented by red symbols were not included in the regression analyses. E also increased acropetally in all species measured (Figure 2.3A and 2.3B), but did not increase in direct proportion to g_{wv} . Since E is a function of g_{wv} and the vapor pressure gradient across the leaf surface, decreases in T_{Leaf} along the blade would reduce the vapor pressure gradient and reduce the acropetal increase in E .

Photosynthetic rates (A) increased by 35% and 100% along the leaf blade for the C₃ and C₄ grasses, respectively (Figure 2.3C and 2.3D). C₄ species had greater variability in A (1-18 $\mu\text{mol m}^{-2} \text{s}^{-1}$) compared to C₃ species (5-15 $\mu\text{mol m}^{-2} \text{s}^{-1}$). C₄ species exhibited a greater acropetal increase in A , which may have been partly due to the greater variability within the C₄ functional group. As with g_{wv} , A declined at the tips of the blades when leaf blade angle was < 0° from horizontal (Figures 2.3C and 2.3D, red symbols).

Hydraulic Conductivity

The hydraulic efficiency of the leaf xylem remained relatively constant within the blades when normalized for leaf area. Leaf specific hydraulic conductivity in the xylem (K_{x*leaf} , $\text{mmol mm}^{-1} \text{MPa}^{-1} \text{s}^{-1}$) did not change significantly within blades of any species measured (Figure 2.4). So, for a given amount of leaf area, the capacity to move water through the xylem did not change along the blades. The C₄ species selected tended to have higher K_{x*leaf} , *Sonu* had K_{x*leaf} of 1.19, which was significantly greater ($p < 0.01$) than *Ange* (0.90). There was no significant difference in K_{x*leaf} between the other species measured.

Leaf Anatomy

Leaf structure varied significantly along the blades of all species measured (Table 2.2, Figure 2.5). Guard cell length increased slightly for *Elca*, but did not change in the other species. Both stomatal density and SPI were constant along the blade for all species measured (Table 2.2). The selected C₃ species had significantly lower stomatal densities than the C₄ species; stomatal densities ranged from 30-100 mm⁻² and 75-310 mm⁻² for C₃ and C₄ species, respectively. The guard cell length, however, was significantly longer for the C₃ species (range 60.36-62.19 μm) than the C₄ species (range 15.62-17.48 μm). SPI varied minimally within each functional group (Table 2.2), but there were significant differences between C₃ and C₄ species. Significant decreases in inter-veinal distance (Figure 2.5A and 2.5B) coupled to constant stomatal density and SPI (Table 2.2) should lead to shorter distances for water movement from a vascular bundle to stomate. The diffusional distance for water movement, measured as the distance from a vascular bundle to stomatal complex, decreased acropetally in all plants measured in this study (Figure 2.5C and 2.5D). This decrease in D_m was also correlated to rates of gas exchange, as there was a significant negative relationship between D_m and g_{wv} (Figure 2.6).

Discussion

Functional Changes Along Grass Leaves

I have identified a tight correlation between structure and function within individual grass blades across a range of species. A and g_{wv} increased acropetally along the blades of all species measured, which correlated to changes in the hydraulic architecture of blades. Previous studies investigating the heterogeneity of gas exchange in grasses also identified large increases in A and g_{wv} that were correlated with large light gradients from base to tip (Meinzer and Saliendra 1997). In this study, I build on this fundamental work to investigate the relationship between these changing rates of gas exchange in relation to the unique hydraulic architecture of grass leaves.

Our results show stomatal conductance to water vapor (g_{wv}) and carbon assimilation (A) increased acropetally (Figure 2.2 and Figure 2.3) for all species measured,

which is consistent with previous work (Miranda, Baker and Long 1981a, Long *et al.* 1989, Meinzer and Saliendra 1997). Despite differences in the absolute values of g_{wv} , the relative increase in g_{wv} was similar between the two functional groups; C₃ species increased by 105% while C₄ species increased by 140%. g_{wv} increased acropetally despite no change in light intensity along blades under the growth conditions of this study. A also increased acropetally along the blades of all species measured. The relative increase for C₄ plants was greater (100%) than C₃ plants (35%), which is somewhat surprising since C₄ photosynthesis is considered less sensitive to internal CO₂ concentrations due to their ability to concentrate CO₂ at the sites of carboxylation. The steep increase in A for C₄ species is driven, at least in part, by the low photosynthetic rates in the basal sections of the blade for some of the individual C₄ plants (Figure 2.3D), which is likely a result of a greater proportion of the leaf consisting of vasculature near the base (Figure 2.4). It has been suggested acropetal increases in A are an adaptation to the growth form of grasses (Long *et al.* 1989) and the measurements of Meinzer and Saliendra (1997) support this idea. If the basal portion of the grass blade is shaded by the tiller and upper leaves, resources will be allocated to the distal regions of leaves to maximize photosynthesis where light availability is typically higher. The native grasses of the tallgrass prairie I selected have relatively narrow leaves and so the effect of self-shading may not be as severe as for *Zea mays* L. and sugarcane (Long *et al.* 1989, Meinzer and Saliendra 1997). Even so, the changes in A and g_{wv} measured here agree with the idea that these grasses have adapted to a growth form where light gradients exist along their blades. It must be noted, however, that acropetal increases in g_{wv} have been found in leaves of tobacco (Nardini *et al.* 2008), which suggests that the systematic changes in gas exchange along leaves is not exclusive to monocots. This pattern of increasing rates of gas exchange may be a fundamental consequence of moving water through a series of channels that exists in all growth forms. Measurements on a wider set of species with a range of growth characteristics would be valuable in further understanding the patterns of gas exchange in leaves.

What then, is the underlying mechanism(s) driving increased in g_{wv} along grass leaves? Plants tend to adjust stomatal conductance to maintain the CO₂ concentration inside the leaf (c_i) at an optimal level across a range of conditions (Cernusak and Marshall 2001). Mott and Buckley (1998) suggested that the maintenance of c_i is a likely signal for

the control of ‘patchy’ stomatal conductance within the individual. The increase in g_{wv} along grass blades could exist to maintain c_i at an optimum level for the increasing rates of photosynthesis. I can evaluate this mechanism as the driver of acropetal increases in g_{wv} for this study with a simple modeling exercise based on established equations. Using A and g_{wv} calculated from the linear regressions for C₃ leaves (Figures 2.2 and 2.3) and converting g_{wv} to stomatal conductance for CO₂ ($g_c = g_{wv}/1.6$), c_i was calculated by rearranging the linear equation for photosynthesis:

$$A = g_c (c_a - c_i) \quad (\text{Eqn. 2.2})$$

where c_a was set to 400 ppm (conditions inside chamber during gas exchange measurements). This simple modeling approach assumes that boundary layer conductance is large compared to g_{wv} and that changes in conductance along the leaf are driven by changes in g_{wv} . This assumption is valid for the conditions of this study, as boundary layer conductance of ~ 2 orders of magnitude greater than g_{wv} during gas exchange measurements (data not shown). In order to maintain a constant c_i , the modeled increase in g_{wv} was 35% acropetally along the blade, which is a smaller increase than I measured for C₃ leaves. This suggests that the changes in A and g_{wv} observed in this study would lead to increases in c_i along the leaves in the species measured. This is the opposite trend compared to field grown sugarcane (Meinzer and Saliendra 1997), where c_i values decreased acropetally. The difference in c_i patterns may be due, in part, to the different photosynthetic pathways utilized by the plants of interest. Our modeling exercise was carried out for C₃ grasses, which have photosynthetic rates that saturate at higher c_i values than C₄ plants (like sugarcane) and may have a relatively larger change in g_{wv} to maintain higher levels of c_i . Measurement conditions may also contribute to the different patterns of c_i in our model compared to the results from sugarcane. Changes in the rates of gas exchange for sugarcane were measured in the presence of large light gradients along the blades; our measurements were made on leaves growing with a uniform light environment along the blades. The increased light availability along sugarcane blades may change the pattern of g_{wv} compared to our results. The range of A values measured along grass blades, however, was quite similar between the two studies and so it is unclear how leaf-level light gradients would have affected our results. Finally, it is also possible that some unknown

'signal' besides c_i results in g_{wv} adjustments and may have driven the increase in stomatal conductance I observed. Further work needs to be done comparing C_3 and C_4 patterns of g_{wv} and A along leaves under a range of conditions (e.g., light gradients, boundary layer gradients, etc.).

Structural Changes Along Grass Leaves

Water flow within leaves can be divided into two broad structural categories; flow within the xylem, and flow outside the xylem as water moves out of the vascular bundle to sites of evaporation. The capacity for water movement within the xylem, calculated as leaf specific hydraulic conductivity (K_{x*leaf} , $\text{mmol mm}^{-1} \text{s}^{-1} \text{MPa}^{-1}$), remained relatively constant (Figure 2.4) along the grass blades, which is consistent with other studies of grass hydraulic architecture (Martre and Durand, 2001). Martre and Durand (2001) showed K_{x*leaf} increased along the sheath, but then remained constant along the blade with a slight increase in the tips using leaves of *Festuca arundinacea* Schreb cv. Clarine. Similarly, others have identified reductions in hydraulic conductivity and total vessel area along grass blades as leaf area declines (Colbert and Evert 1982, Russell and Evert 1985, Dannenhoffer *et al.* 1990), but in these studies leaf specific hydraulic conductance was not reported.

The conductance of water outside the xylem (K_{ox} , $\text{mmol mm s}^{-1} \text{MPa}^{-1}$) can be a significant source of resistance within leaves (Martre, Cochard and Durand 2001, Cochard, Nardini and Coll 2004, Mott 2007) and has been related to the internal structure of the leaves (Sack and Frole 2006, Brodribb *et al.* 2007). Increases in vascular density coupled to constant or increasing stomatal density resulted in shorter pathlengths (D_m) for the movement of water from vascular bundles to the site of evaporation (Figure 2.5). Vascular density also increased in *Festuca arundinacea* Schreb cv. Clarine (Martre and Durand 2001) but was less variable in 7-day old *Zea mays* L. (Miranda *et al.* 1981b), where inter-veinal distances remained constant over most of the leaf. Based on previous findings (Sack and Frole 2006, Brodribb *et al.* 2007), the decrease in D_m acropetally found here would reduce the resistance to water movement outside the xylem facilitating greater g_{wv} in distal portions of grass leaves without drastic increases in the $\Delta\Psi$ from vascular bundle to site of

evaporation. Increases in the K_{ox} along grass blades while K_{x*leaf} remains constant changes the relative proportions of these conductances within individual leaves may facilitate the increase in g_{wv} along grass blades, but much work remains on the complex relationship of liquid and vapor phase resistances within leaves (Meinzer 2002) to fully understand these increases in g_{wv} along grass blades.

Implications

Despite the uncertainty of the mechanism controlling g_{wv} , it is apparent that there is a tight correlation between hydraulic architecture and rates of gas exchange within leaves of grasses. The changes in architecture likely minimize the water potential gradients within the leaf as the rate of water loss increases acropetally. Assuming D_m to be directly proportional to leaf conductance outside the xylem (Sack and Frole 2006, Brodribb *et al.* 2007), I used an electrical analog approach to model the effect of changes in extra-xylery conductance on the water potential gradient from vascular bundle to the epidermis ($\Delta\Psi_{vb-e}$). $\Delta\Psi_{vb-e}$ was calculated along the blade as:

$$\Delta\Psi_{vb-e} = \frac{E}{K_{ox}} * l \quad \text{(Eqn. 2.3)}$$

where K_{ox} ($\text{mmol mm s}^{-1} \text{MPa}^{-1}$) is the hydraulic conductance outside the xylem from vascular bundle to epidermis and l is equal to D_m for this exercise. I set K_{ox} to an arbitrary value of $0.7 \text{ mmol mm s}^{-1} \text{MPa}^{-1}$ (which is one-tenth the value of measured axial hydraulic conductance) and was assumed to be constant along the leaf so that only E and l changed according to our measurements on C_3 leaves. The absolute value of K_{ox} , however, is not important for this simulation since I am interested in the effect of changing D_m on $\Delta\Psi_{vb-e}$ from vascular bundle to epidermis as g_{wv} increases. Using this approach, the advantage of decreasing D_m as g_{wv} increases is apparent (Figure 2.7), as the relative change in $\Delta\Psi_{vb-e}$ was 63% less at the leaf tip than if there was no acropetal change in D_m . This suggests that the structural change in grass leaves minimizes the water potential gradients across the leaf mesophyll as g_{wv} increases. The hydraulic conductance through both xylem and mesophyll (K_{leaf}) has been shown to decrease acropetally in tobacco leaves (Nardini *et al.* 2008) and was inversely related to g_{wv} . Nardini *et al.* (2008) suggest that g_{wv} would increase as K_{leaf}

decreased to maintain a constant Ψ_{leaf} , as no significant difference in Ψ_{leaf} were identified between basal and apical leaf sections in their study. While it is unlikely that Ψ_{leaf} remained constant along grass blades in this study due to the need for a water potential gradient to exist to move water from the base to tip (Zwieniecki *et al.* 2004), g_{wv} may still be increasing to minimize changes in leaf water status as K_{leaf} decreases along grass blades.

Conclusions

Our results highlight the tight correlation between the structure and function within individual grass blades. The increasing rates of photosynthesis along grass blades demand greater g_{wv} in order to maintain c_i values at an optimum level. Decreases in the extra-xylery pathway to water movement should allow greater movement of water without increasing water potential gradients from vascular bundles to the site of evaporation. This coupling of structure and function allow the often long, narrow leaves of monocots to maximize resources while minimizing pressure gradients along the blades.

Acknowledgements

I greatly appreciate the technical assistance of Whitley Jackson and Johanna Burniston; the expertise of Dr. Dan Boyle in helping in florescence microscope imaging; and Dr. Kendra McLauchlan for the use of laboratory facilities. The Kansas Technology Enterprise Corporation and the Konza Prairie LTER (DEB-0823341) provided financial support.

Literature Cited

- Affek H., Krisch M., and Yakir D. 2006. Effects of intraleaf variations in carbonic anhydrase activity and gas exchange on leaf $C^{18}O$ isoflux in *Zea mays*. *New Phytologist* 169, 321-329.
- Brodribb T.J., Holbrook N.M., and Gutierrez M.V. 2002. Hydraulic and photosynthetic coordination in seasonally dry tropical forest trees. *Plant, Cell and Environment* 25, 1435-1444.
- Brodribb T.J., Holbrook N.M., Zwieniecki M.A., and Palma B. 2005. Leaf hydraulic capacity in ferns, conifers and angiosperms: Impacts on photosynthetic maxima. *New Phytologist* 165, 839-846.

- Brodrigg T.J., Feild T.S., and Jordan G.J. 2007. Leaf maximum photosynthetic rate and venation are linked by hydraulics. *Plant Physiology* 144, 1890-1898.
- Buckley T.N., and Mott K.A. 2000. Stomatal responses to non-local changes in PFD: evidence for long-distance hydraulic interactions. *Plant, Cell and Environment* 23, 301- 309.
- Buckley T., Farquhar G., and Mott K. 1999. Carbon-water balance and patchy stomatal conductance. *Oecologia* 118, 132-143.
- Cernusak L.A., and Marshall J.D. 2001. Responses of foliar ¹³C, gas exchange and leaf morphology to reduced hydraulic conductivity in *Pinus monticola* branches. *Tree Physiology* 21, 1215-1222.
- Cochard H., Nardini A., and Coll L. 2004. Hydraulic architecture of leaf blades: where is the main resistance? *Plant, Cell and Environment* 27, 1257-1267.
- Colbert J., and Evert R. 1982. Leaf vasculature in sugarcane (*Saccharum-officinarum* L.). *Planta* 156, 136-151.
- Dannenhoffer J., Ebert W., and Evert R. 1990. Leaf vasculature in barley, *Hordeum vulgare* (Poaceae). *American Journal of Botany* 77, 636-652.
- Helliker B.R., and Ehleringer J.R. 2000. Establishing a grassland signature in veins: O-18 in the leaf water of C-3 and C-4 grasses. *Proceedings of the National Academy of Sciences of the United States of America* 97, 7894-7898.
- Long S., Bolharnordenkamp H., Croft S., Farage P., Lechner E., and Nugawela A. 1989. Analysis of spatial variation in CO₂ uptake within the intact leaf and its significance in interpreting the effects of environmental-stress on photosynthesis. *Philosophical Transactions of the Royal Society of London Series B-Biological Sciences* 323, 385-395.
- Marenco R.A., Siebke K., Farquhar G.D., and Ball M.C. 2006. Hydraulically based stomatal oscillations and stomatal patchiness in *Gossypium hirsutum*. *Functional Plant Biology* 33, 1103-1113.
- Martre P., Durand J.L., and Cochard H. 2000. Changes in axial hydraulic conductivity along elongating leaf blades in relation to xylem maturation in tall fescue. *New Phytologist* 146, 235-247.
- Martre P., and Durand J.L. 2001. Quantitative analysis of vasculature in the leaves of *Festuca arundinacea* (Poaceae): Implications for axial water transport. *International Journal of Plant Sciences* 162, 755-766.
- Martre P., Cochard H., and Durand J.L. 2001. Hydraulic architecture and water flow in growing grass tillers (*Festuca arundinacea* Schreb.). *Plant, Cell and Environment* 24, 65-76.

- Meinzer F.C., and Saliendra N.Z. 1997. Spatial patterns of carbon isotope discrimination and allocation of photosynthetic activity in sugarcane leaves. *Australian Journal of Plant Physiology* 24, 769-775.
- Meinzer F.C. 2002. Co-ordination of vapour and liquid phase water transport properties in plants. *Plant, Cell and Environment* 25, 265-274.
- Miranda V., Baker N., and Long S. 1981a. Limitations of photosynthesis in different regions of the *Zea mays* leaf. *New Phytologist* 89, 179-190.
- Miranda V., Baker N., and Long S. 1981b. Anatomical variation along the length of the *Zea mays* leaf in relation to photosynthesis. *New Phytologist* 88, 595-605.
- Mott K.A., and Buckley N. 1998. Stomatal heterogeneity. *Journal of Experimental Botany* 49, 407-417.
- Mott K.A. 2007. Leaf hydraulic conductivity and stomatal responses to humidity in amphistomatous leaves. *Plant, Cell and Environment* 30, 1444-1449.
- Nardini A., Gortan E., Ramani M., and Salleo S. 2008. Heterogeneity of gas exchange rates over the leaf surface in tobacco: an effect of hydraulic architecture? *Plant, Cell and Environment* 31, 804-812.
- Ogee J., Cuntz M., Peylin P., and Bariac T. 2007. Non-steady-state, non-uniform transpiration rate and leaf anatomy effects on the progressive stable isotope enrichment of leaf water along monocot leaves. *Plant, Cell and Environment* 30, 367-387.
- Pickard W.F. 1981. How does the shape of the substomatal chamber affect transpirational water loss? *Mathematical Biosciences* 56, 111-127.
- Pinheiro J., Bates D., DebRoy S., Sarkar D., and the R Core team (2008). nlme: Linear and Nonlinear Mixed Effects Models. R package version 3.1-90.
- R Development Core Team, 2008. R: A language and environment for statistical computing. R Foundation for Statistical Computing, Vienna, Austria. ISBN 3-900051-07-0, URL <http://www.R-project.org>.
- Rasband W.S., ImageJ, U. S. National Institutes of Health, Bethesda, Maryland, USA, URL <http://imagej.nih.gov/ij/>, 1997-2011.
- Russell S., and Evert R. 1985. Leaf Vasculature in *Zea mays* L. *Planta* 164, 448-458.
- Ruzin S.E. 1999. *Plant Microtechnique and Microscopy*, Oxford University Press, USA.
- Sack L., Cowan P.D., Jaikumar N., and Holbrook N.M. 2003. The 'hydrology' of leaves: co-ordination of structure and function in temperature woody species. *Plant, Cell and Environment* 26, 1343-1356.

- Sack L., and Frole K. 2006. Leaf structural diversity is related to hydraulic capacity in tropical rain forest trees. *Ecology* 87, 483-491.
- Sperry J., Donnelly J., and Tyree M. 1988. A method for measuring hydraulic conductivity and embolism in xylem. *Plant, Cell and Environment* 11, 35-40.
- West G.B., Brown J.H., and Enquist B.J. 1999. A general model for the structure and allometry of plant vascular systems. *Nature* 400, 664-667.
- Westgate M.E., and Steudle E. 1985. Water transport in the midrib tissue of maize leaves: direct measurement of the propagation of changes in cell turgor across a plant tissue. *Plant Physiology* 78, 183.
- Ye Q., Holbrook N.M., and Zwieniecki M.A. 2008. Cell-to-cell pathway dominates xylem-epidermis hydraulic connection in *Tradescantia fluminensis* (Vell. Conc.) leaves. *Planta* 227, 1311-1319.
- Zwieniecki M.A., Melcher P.J., Boyce C.K., Sack L., and Holbrook N.M. 2002. Hydraulic architecture of leaf venation in *Laurus nobilis* L. *Plant, Cell and Environment* 25, 1445-1450.

Tables and Figures

Table 2.1 Leaf characteristics for the 5 species used in this study. Mean (sd) values for 5 replicates are shown for grass blade length and the blade width at 50% of the blade length.

Species	Blade Length (cm)	Blade Width (cm)
<i>Ange</i> (<i>Andropogon gerardii</i> Vitman, C ₄ NADP-ME)	30.8 (3.4)	0.57 (0.14)
<i>Scsc</i> (<i>Schizachyrium scoparium</i> Nash, C ₄ NADP-ME)	27.0 (2.9)	0.43 (0.74)
<i>Sonu</i> (<i>Sorghastrum nutans</i> Nash, C ₄ NADP-ME)	38.8 (3.1)	0.95 (0.18)
<i>Elca</i> (<i>Elymus canadensis</i> L., C ₃)	35.3 (5.1)	0.87 (0.29)
<i>Brin</i> (<i>Bromus inermis</i> Leyss, C ₃)	27.2 (2.4)	0.64 (0.14)

Table 2.2 Relationship between leaf position and anatomical characteristics within grass leaves. Mean \pm SD values of each leaf segments for all species are reported. Large interspecies differences were still apparent despite the acropetal variability that was the focus of this study. The slope and p-value of the regression between the anatomical variable and leaf position are also shown. The slope of leaf position and inter-veinal distance is the most consistently significant relationship.

Species	Stomatal Density [mm ⁻²]			Guard Cell Length [μ m]			Stomatal Pore Index			Interveinal distance [mm]		
	Mean	Slope	p-value	Mean	Slope	p-value	Mean	Slope	p-value	Mean	Slope	p-value
<i>Ange</i>	170.3 \pm 52.1 ^a	0.06	0.57	16.67 \pm 0.87 ^a	-10.86	0.19	0.044 \pm 0.004 ^a	0.0000	0.94	0.11 \pm 0.02 ^a	-0.0003	<0.001
<i>Scsc</i>	143.8 \pm 33.14 ^a	0.12	0.59	17.48 \pm 1.09 ^a	0.46	0.95	0.043 \pm 0.009 ^a	0.0002	0.44	0.22 \pm 0.04 ^b	-0.0008	<0.01
<i>Sonu</i>	234.9 \pm 49.27 ^a	0.00	0.44	15.62 \pm 1.36 ^a	4.44	0.32	0.056 \pm 0.011 ^a	0.0000	0.99	0.11 \pm 0.01 ^a	-0.0003	0.02
<i>Elca</i>	58.6 \pm 8.08 ^b	0.54	0.49	61.67 \pm 5.40 ^b	2.31	0.04	0.224 \pm 0.048 ^b	0.0014	0.19	0.30 \pm 0.05 ^c	-0.0014	<0.01
<i>Brin</i>	49.8 \pm 6.59 ^b	0.60	0.48	62.19 \pm 3.53 ^b	2.34	0.13	0.193 \pm 0.032 ^c	0.0014	0.12	0.24 \pm 0.03 ^b	-0.0011	<0.01

Figure 2.1 Cross section of an *Elymus canadensis* blade double stained with Safranin-O and Fast Green taken on a light microscope at 40X magnification. Key anatomical characteristics are labeled as well as the measurements used to calculate D_m (Eqn. 2.1). D_v was measured from the top of the vascular bundle to the outer edge of the epidermis, and D_h was measured as the transverse distance from the edge of the vascular bundle to the center of the stomatal pore.

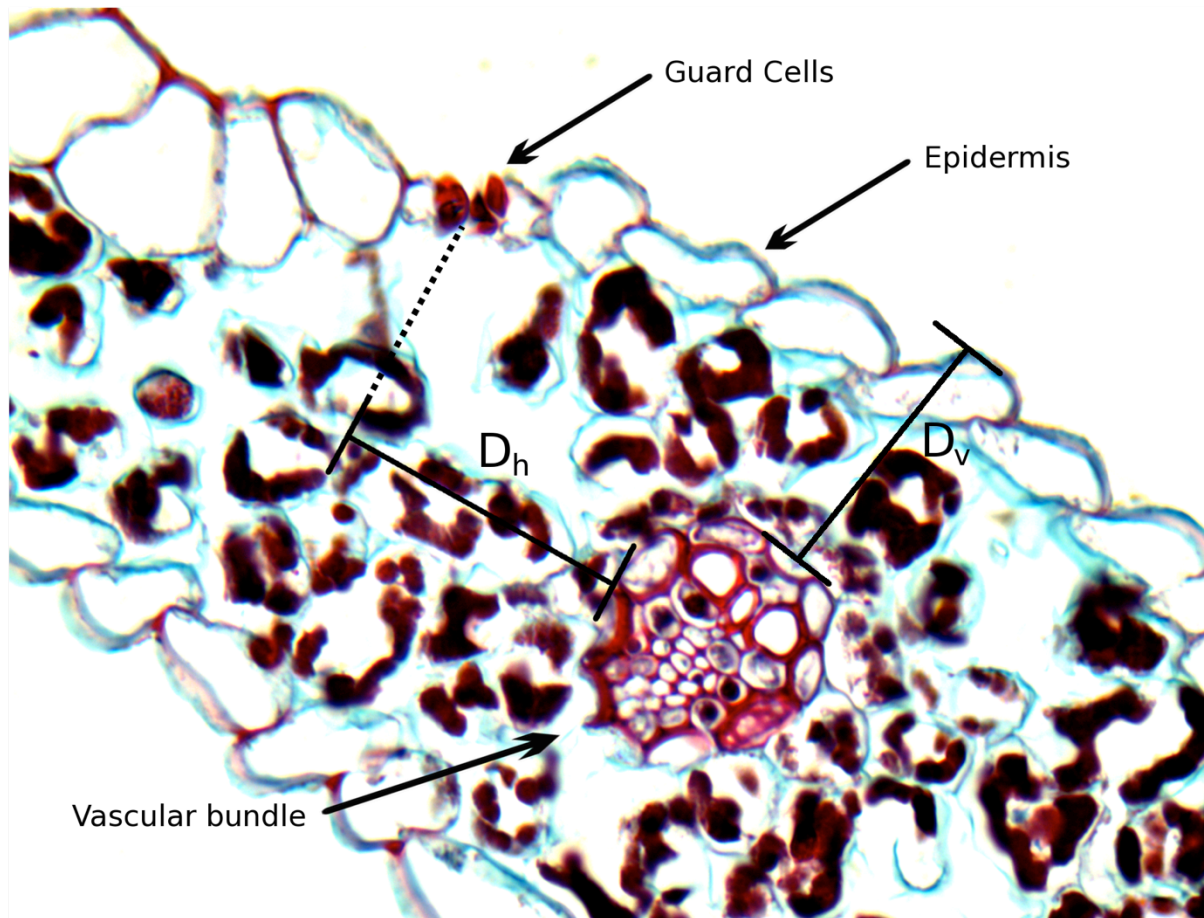


Figure 2.2 Relationship between stomatal conductance (g_{wv} , panels A and B), leaf temperature (T_{Leaf} , panels C and D) and leaf blade position, reported as the percentage of leaf length measured from the ligule. Black symbols are measurements made on leaf sections with an angle $>0^\circ$ from horizontal, red symbols are measurements made where the leaf tip was drooping and leaf angle was $<0^\circ$ from horizontal. g_{wv} increased acropetally for all species when leaf angle was $>0^\circ$.

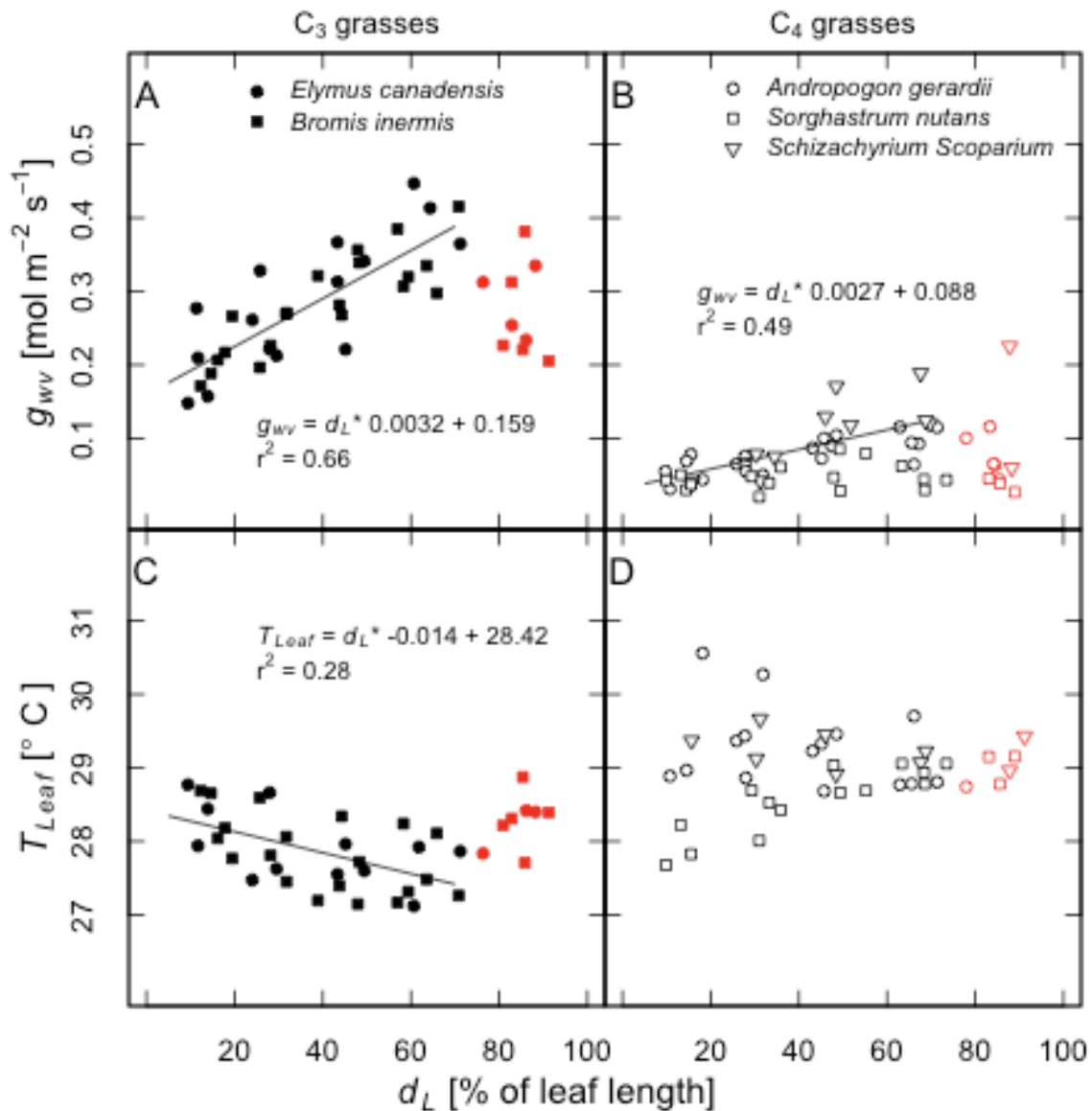


Figure 2.3 Relationship between Transpiration (E , panels A and B), Photosynthetic rate (A , panels C and D) and leaf blade position reported as the percentage of leaf length measured from the ligule. Black symbols are measurements made on leaf sections with an angle $>0^\circ$ from horizontal, red symbols are measurements made where the leaf tip was drooping and leaf angle was $<0^\circ$ from horizontal. Data represented by the red symbols were not included in the regression analyses.

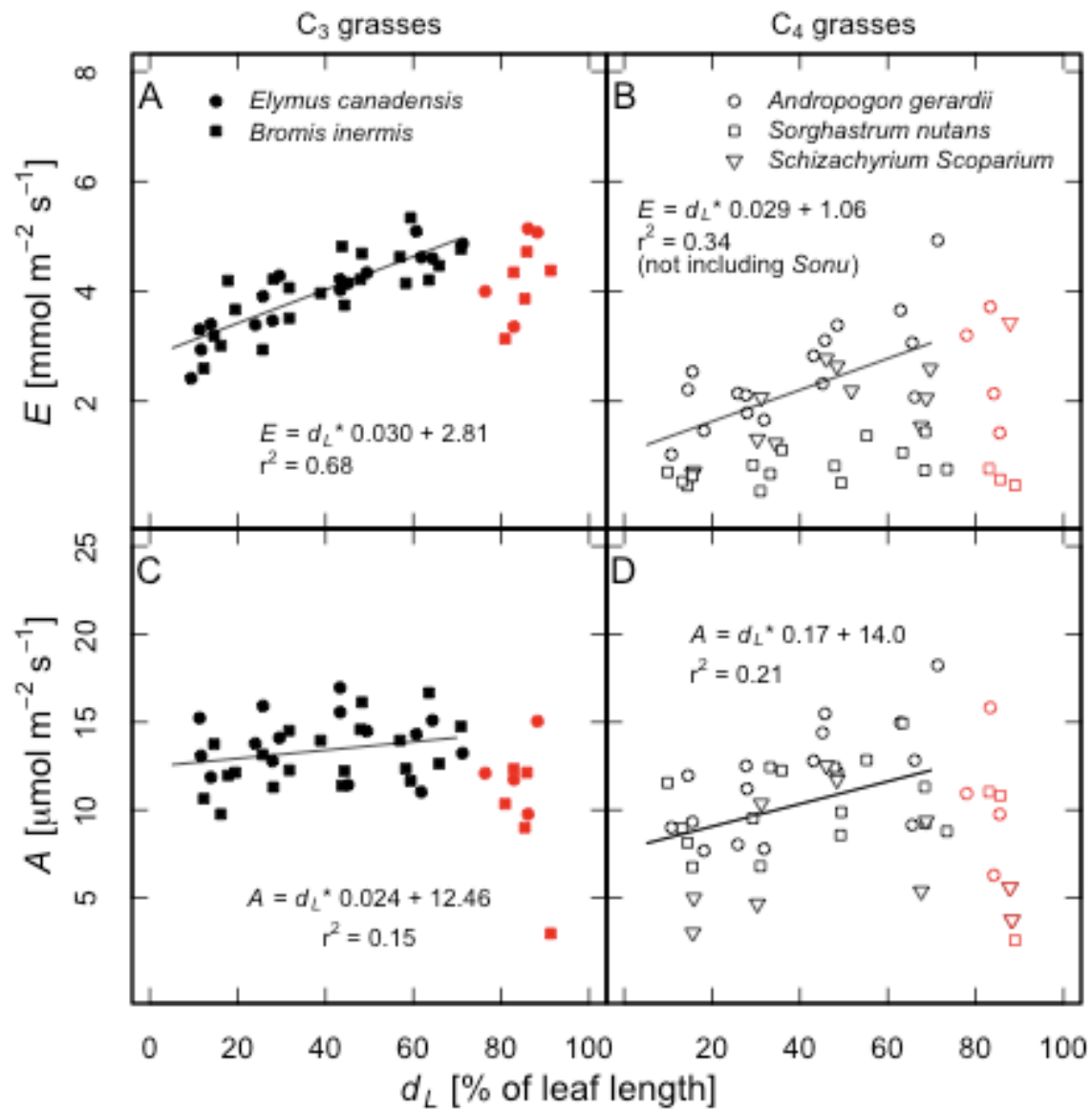


Figure 2.4 Leaf specific hydraulic conductivity (K_{x^*leaf}) as a function of leaf blade position. K_{x^*leaf} remained relatively constant for all species measured as the linear regression between K_{x^*leaf} and leaf position was not significant at the $p < 0.05$ level within a functional group or for any individual species. When K_{x^*leaf} of all leaf segments were pooled, *Sonu* (*Sorghastrum nutans* Nash) had the highest K_{x^*leaf} (1.19) followed by *Ange* (*Andropogon gerardii* Vitman; 0.90) and no significant differences between the other species.

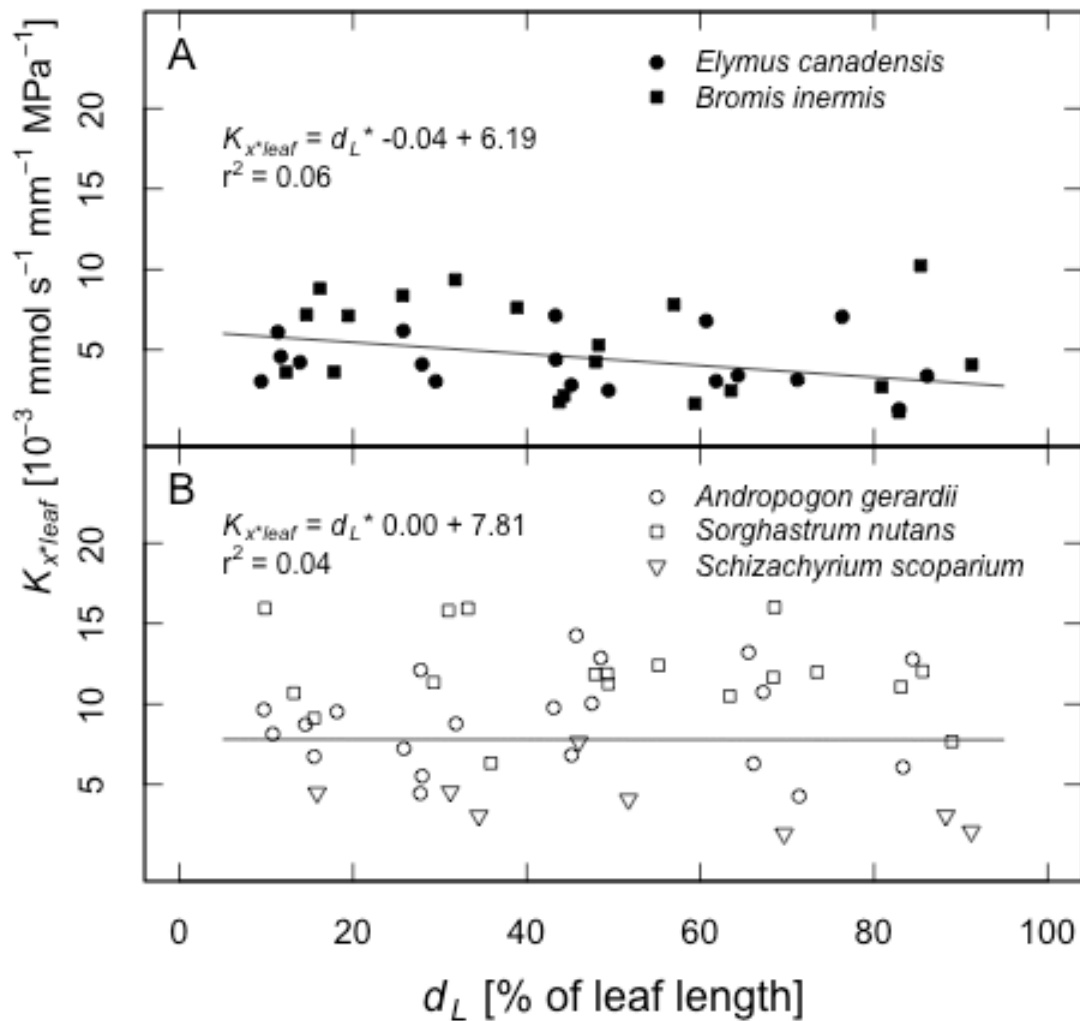


Figure 2.5 Changes in structural characteristics along grass blades. Inter-veinal distance (panels A and B) and diffusional path from vascular bundle to stomatal pore (D_m , panels C and D) decreased acropetally for all species in this study. *Ange* (*Andropogon gerardii* Vitman) and *Sonu* (*Sorghastrum nutans* Nash) had the smallest change along their blades compared to the other species measured.

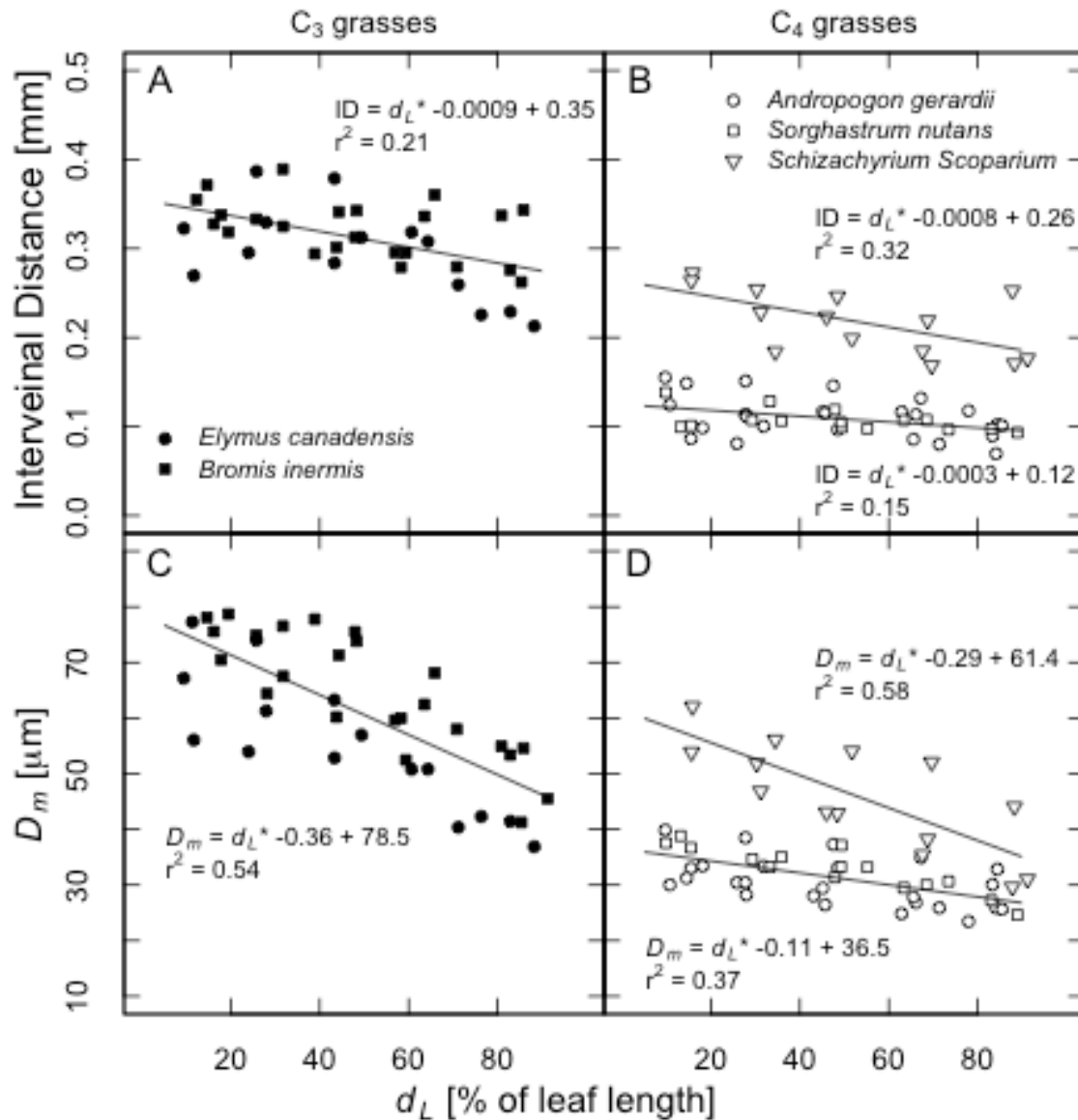


Figure 2.6 Structure-function relationship within grass leaves. D_m is the distance of the diffusional path from vascular bundle to stomatal pore within grass blades. For well-watered plants, g_{wv} is closely related to D_m within individual leaf blades. Analysis was performed using mixed-effects modeling and were significant at the $p < 0.001$ level for pooled C_3 species and *Scsc* (*Schizachyrium scoparium* Nash), but only significant at the $p < 0.1$ level for *Ange* (*Andropogon gerardii* Vitman) and *Sonu* (*Sorghastrum nutans* Nash).

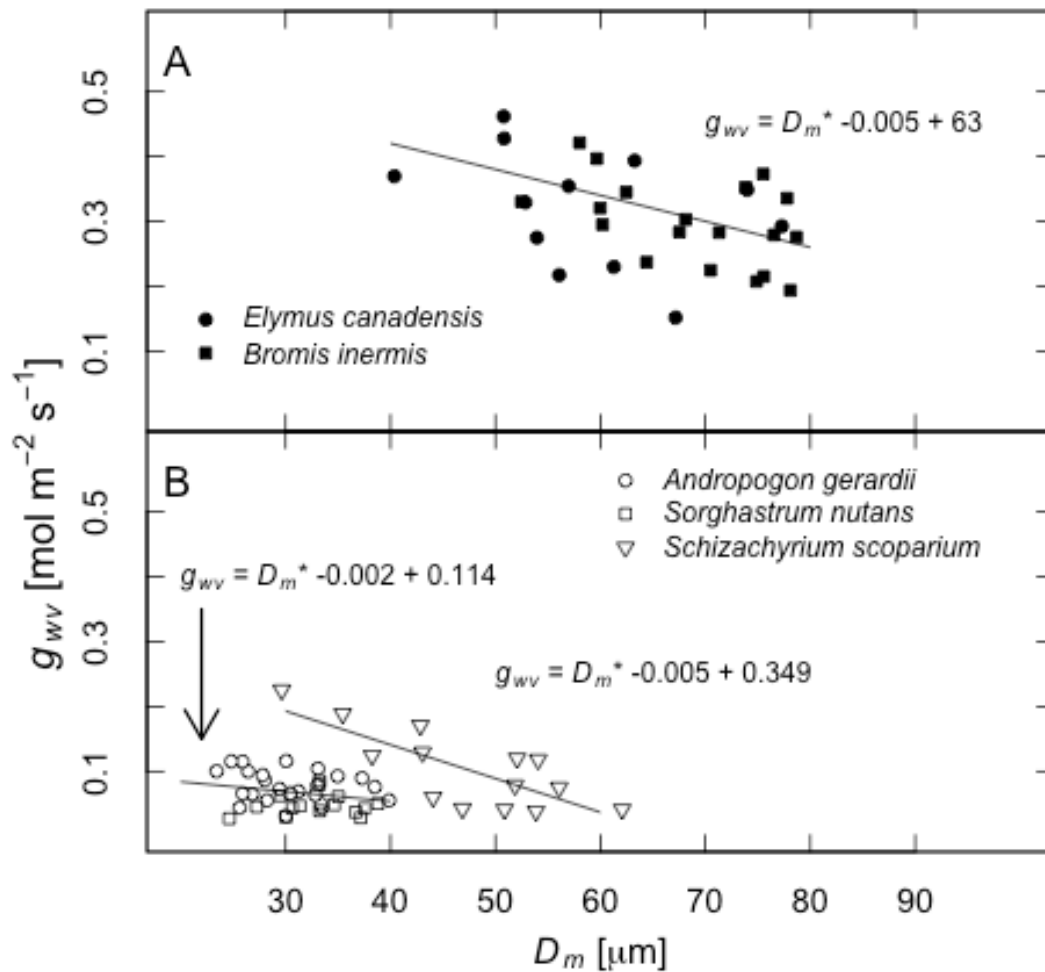
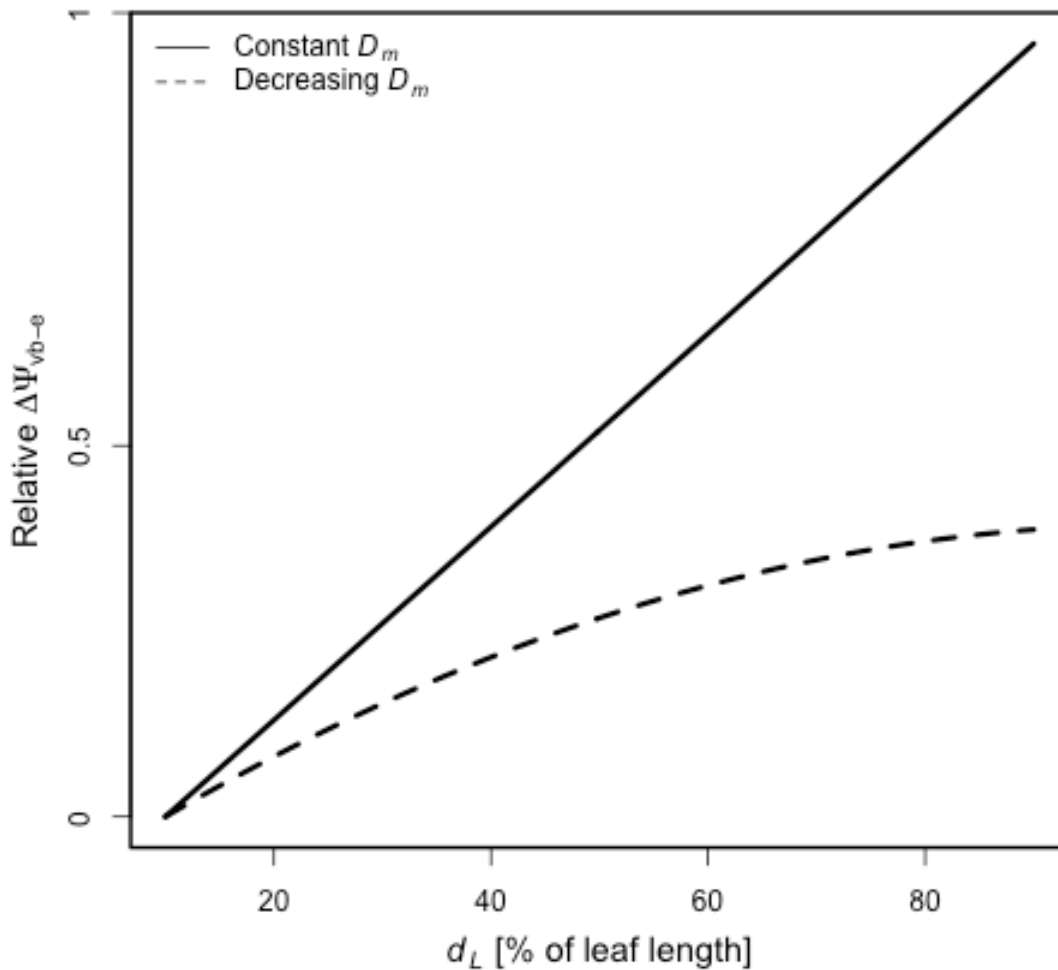


Figure 2.7 The modeled change in water potential gradient between the vascular bundle to epidermis ($\Delta\Psi_{vb-e}$) for a C_3 grass blade. The solid line represents the increase in $\Delta\Psi_{vb-e}$ assuming no acropetal change in D_m . When D_m decreased, as observed for C_3 grass blades in this study, the increase in $\Delta\Psi_{vb-e}$ was 63% less than when D_m remained constant along the blade.



Chapter 3 - Partitioning hydraulic resistances in grass leaves reveals unique correlations with stomatal conductance during drought

Abstract

The hydraulic resistance of leaves plays an important role in plant responses to drought by minimizing the pressure gradient from soil to leaf and by maintaining the integrity of the water column. I partitioned the hydraulic resistance in leaves of six genotypes of *Sorghum bicolor* L. (Moench) into two possible components: the hydraulic resistance within the xylem (r_x) and outside the xylem (r_{ox}). I then compared stomatal (g_s) conductance and photosynthesis (A) responses to drought in relation to the different components of leaf resistance. In four of the six genotypes the greatest resistance to water movement was outside the xylem. I found g_s under well-watered conditions had the strongest statistical correlation with r_{ox} ($r^2 = 0.63$), but as soil moisture became limiting, g_s was predicted better by r_x ($r^2 = 0.83$). I interpret these results to suggest that r_{ox} limits maximum rates of gas exchange, but as soil moisture becomes limiting to growth, the ability to efficiently move water from the soil to leaves (low r_x) becomes more important for the maintenance of cell turgor and gas exchange in leaves. Furthermore, high r_{ox} resulted in lower rates of A when soil moisture was readily available but did not decrease much in response to drought. In contrast, low r_{ox} correlated to high initial rates of photosynthesis but rates of gas exchange declined quickly during the drought for these genotypes. The genotype with high r_{ox} achieved greater final aboveground biomass ($p < 0.05$) despite lower initial rates of A . These results illustrate the key role of leaf resistance compartmentalization as a drought response strategy in a common, broadly-adapted cereal crop species.

Introduction

Leaf hydraulics provide an important constraint on whole plant gas exchange, as the major resistance to the movement of water can occur in the last few μm of water's path through plants from roots to atmosphere (Brodribb *et al.* 2007). Resistances in the leaf can be divided into two broad categories; axial resistance within the xylem (r_x), and resistance outside the xylem (r_{ox}) as water moves from the vascular bundle through the leaf mesophyll. The relative proportion of these two resistances in leaves remains inconclusive; measurements partitioning these two resistances have found that r_{ox} is 26-80% of total leaf resistance (Martre, Cochard, and Durand 2001, Zwieniecki *et al.* 2002, Sack, Streeter, and Holbrook. 2004, Cochard, Nardini and Coll 2004, Nardini and Salleo 2005). Across a range of species, r_{ox} and r_x have been linked to maximum rates of gas exchange (Sack *et al.* 2005, Sack and Frole 2006, Brodribb *et al.* 2007) but the functional significance of changes in the relative proportions of these two resistances has yet to be explored.

To better understand the significance of varying leaf resistances, the hydraulic architecture of plants has been studied across broad climatic gradients. Low resistance to water movement through the plant stem (low r_x) is correlated with high stomatal conductance in a broad range of plant species (Meinzer and Grantz 1990, Saliendra, Sperry and Comstock 1995, Hubbard *et al.* 2001), but is typically negatively correlated with drought tolerance as there is a trade-off between hydraulic safety and efficiency (Tyree and Zimmerman 2002). In xeric systems, the ability to withstand cavitation is important in maintaining plant growth and provides a competitive advantage when soil moisture is limited. The hydraulic architecture of leaves is also important in plant function and often represents the greatest resistance to water movement within plants (Nardini and Salleo 2000). The hydraulic resistance of the whole leaf is directly correlated with maximum photosynthesis and g_s (Brodribb *et al.* 2007) and responds to changes in leaf hydration status (Nardini, Salleo and Raimondo 2003, Kim and Steudle 2007, Heinen, Ye and Chaumont 2009). To our knowledge, the role of these two leaf resistances in regulating stomatal responses to decreasing soil moisture has not been investigated. Grasses offer an interesting perspective on the hydraulic pathway because the majority of the aboveground

pathway for water movement occurs in leaves, and therefore, understanding leaf resistance to water movement is vital to understanding drought responses in this growth form.

The extra-xylery pathway of water movement through leaves can represent up to 80% of the resistance to water movement through plants, even though this segment of water movement may be a small fraction of the total distance travelled (Sack *et al.* 2004). The distance from vascular bundle to stomata has been shown to correlate with stomatal conductance between species (Brodrribb *et al.* 2007) and within individual leaves (Kodama *et al.* 2011, Ocheltree *et al.* 2012) under well-watered conditions, but the only direct comparison of g_s with measurements of r_{ox} found a weak correlation between the two variables (Nardini and Salleo 2000). In this study, r_x was better correlated with g_s , but these results were from a field study and the water status of the plants was not presented. It is still unclear, however, if r_{ox} correlates with g_s when soil water is freely available in plants.

The efficient transport of water through the plant-atmosphere-continuum allows plants to maintain maximum stomatal conductance while minimizing the water potential gradient from the soil matrix to leaf surface (Tyree and Zimmerman 2002), which is described by applying Darcy's law to plants:

$$E = \frac{1}{r_{plant}} * (\Psi_{soil} - \Psi_{leaf}) \quad (\text{Eqn. 3.1})$$

where, E is the transpiration rate, r_{plant} is the hydraulic resistance of the plant, and Ψ_{soil} and Ψ_{leaf} are the water potentials of the soil and leaf, respectively. If two plants that maintained Ψ_{leaf} at the same value were compared, the plant with lower r_{plant} would be able to maintain higher rates of E as the soil dried out (decreasing Ψ_{soil}), assuming the water potential in the xylem remained above the threshold of widespread cavitation. So within some range of soil water potential r_{plant} would confer greater stomatal conductance, but as the soil continues to dry the resistance to cavitation within the leaf xylem would become more important in controlling stomatal conductance (Blackman, Brodrribb and Jordan 2010). These studies demonstrate the importance of maximum hydraulic conductivity within the xylem of leaves for the maintenance of leaf-level gas exchange.

Both r_{ox} and r_x correlate with maximum rates of gas exchange under well-watered conditions across a range of species, but how does the relative proportion of these

resistances within leaves affect plant performance as soils dry? The objective of this study was to investigate how the partitioning of hydraulic resistance between xylery and extra-xylery tissue in leaves related to temporal patterns of stomatal conductance as soil moisture declined. I hypothesize that: 1) maximum rates of gas exchange will be correlated with r_{ox} under well-watered conditions, but 2) as water becomes limiting to plant growth, rates of gas exchange will be correlated with r_x , to minimize the water potential gradient from soil to leaf. As such, individuals with high r_{plant} within the xylem will be able to maintain higher rates of gas exchange. Furthermore, I hypothesize that the plants with greater r_{ox} will have lower initial growth rates but will maintain these rates further into the drought.

Materials and Methods

Plant Material

Six genotypes of *Sorghum bicolor* L. (Moench) were selected for this study; 3 strains being developed (SC1019, SC1205, and SC15) and 3 inbred lines (TX-7078, BTx7078 and B35). The study was divided into two sections to allow for a thorough characterization of both leaf hydraulic resistances and response of gas exchange to drought. The first component of the study was to determine the Hydraulic Architecture (HA) of the leaves and the second component was a Drought Response experiment (DR). In both studies 2 seeds were planted in 20 L pots filled with ~ (Metro-Mix 360, Sun-Gro Horticulture Canada Ltd., Vancouver, British Columbia, Canada) soil, supplied with controlled-release fertilizer (Scotts-Sierra Horticultural Products Co., Marysville, Ohio, USA) and watered daily. Plants were thinned to one individual per pot after germination. For the HA experiment, 2 replicates of each genotype were planted each week so that plants would develop in stages to allow sampling of replicates at the same developmental stage. Plants were grown in a greenhouse where maximum daily PAR was between 800-1200 $\mu\text{mol m}^{-2} \text{s}^{-1}$ and daily temperatures were maintained between 22-26°C. For the HA experiment all measurements were made on the 5th or 6th leaf of each plant. For the DR experiment 8 replicates of each genotype were planted at the same time and grown under well-watered

conditions until the 5th leaf had fully expanded and then water was withheld to initiate the drought treatment.

Hydraulic Conductivity

Hydraulic resistance was measured using a hydrostatic gradient to force water through the sample (Sperry, Donnelly and Tyree 1988) with a custom chamber designed for large grass leaves. The chamber was constructed to accommodate the large leaves of sorghum, which allowed me to quantify both axial resistance within the xylem (r_x), and extra-xylery resistance as water moved from the vascular bundle through the leaf mesophyll (r_{ox}). The hydraulic chamber consisted of two compartments; 1) a small compartment where the basal cut section of the leaf would be placed and water forced into the leaf, and 2) a collection compartment where water flowing through the uncut leaf surface (for measurement of r_{leaf}) or the cut leaf surface (for determination of r_x) was collected and diverted to a balance through 3.2 mm ID tubing (Bev-a-Line). Pressure transducers (model 68075, Cole-Parmer Instrument Company, Vernon Hills, Illinois, USA) were placed on both inlet and outlet tubing to measure the pressure gradient across the leaf and a thermocouple measured water temperature in the collection compartment. Pressure of the inlet water was maintained at ~20 kPa during measurements and water passing through the leaf was collected on a balance (± 0.0001 g, Pioneer PA214, Ohaus Corporation, Pine Brook, New Jersey, USA) connected to a datalogger (CR1000, Campbell Scientific, Inc., Logan, Utah, USA) to monitor the rate of water flow through the systems at 1s intervals. The background flow was determined by equilibrating the pressure on each side of the leaf so that no pressure gradient existed across the leaf segment and the flow was measured for 5 min. This was performed before and after each measurement, and the average of the two measurements was subtracted from pressurized flow and the result divided by the pressure gradient to yield hydraulic resistance ($\text{MPa mmol}^{-1} \text{ s}$).

Plants were watered to pot-holding capacity and placed in a dark chamber overnight prior to hydraulic measurements to force stomatal closure and allow the plants to fully hydrate so no vessels would be embolized. The most recently matured leaf (5th or 6th leaf) was cut from the plant under water and placed in the chamber for hydraulic conductivity. Each leaf was placed in the chamber so the longitudinal mid-point of the leaf

was centered in the collection compartment of the hydraulic chamber to minimize any systematic bias of leaf position between measurements. To determine r_{leaf} the basal portion of the leaf was re-cut with a razorblade and immediately sealed in the pressurized compartment of the chamber. The distal portion of the leaf was left intact and $\sim 50 \text{ cm}^2$ of leaf area placed in the collection compartment, but also extended beyond it, and was connected to a reservoir on the balance. In this way, water flowed through the basal end of the leaf and exited through the stomata into the collection chamber allowing quantification of total leaf hydraulic resistance (r_{leaf} , $\text{MPa mmol}^{-1} \text{ s}$). The collection compartment was illuminated at $2000 \mu\text{mol m}^{-2} \text{ s}^{-1}$ PAR to using a fiber-optic light source (FL-150, Meiji Techno Company, Saitama, Japan). Light intensity incident on the leaf surface was estimated by using a PAR sensor (Li-190, Li-Cor, Inc., Lincoln, Nebraska, USA) sealed in an acrylic chamber (similar to the hydraulic chamber) submerged under water at the same level as the leaf.

Following measurement of r_{leaf} the collection compartment was opened and a transverse cut was made across the leaf to remove most of the leaf area and exposed the xylem for determination of axial hydraulic resistance. A fresh transverse cut was also made on the basal end of the leaf and then both chambers were re-sealed. These cuts removed the extra-xylery portion of the leaf from the measurement and now only the axial hydraulic resistance was measured. Flow rate through the xylem proceeded as previously described. Following hydraulic resistance measurements, the leaf area of the entire leaf was measured so that both r_x and r_{ox} could be normalized for leaf area.

I used an electrical analog approach to partition the resistances between r_x and r_{ox} components. I assumed r_{leaf} consisted of two resistances in series, r_x and r_{ox} , which allowed r_{ox} to be calculated based on direct measurements of r_{leaf} and r_x (Eqn. 3.2a). r_{ox} was normalized for the amount of leaf area (LA, m^2) inside the collection chamber (Eqn. 3.2b, $\text{MPa mmol}^{-1} \text{ s m}^2$) and r_x was normalized by the length of the leaf section measured (l_{seg} , m) and the leaf area distal (LA, m^2) to this section (Eqn. 3.2c, $\text{MPa mmol}^{-1} \text{ s m}$).

$$r_{ox} = r_{leaf} - r_x \quad \text{Eqn. 3.2a}$$

$$r_{ox*LA} = \frac{r_{ox}}{LA} \quad \text{Eqn. 3.2b}$$

$$r_{x*LA} = \frac{r_x}{LA * l_{seg}} \quad \text{Eqn. 3.2c}$$

Gas Exchange

Gas exchange measurements for the DR experiment were made on the second set of plants during a simulated drought. After plants had 5 mature leaves, water was completely withheld to simulate drought. Gas exchange rates were measured (Li-6400 Li-Cor, Inc., Lincoln, NE, 68504) on the center of the leaf, as rates of gas exchange vary with leaf position in grass leaves (Ocheltree *et al.* 2012). All measurements were made between 11 AM and 3 PM with clear skies to maximize light availability in the greenhouse to best estimate maximum rates of gas exchange for that day. Measurements were repeated every 3-4 days to capture the response of leaf-level gas exchange rates to drying soils. Prior to gas exchange measurements the weight of each potted plant was measured (± 50 g, model CTB-600, Citizen Scales, Mumbai, India).

Biomass Production

After the drought experiment was complete, plants were harvested and divided into above and belowground components. Soil was washed from the roots with a low-pressure spray nozzle and the dislodged soil was collected in a large bucket to sit overnight to allow the soil to separate gravimetrically. After ~ 24 hours the majority of water was siphoned off the top and the soil was dried at 60°C in a shallow pan for 7 days to measure dry soil weight (± 0.01 g, Pioneer PA3102, Ohaus Corporation, Pine Brook, New Jersey, USA). Several soil samples were weighed everyday during the drying process and it was determined that the soils were $>99\%$ dry by the end of 7 days; all subsequent soil samples were dried and weighed at the end of 7 days. Above- and belowground plant biomass was dried at 60°C for 48 hours and then weighed (± 0.0001 g, Pioneer PA214, Ohaus Corporation, Pine Brook, New Jersey, USA). Soil Water Content (SWC_{mass}) was determined on a mass basis from the measurements of the potted plants during the experiment and the dry soil;

$$\text{SWC}_{\text{mass}} = \frac{w_{\text{wet}} - w_{\text{dry}}}{w_{\text{wet}}} \quad \text{Eqn. 3.3}$$

where, w_{wet} (kg) is the weight of the potted plant at during the experiment and w_{dry} (kg) is the weight of the dry soil. The weight of the plant was included in the measurement

of w_{wet} , and so changes in SWC_{mass} based on our measurements would reflect changes in both soil moisture content and relative water content of the plant tissue. The plant weight was small in comparison to the total pot weight throughout the study and so changes in SWC_{mass} based on Eqn. 3 were mainly driven by changes in soil moisture.

Leaf Water Potential

Leaf water potential (Ψ_{leaf}) measured throughout the drought experiment. All water potential measurements were made using thermocouple psychrometers (70 series, JRD Merrill, Logan, Utah, USA) attached to a CR7 datalogger (Campbell Scientific Ltd, Logan, Utah, USA). Leaf water potential measurements were made following gas exchange measurements. A 5mm leaf disc was removed using a disposable biopsy punch (Integra Miltex, York, Pennsylvania, USA) and immediately placed in the psychrometer chamber. All psychrometer chambers were placed in a 25°C water bath to equilibrate for 1 hour before measuring. The measurement of wet-bulb depression was made according to Comstock (2000) and converted to Ψ_{leaf} based on the calibration of NaCl standards measured in the same manner as leaf discs.

All statistical analyses were performed using the R open source statistical software package (R Development Core Team, 2008).

Results

Hydraulic Conductivity

I found significant differences among the six genotypes of *Sorghum bicolor* L. (Moench), in both r_x and r_{ox} (Figure 3.1). r_x ranged from 0.18-0.41 MPa mmol⁻¹ s m across the six genotypes, which highlights the potential variability within a single species. r_{ox} ranged from 0.12-0.45 MPa mmol⁻¹ s m², but there was greater variability within each genotype than for r_x , which is likely because r_{ox} incorporates the uncertainty associated with measurements of both r_{leaf} and r_x (Eqn. 3.2a). The proportion of hydraulic resistance in the xylem was 0.31-0.78 for all genotypes (Figure 3.1C). Four of the genotypes had ~30-40% of total leaf resistance in the xylem, with the remaining resistance being outside the

xylem as water moved from the vascular bundle to the leaf surface. The remaining two genotypes had nearly ~80% of their resistance inside the xylem.

Gas Exchange

Stomatal conductance correlated with different components of leaf hydraulic resistance as soil moisture declined (Figure 3.2). When SWC_{mass} was high (>3.5 kg/kg) stomatal conductance was inversely related to r_{ox} (Figure 3.2A) but not significantly correlated to r_x (Figure 3.2B). As SWC_{mass} decreased to the range of 1.5-3.5 kg/kg, g_s of most species declined and was best correlated with r_x (Figure 3.2D) rather than r_{ox} (Figure 3.2C), although the relationship between r_{ox} and g_s was still significant. When soil moisture dropped below 1.5 kg/kg, there was no correlation between either r_{ox} or r_x (Figure 3.2C and 3.2F) as there was very little variability in g_s at this level of soil moisture.

Leaf Water Potential

There was no significant difference in leaf water potential throughout the experiment between the six genotypes (Table 3.1), and the average Ψ_{leaf} was -1.5 MPa for all sampling periods. There were no significant difference between genotypes in Ψ_{leaf} for any of the sampling periods, and there was no significant difference in Ψ_{leaf} between sampling periods within any genotype. This suggests that all genotypes regulated g_s to help maintain Ψ_{leaf} at identical values throughout the experiment.

Biomass Production

Few differences in final biomass production were found between genotypes when grown under drought (Table 3.1). SC15, the genotype with the greatest resistance in the leaves, had the highest aboveground biomass (Figure 3.2). Aboveground biomass in the control treatment showed greater variability but was not correlated to either r_x or r_{ox} (data not shown). Root biomass varied by genotype (Table 3.1) and was correlated with r_{leaf} (Figure 3.3). Plants with greater resistance in their leaves (and lower g_s) had less root biomass (Figure 3.3A) and smaller root:shoot ratios (Figure 3.3B). Major vein density was correlated with r_x (Figure 3.4A) rather than r_{ox} , suggesting the bulk of axial water movement was in this vein order. The distance of water movement from the vascular

bundle to stomata (D_m) was weakly correlated (not significant at $p < 0.05$) with r_{ox} (Figure 3.4B).

The temporal pattern of photosynthesis (A) as soil moisture declined was compared for two genotypes that differed in r_{ox} (Figure 3.5). A cubic spline fit to the g_s data for a genotype with high r_{ox} (genotype SC15) and low r_{ox} (genotype SC1019) were compared and final biomass shown in the inset (Figure 3.5). In the example presented, the genotype with high r_{ox} had lower A early in the drought experiment when soil moisture was readily available and was able to maintain those rates further into the drought. The genotype with low r_{ox} (genotype SC 1019) had higher initial A but declined quickly. For this experiment, the high r_{ox} genotype was able to accumulate greater aboveground biomass by maintaining its maximum A for a longer period of time (Figure 3.5, insert).

Discussion

Here I show significant correlations between the hydraulic architecture of grass blades and the response of leaf-level gas exchange to decreasing soil moisture. To my knowledge, this is the first time that the functional significance of leaf partitioning of hydraulic resistance between xylem and extra-xylery components in relation to drought has been shown. When soil moisture was readily available, the resistance outside the xylem (r_{ox}) was tightly correlated with maximum rates of gas exchange. As soil moisture decreased, the axial resistance within the xylem of grass blades (r_x) became more important in maintaining high rates of gas exchange.

Within a single species I found r_{ox} to vary from 21-69% of total leaf resistance, which spans almost the entire range of previously reported values for a range of woody species (Zwieniecki *et al.* 2002, Cochard *et al.* 2004, Sack *et al.* 2004, Nardini and Salleo 2005, Sack, Tyree and Holbrook 2005). Since these genotypes were developed to maximize grain production in a variety of conditions, these results likely represent a maximum level of plasticity possible for a species. In previous studies, the relative contributions of xylem and extra-xylery resistances to whole leaf hydraulics based on different species and techniques has been debated (Zwieniecki *et al.* 2002, Cochard *et al.* 2004). Using a common technique across six genotypes I found the same range of values,

suggesting that the proportion of these leaf resistances is highly variable and is both species and genotype specific.

In networks where component resistances act in series, such as the leaf venation system studied here, the greatest resistance should limit the rate of water use (Meinzer 2002). Four of the six genotypes I studied had the greatest resistance outside the xylem in their leaves (Figure 3.1C) and consistent with theory, I found the resistance outside the xylem to be tightly correlated with g_s when soil moisture was readily available (Figure 3.2A). This is consistent with previous work that found indirect estimates of r_{ox} to correlate with maximum rates of gas exchange, as the distance from vascular bundle to stomata was correlated with g_s within grass leaves (Ocheltree *et al.* 2012) and between eudicot leaves (Brodribb *et al.* 2007). The results presented here differ from previous results in that I show a link between direct measurements of extra-xylery resistance and maximum g_s . I did not, however, find a correlation between D_m and g_s in this study (Figure 3.5B), but the range of D_m values across the six genotypes of *Sorghum bicolor* L. (Moench) was small (390-480 μm) compared to previous studies ($\sim 100\text{-}1200$ μm , Brodribb *et al.* 2007), so it may be that variability in r_{ox} within a species may be a function of factors other than just D_m . The movement of water from vascular bundle to stomata is likely a combination of symplastic and apoplastic pathways, and as such, differences in r_{ox} between genotypes could result from differences between either of these pathways, such as: differential aquaporin regulation (Fletcher *et al.* 2007), different proportions of symplastic/apoplastic pathways, or membrane composition that differ in their ability to transport water (Canny 1995).

As water becomes limiting to plant growth and plants must reduce g_s in order to maintain cell turgor, the ability to efficiently transport water to leaf cells should be extremely important. According to Eqn. 3.1, at a given water potential gradient ($\Psi_{soil} - \Psi_{leaf}$) the efficiency to move water through the xylem (r_{leaf} in Eqn. 3.1) controls water flux from leaves. Since all of the genotypes I studied maintained Ψ_{leaf} at the same level (Table 3.1) then the hydraulic efficiency of the xylem should control transpiration rates for a given SWC_{mass} . Our data support this idea (Figure 3.2D) as there was a tight correlation between g_s and r_x when soil moisture was limiting that did not exist under well-watered conditions

(Figure 3.2B). These results highlight the importance of axial resistance in the xylem to maintaining rates of gas exchange for growth under moderate water stress.

I found significant correlations between leaf structure and hydraulic resistances within the xylem of the genotypes I studied. Major vein density correlated strongly with r_x across these six genotypes (Figure 3.5A). The dimensions and number of vessel members in the major veins was similar across genotypes (data not shown), so any differences in r_x between genotypes resulted from major vein density (Figure 3.5A). This matches model simulations of leaves, where increasing major vein density led to a linear decrease in xylem resistance (McKown, Cochard, and Sack 2010).

Implications for Plant Strategies

Since the hydraulic resistance of different leaf components affects g_s at different levels of soil moisture, the partitioning of leaf resistances between xylem and extra-xylery components should influence plant responses to drought. Photosynthesis (A) correlated closely with g_s throughout our study ($r^2 = 0.92$, data not shown), so changes in g_s reflect changes in carbon assimilation as soil moisture declined. The response of A for two genotypes on either end of the r_{ox} spectrum were plotted (Figure 3.5); genotype SC15 had high r_{ox} , which correlated with low rates of A compared to genotype SC1019 when soil moisture was readily available. After water was withheld, A quickly declined in SC1019 as soil moisture was quickly depleted as a result of higher rates of g_s early in the drought treatment. Genotype SC15, which had effectively 'conserved' water with its greater resistance to water loss (high r_{ox}), was able to maintain higher rates of A longer into the drought experiment. For the time period of this experiment this strategy led to greater aboveground biomass for SC15 despite its' lower initial rates of gas exchange. Across all six genotypes the root:shoot ratio was significantly correlated with the resistance of leaves (Figure 3.5B). Like SC15, high resistance in the leaf led to less demand for water and so more resources were allocated aboveground. This strategy would only be beneficial if there was no competition for water, as in agricultural mono-cropping systems.

In natural ecosystems it is unclear which strategy would be competitively advantageous for plants; dominant species are often inefficient users of water (Delucia and Schlesinger 1991), so large r_{ox} that limits water use and conserves water may not be a

competitive strategy in many systems. In mesic systems where drought is typically moderate, minimizing r_{ox} and maximizing the efficiency of water transport through the xylem to maintain hydrated cells should be advantageous. And indeed, in many systems the fast growing species often have the highest stem hydraulic conductance (Brodribb and Feild 2000, Markesteijn *et al.* 2011). In xeric systems where competition for water may not be as important as tolerating long periods of drought, conserving water may be advantageous to growth and survival. In addition to conserving water, being able to tolerate low soil moisture and low leaf water potentials will also be more important, which is a result of the characteristics of the individual vessel elements (Wheeler *et al.* 2005, Hacke *et al.* 2006, Blackman *et al.* 2010) and vein density of leaves (Scoffoni *et al.* 2011).

Conclusions

Our results show the correlation between the hydraulic architecture of grass leaves and the response of leaf-level gas exchange to drying soils. High resistance outside the xylem correlates to low rates of gas-exchange when soil moisture is readily available to plants, but these plants conserved water and were able to maintain higher rates of gas exchange at lower levels of soil moisture. Furthermore, the efficient transport of water within the xylem was important to maintaining leaf-level gas exchange under moderate drought. Future work should focus on understanding leaf function under severe drought, and measuring leaf resistance partitioning across a broader range of species. Our results suggest that the partitioning of hydraulic resistance within leaves provides the framework for how plants respond and grow under a range of soil moisture conditions.

Acknowledgements

I would like to thank George Mahama for assistance in setting-up and caring for the plants in this experiment and Jeff Hartman for assistance with hydraulic conductivity measurements. I would also like to thank Dr. Tom Sinclair for discussion and comments that helped improve this manuscript. The Kansas Technology Enterprise Corporation and the Konza Prairie LTER (DEB-0823341) provided financial support.

Literature Cited

- Blackman C.J., Brodribb T.J., and Jordan G.J. 2010. Leaf hydraulic vulnerability is related to conduit dimensions and drought resistance across a diverse range of woody angiosperms. *New Phytologist* 188, 1113-1123.
- Brodribb T.J., and Feild T.S. 2000. Stem hydraulic supply is linked to leaf photosynthetic capacity: evidence from New Caledonian and Tasmanian rainforests. *Plant, Cell and Environment* 23, 1381-1388.
- Brodribb T.J., Field T.S., and Jordan G.J. 2007. Leaf maximum photosynthetic rate and venation are linked by hydraulics. *Plant Physiology* 144, 1890-1898.
- Canny M. 1995. Apoplastic water and solute movement - new rules for an old space. *Annual Review of Plant Physiology and Plant Molecular Biology* 46, 215-236.
- Cochard H., Nardini A., and Coll L. 2004. Hydraulic architecture of leaf blades: where is the main resistance? *Plant, Cell and Environment* 27, 1257-1267.
- Delucia E., and Schlesinger W. 1991. Resource-use efficiency and drought tolerance in adjacent great-basin and sierran plants. *Ecology* 72, 51-58.
- Fletcher A.L., Sinclair T.R., and Allen L.H. 2007. Transpiration responses to vapor pressure deficit in well watered "slow-wilting" and commercial soybean. *Environmental and Experimental Botany* 61, 145-151.
- Hacke U.G., Sperry J.S., Wheeler J.K., and Castro L. 2006. Scaling of angiosperm xylem structure with safety and efficiency. *Tree Physiology* 26, 689-701.
- Heinen R.B., Ye Q., and Chaumont F. 2009. Role of aquaporins in leaf physiology. *Journal of Experimental Botany* 60, 2971-2985.
- Hubbard R.M., Ryan M.G., Stiller V., and Sperry J.S. 2001. Stomatal conductance and photosynthesis vary linearly with plant hydraulic conductance in ponderosa pine. *Plant, Cell and Environment* 24, 113-121.
- Kim Y.X., and Steudle E. 2007. Light and turgor affect the water permeability (aquaporins) of parenchyma cells in the midrib of leaves of *Zea mays*. *Journal of Experimental Botany* 58, 4119-4129.
- Kodama N., Cousins A., Tu K.P., and Barbour M. 2011. Spatial variation in photosynthetic CO₂ carbon and oxygen isotope discrimination along leaves of the monocot triticales (*Triticum × Secale*) relates to mesophyll conductance and the Péclet effect. *Plant, Cell and Environment* 34, 1548-1562.

- Markesteyn L., Poorter H., Paz H., Sack L., and Bongers F. 2011. Ecological differentiation in xylem cavitation resistance is associated with stem and leaf structural traits. *Plant, Cell and Environment* 34, 137-148.
- Martre P, Cochard H., and Durand J.L. 2001. Hydraulic architecture and water flow in growing grass tillers (*Festuca arundinacea* Schreb.). *Plant, Cell and Environment* 24, 65-76.
- McKown AD, Cochard H., and Sack L. 2010. Decoding Leaf Hydraulics with a Spatially Explicit Model: Principles of Venation Architecture and Implications for Its Evolution. *The American Naturalist* 175, 447-460.
- Meinzer F.C., and Grantz D. 1990. Stomatal and hydraulic conductance in growing sugarcane - stomatal adjustment to water transport capacity. *Plant, Cell and Environment* 13, 383-388.
- Meinzer F.C. 2002. Co-ordination of vapour and liquid phase water transport properties in plants. *Plant, Cell and Environment* 25, 265-274.
- Mott K.A. 2007. Leaf hydraulic conductivity and stomatal responses to humidity in amphistomatous leaves. *Plant, Cell and Environment* 30, 1444-1449.
- Nardini A., and Salleo S. 2000. Limitation of stomatal conductance by hydraulic traits: sensing or preventing xylem cavitation? RID C-6525-2009. *Trees-Structure and Function* 15, 14-24.
- Nardini A., and Salleo S. 2005. Water stress-induced modifications of leaf hydraulic architecture in sunflower: co-ordination with gas exchange. *Journal of Experimental Botany* 56, 3093-3101.
- Nardini A., Salleo S., and Raimondo F. 2003. Changes in leaf hydraulic conductance correlate with leaf vein embolism in *Cercis siliquastrum* L. *Trees-Structure and Function* 17, 529-534.
- Ocheltree T.W., Nippert J.B., and Prasad P.V.V. 2012. Changes in stomatal conductance along grass blades reflects changes in leaf structure. *Plant, Cell and Environment*. 35, 1040-1049.
- R Development Core Team. 2008. R: A language and environment for statistical computing. R Foundation for Statistical Computing, Vienna, Austria. ISBN 3-900051-07-0, URL <http://www.R-project.org>.
- Sack L., and Frole K. 2006. Leaf structural diversity is related to hydraulic capacity in tropical rain forest trees. *Ecology* 87, 483-491.
- Sack L., Streeter C.M., and Holbrook N.M. 2004. Hydraulic analysis of water flow through leaves of sugar maple and red oak. *Plant Physiology* 134, 1824-1833.

- Sack L., Tyree M.T., and Holbrook N.M. 2005. Leaf hydraulic architecture correlates with regeneration irradiance in tropical rainforest trees. *New Phytologist* 167, 403-413.
- Saliendra N., Sperry J.S., and Comstock J. 1995. Influence of leaf water status on stomatal response to humidity, hydraulic conductance, and soil drought in *Betula occidentalis*. *Planta* 196, 357-366.
- Scoffoni C., Rawis M., McKown A., Cochard H., and Sack L. 2011. Decline of leaf hydraulic conductance with dehydration: relationship to leaf size and venation architecture. *Plant Physiology* 156, p. 832.
- Sperry J.S., Donnelly J., and Tyree M.T. 1988. A method for measuring hydraulic conductivity and embolism in xylem. *Plant, Cell and Environment* 11, 35-40.
- Tyree M.T., and Zimmerman M.H. 2002. *Xylem Structure and the Ascent of Sap* Second., Berlin: Springer-Verlag.
- Wheeler J.K., Sperry J.S., Hacke U.G., and Hoang N. 2005. Inter-vessel pitting and cavitation in woody Rosaceae and other vesselled plants: a basis for a safety versus efficiency trade-off in xylem transport. *Plant, Cell and Environment* 28, 800-812.
- Zwieniecki M.A., Melcher P.J., Boyce C.K., Sack L., and Holbrook N.M. 2002. Hydraulic architecture of leaf venation in *Laurus nobilis* L. *Plant, Cell and Environment* 25, 1445-1450.

Tables and Figures

Table 3.1 Mean (SE) values for aboveground biomass, root biomass, and Ψ_{leaf} for the six genotypes of *Sorghum bicolor* L. (Moench). Lowercase letters indicate significant differences at the $p < 0.05$ level. Aboveground biomass is shown for a ‘control’ group that was grown under well-watered conditions and the ‘drought’ treatment group. Root biomass and Ψ_{leaf} are shown only for the ‘drought’ treatment group. The p-value for the sampling date in a mixed-effects model is shown for each genotype, indicating that there was no significant difference in Ψ_{leaf} throughout the drought treatment experiment.

Genotype	Aboveground Biomass, Control [g]	Aboveground Biomass, drought [g]	Root Biomass drought [g]	Ψ_{leaf} drought [Mpa]	p-value of sampling date
BTx623	78.4 (5.0) ^a	29.9 (1.6) ^{a,b}	12.2 (0.6) ^a	-1.28 (0.07) ^a	0.37
B35	117.4 (12.0) ^b	28.8 (0.9) ^a	10.9 (0.9) ^{a,b}	-1.43 (0.08) ^a	0.20
SC1019	182.1 (13.3) ^c	30.5(1.5) ^{a,b}	11.8 (0.8) ^a	-1.14 (0.08) ^a	0.10
SC1205	119.6 (10.1) ^b	29.7 (1.3) ^{a,b}	9.4 (0.6) ^b	-1.38 (0.07) ^a	0.11
SC15	71.2 (9.2) ^a	35.5 (1.1) ^b	6.1 (0.5) ^c	-1.15 (0.08) ^a	0.12
Tx7078	76.5 (9.2) ^a	27.4 (1.9) ^a	9.4 (0.5) ^b	-1.36 (0.08) ^a	0.42

Figure 3.1 Hydraulic resistance of different leaf components for six genotypes of *Sorghum bicolor* L. (Moench). Eight replicates of each genotype were measured. The resistance in the xylem (r_x , panel A) and outside the xylem (r_{ox} , panel B) are presented normalized by leaf area. The proportion of leaf resistance in the xylem (panel C) was calculated based on direct measurements of both r_{leaf} and r_x . Lowercase levels indicate significant differences at $p < 0.05$ significance level of pair wise comparisons using a 'Holm' correction for multiple comparisons.

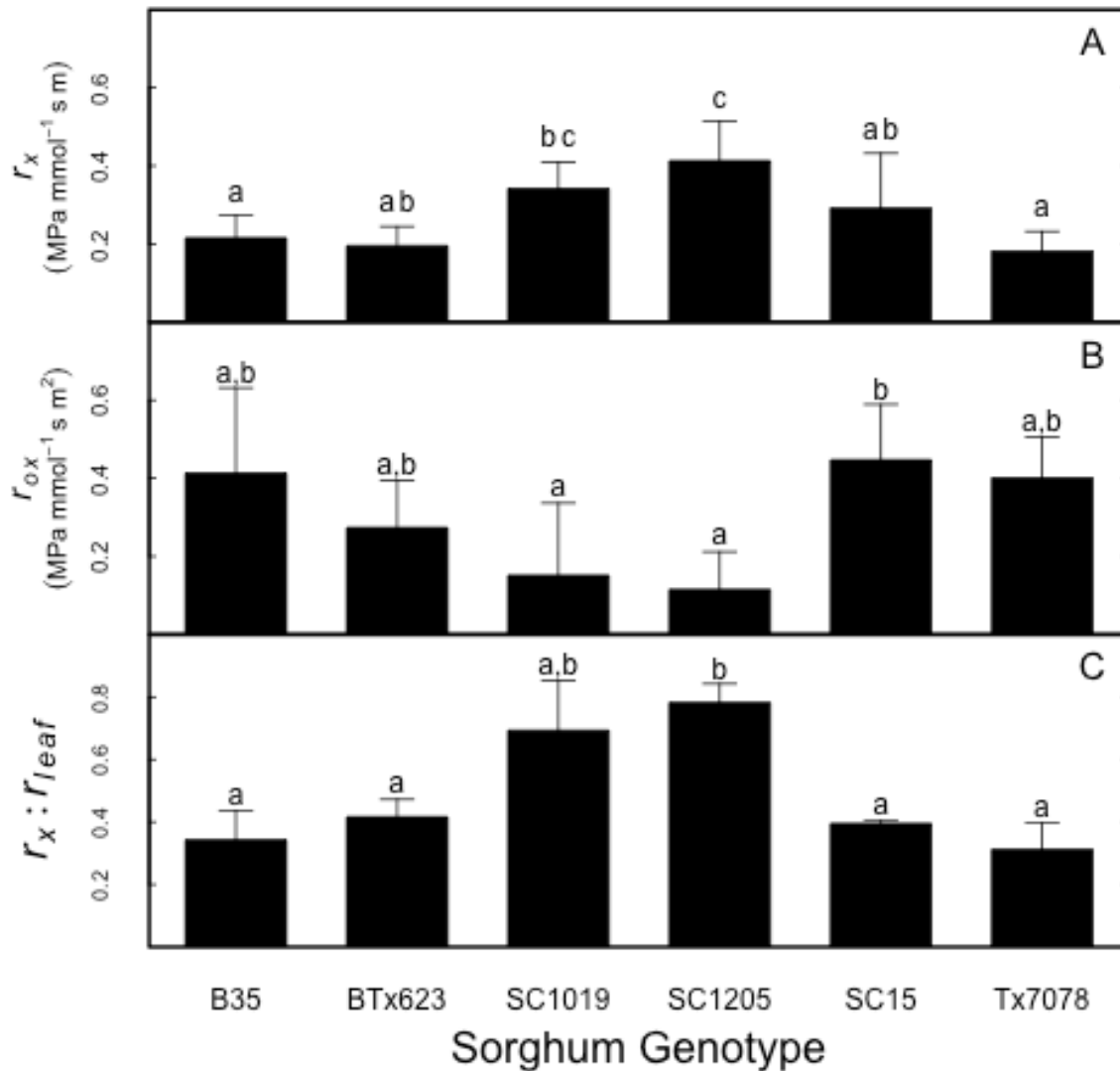


Figure 3.2 Relationship between the stomatal conductance (g_s) and hydraulic resistance in the xylem (r_x) and outside the xylem (r_{ox}) at different levels of Soil Water Content (SWC_{mass}). Panels A, C, and E show r_{ox} values and panels B, D, and F show r_x . The level of soil moisture is shown on the right hand side of the figure for each pair of panels. The equation for the linear regression is given in each panel and its' corresponding r^2 value. The different symbols represent each genotype tested; BTx623 (open circles), B35 (diamonds), SC1019 (triangles), SC1205 (inverted triangles), SC15 (closed circles), and Tx7078 (squares).

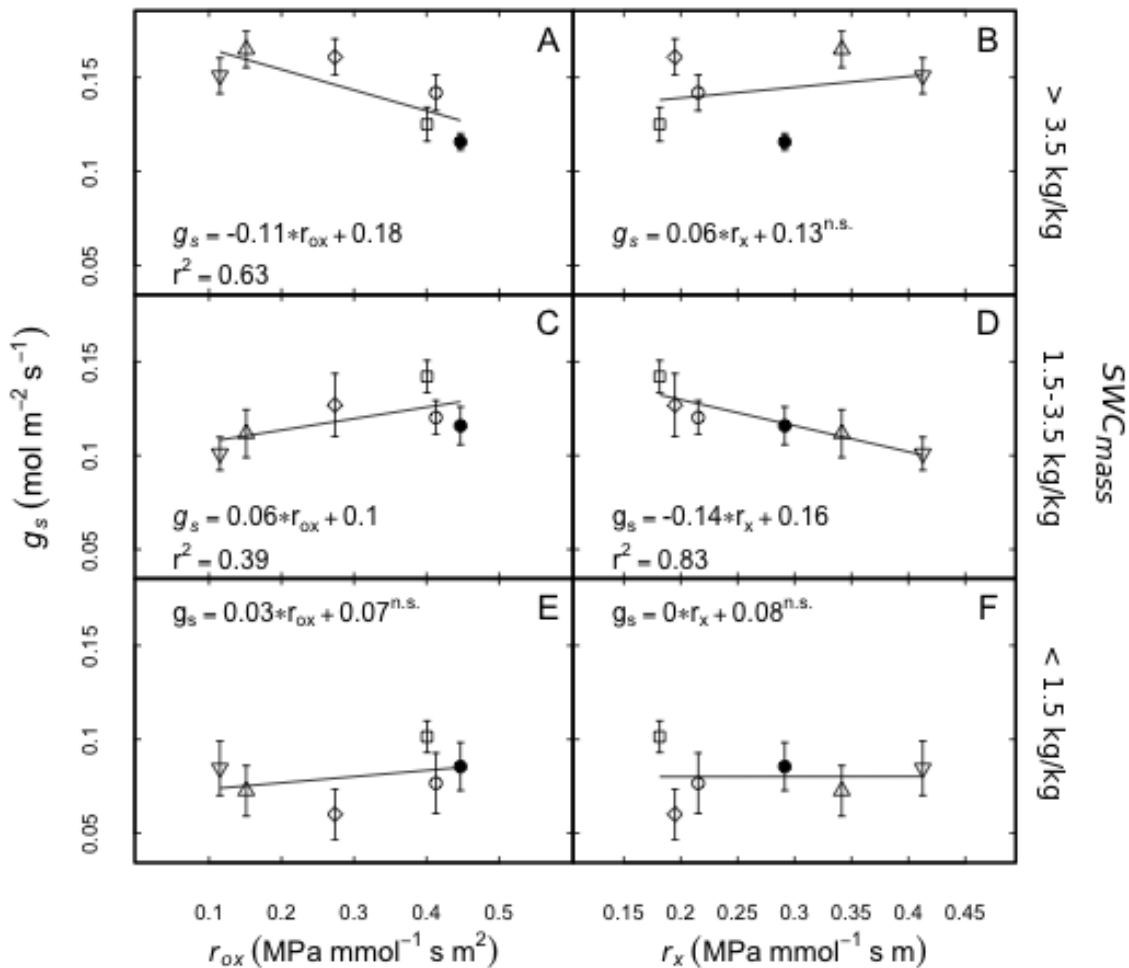


Figure 3.3 Relationship between whole leaf hydraulic resistance and root characteristics of the six genotypes. High water use in the leaves, which correlated to low hydraulic resistance resulted in greater root biomass (panel A) and greater allocation of biomass belowground (panel B) for water acquisition. The equation for the linear regression is given in each panel and its' corresponding r^2 value. The different symbols represent each genotype tested; BTx623 (open circles), B35 (diamonds), SC1019 (triangles), SC1205 (inverted triangles), SC15 (closed circles), and Tx7078 (squares).

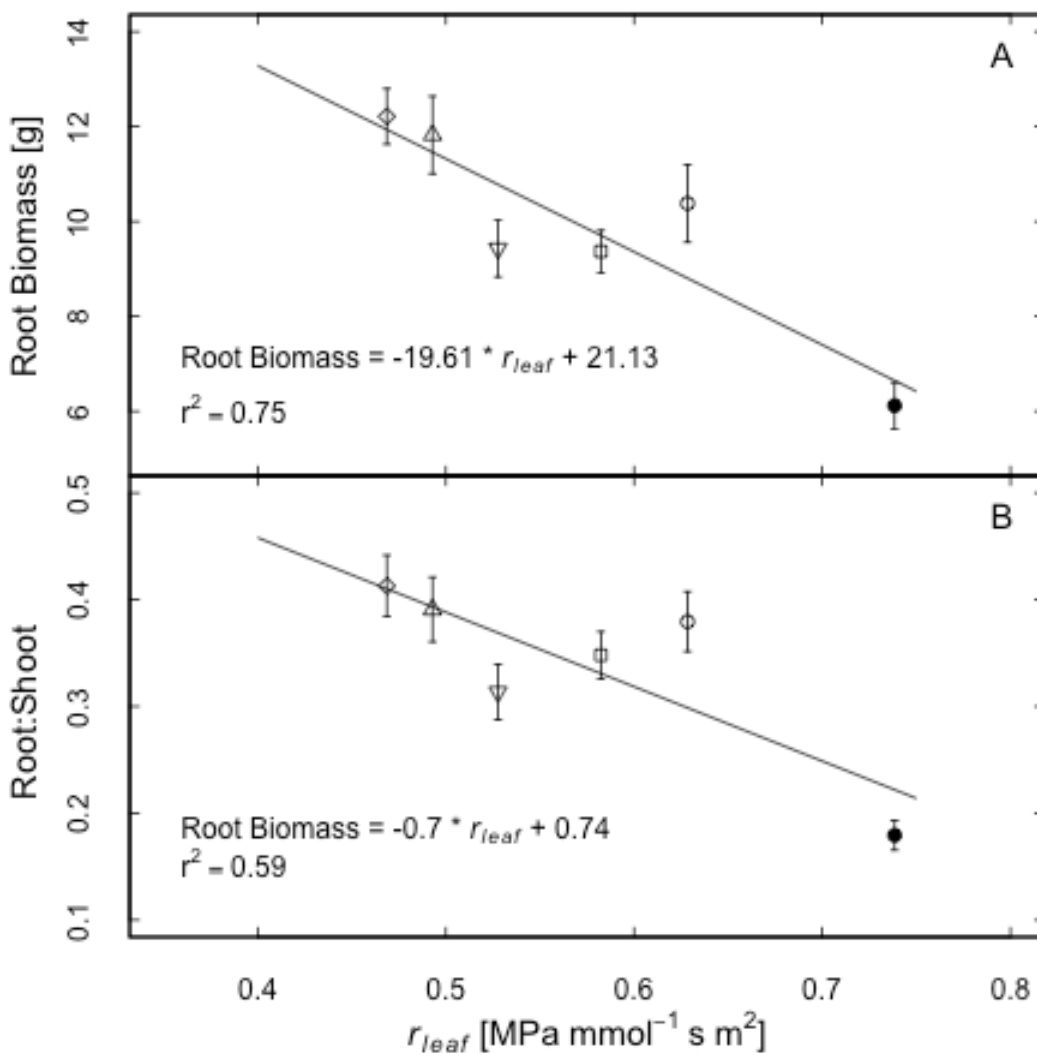


Figure 3.4 Relationship between leaf structure and hydraulic resistance in leaves of *Sorghum bicolor* L. (Moench). There was a significant relationship ($p < 0.05$) between major vein density and axial hydraulic resistance in the xylem (panel A). The relationship between the distance water travels from vascular bundle to stomata (D_m) and resistance outside the xylem was non-significant at the $p < 0.05$ level (panel B). The equation for the linear regression is given in each panel and its' corresponding r^2 value. The different symbols represent each genotype tested; BTx623 (open circles), B35 (diamonds), SC1019 (triangles), SC1205 (inverted triangles), SC15 (closed circles), and Tx7078 (squares).

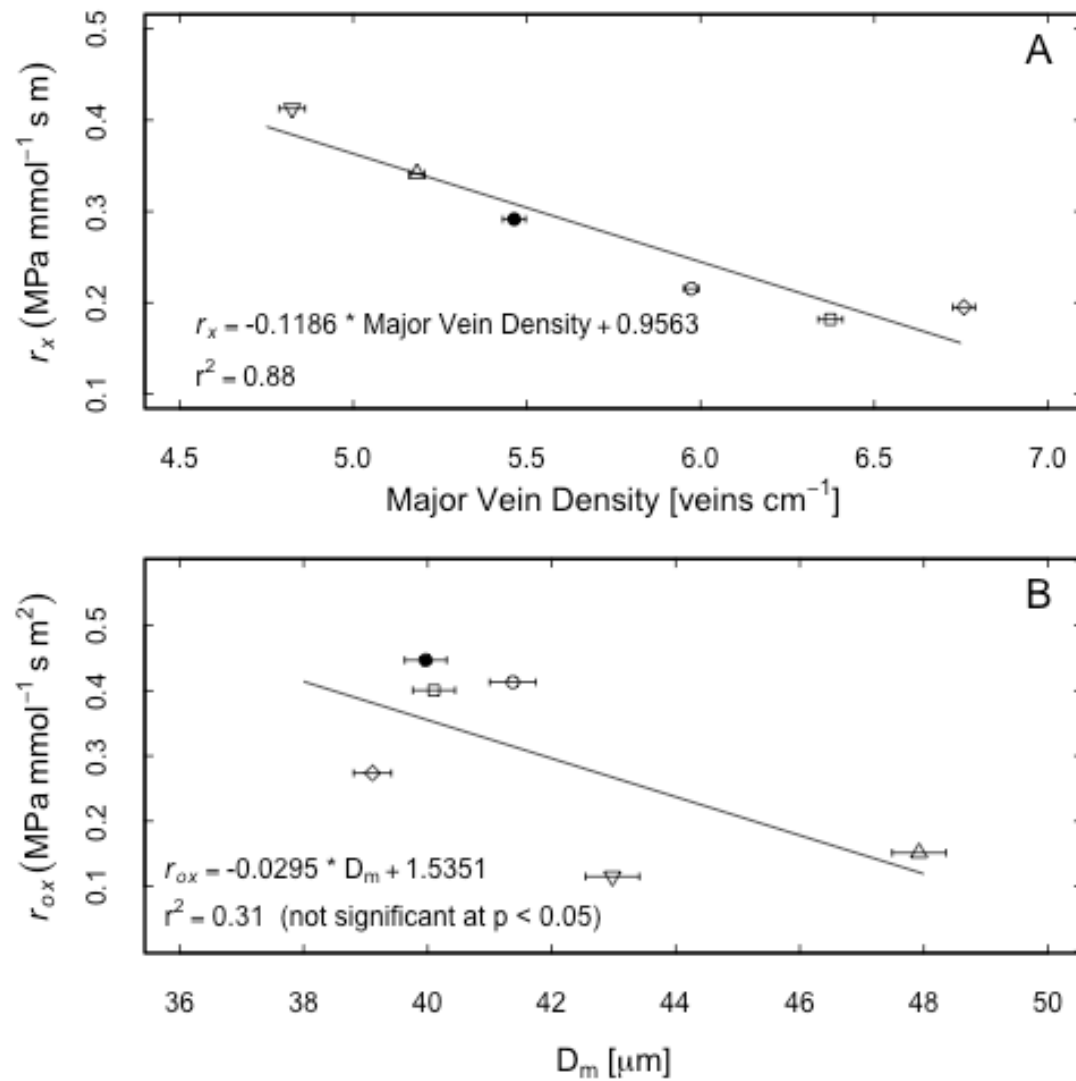
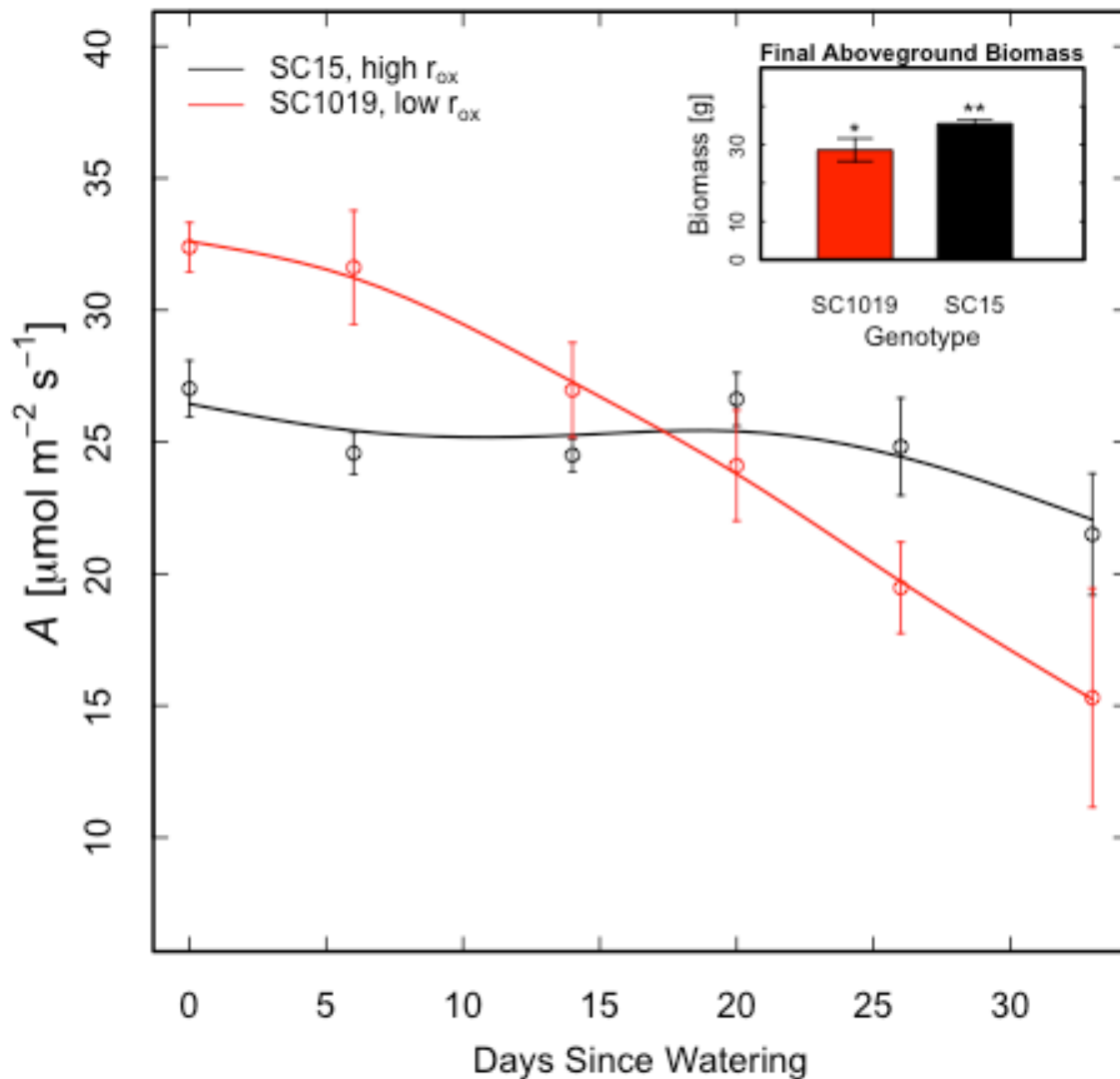


Figure 3.5 Temporal trend in photosynthesis for two contrasting genotypes as soil moisture was depleted from evapotranspiration from the pots. The lines are cubic fit to the mean (SE bars) for each sampling period. Genotype SC15 (black line) had high hydraulic resistance outside the xylem (r_{ox}) compared to SC1019 (red line). Although the initial rates of photosynthesis were lower in genotype SC15, this genotype conserved water for prolonged growth into the drought and results in greater aboveground biomass (insert).



Chapter 4 - Stomatal responses to changes in vapor pressure deficit reflect tissue-specific differences in hydraulic resistance

Abstract

The vapor pressure deficit (D) of the atmosphere can negatively affect plant growth as plants reduce stomatal conductance (g_s) in response to increasing D , which limits the plants ability to assimilate carbon. The sensitivity of g_s to changes in D varies among species and may be related to the hydraulic resistance of different tissues within the plant. I partitioned plant hydraulic resistance between the roots, aboveground xylem, and extra-xylery tissue and correlated these resistances with stomatal responses to increasing D . In general, the greatest resistance to water movement through plants was within the xylem (43% of whole plant resistance) and the lowest resistance was in the root system (26%). There was large variability among species, however, as the proportion of resistance within the xylem ranged from 5-73% of whole plant resistance. The sensitivity of g_s to increasing D was lowest in plants that had a lower proportion of resistance outside the xylem ($r^2=0.36$). Low resistance across the leaf mesophyll would minimize the pressure gradient from vascular bundle to the epidermis, and as D increased, the change in the pressure gradient would be smaller per unit increase in D compared to plants with high resistance through this tissue. Despite reductions in g_s in response to D , transpiration continued to increase, but plants with low hydraulic conductance through the root system limited the rates of transpiration at low levels of D ($r^2=0.79$), which may suggest a plant water conservation strategy. These results show the importance of understanding the partitioning of hydraulic resistances between different tissue types within grass species.

Introduction

Increasing vapor pressure deficits (D) cause stomatal closure and reduced carbon uptake by plants on both diurnal and seasonal timescales. As D increases, the stomatal conductance (g_s) of plants decreases as a mechanism to maintain the hydration of plant tissue. Because of the direct interaction of g_s and photosynthesis (A), reduced g_s in response to D also reduces carbon uptake due to reductions in internal CO_2 concentration. The ability to move water from the rhizosphere to the leaf tissue through the hydraulic pathway plays a vital role in how g_s respond to changes in leaf hydration. A better understanding of how the hydraulic architecture of plants affects the g_s response of plants to changing D will provide insight into the diurnal and seasonal growth patterns of plants.

It has previously been established that g_s declines in response to increasing D , but the exact mechanism driving the reduction is not yet clear. Models of g_s assume that the 'signal' for stomatal closure is the water potential of cells in the leaf (Buckley *et al.* 2003). Alternately, guard cells may be in equilibrium with the water vapor concentration in the stomatal cavity and stomatal closure is in response to changes in internal water vapor concentration (Peak and Mott 2011). Either model would predict stomatal closure if the supply of water to the leaf is inadequate to meet atmospheric demand. Stomatal conductance can also be reduced by biochemical signals from the roots in response to changes in the root water status (Comstock 2002) or from signals coming from other parts of the plant (Bunce 2006). The hydraulic architecture of plants provides the pathway for water to move from soil to the leaf, and so differences between plant species may play a vital role in differential responses of g_s to changes in atmospheric D .

The rate of decrease in g_s with increasing D has been quantified as stomatal sensitivity and correlates with the magnitude of g_s at low D (Oren *et al.* 1999, Addington *et al.* 2004); species with higher maximum rates of g_s are more sensitive to increasing D . Similarly, the sensitivity of C_3 plants tends to be higher than C_4 plants (Maherali *et al.* 2003, Wherley and Sinclair 2009) however this is confounded by the fact that the magnitude of g_s is lower in C_4 species due to fundamental differences in their photosynthetic pathways (Sage and Monson 1999). The sensitivity to D can also be modified by growth conditions, as both drought (Saliendra *et al.* 1995, Addington *et al.* 2004) and atmospheric CO_2

concentration (Wullschleger *et al.* 2002, Maherali *et al.* 2003) reduce the stomatal sensitivity of some species. As the magnitude of g_s is correlated with leaf-specific hydraulic conductance of the plant (Brodribb *et al.* 2002, Addington *et al.* 2004), stomatal sensitivity should also be linked to the hydraulic conductivity of the plant. The sensitivity of g_s has been linked with the hydraulic conductivity of the leaf (Brodribb and Jordan 2008), but it's also likely that the hydraulic conductivity of other plant tissues may play a role in stomatal responses to D .

The transpiration rate from leaves increases in response to D despite the decrease in g_s (example shown in Figure 4.1) but the rate of E asymptotes, or even declines, at some level of D , which has been referred to as the vapor pressure deficit breakpoint (D_{break} , Sinclair *et al.* 2005). D_{break} is related to the hydraulic conductivity of leaves in some plants; genotypes of soybean with low leaf hydraulic conductance had D_{break} values at lower levels of D (Sinclair *et al.* 2008), which resulted in a more conservative water use than genotypes with greater hydraulic conductance. D_{break} also differs between photosynthetic pathways; D_{break} is lower in C_3 compared to C_4 turfgrass (Wherley and Sinclair 2009). The relationship between D_{break} and leaf hydraulic conductance has not been tested on a wide range of species and functional groups to investigate the generality of this relationship. Furthermore, Sadok and Sinclair (2010) found that the hydraulic conductivity of some plants did not correlate well with leaf hydraulics, suggesting that a stronger relationship may exist between the D_{break} and the hydraulics of other plant tissues .

Water must pass through two general compartments, the xylem conduits and the leaf mesophyll, as it moves through the leaf. The proportion of whole leaf resistance that each of these components represents varies greatly among a range of species (Zwieniecki *et al.* 2002, Cochard *et al.* 2004, Sack *et al.* 2004, Sack *et al.* 2005, Mott 2007) but has never been investigated in grass leaves. The only functional consequence of differential partitioning of leaf resistances has been linked to shade-tolerance. Shade tolerant species tended to have a larger proportion of leaf resistance outside the xylem (Sack *et al.* 2005). No other functional consequences of this partitioning have been identified. Although K_{leaf} has been linked to the sensitivity to D , K_{leaf} can occur as a result of many different combinations of xylem and extra-xylery resistances (Sack *et al.* 2004) and as such, the response of g_s to changes in D would correlate with a specific component of K_{leaf} .

Specifically, the efficient supply of water to the mesophyll would occur if the proportion of resistance in the xylem was low, and so the sensitivity of g_s may be better correlated with the hydraulic conductivity of leaf xylem rather than the whole leaf.

It is not yet clear where, within the plant hydraulic pathway, hydraulic resistance may be most closely correlated with stomatal responses to D . Therefore, the objective of this study was to measure the hydraulic resistance of three major tissue types (root system, xylem, extra-xylery tissue in leaves) and correlate these resistances with stomatal sensitivity to D and to D_{break} . I hypothesized that: 1) the proportion of leaf resistance would be evenly distributed between xylem and extra-xylery tissues, 2) the proportion of whole plant hydraulic resistance in the roots would be the lowest, 3) the sensitivity to D would be related the hydraulic conductivity of leaf xylem, and 4) that D_{break} would correlate negatively with the resistance in the xylem, rather than the resistance outside the xylem.

Materials and Methods

Plant Material

Prior data for hydraulic conductivity and D_{break} was not available for many grass species when this experiment was conducted. In order to capture a wide range of values, I measured many grass species that covered a large gradient in D_{break} . The large number of species with low replication within species limits our ability to make conclusions about any particular species or species differences, but allows us to identify general patterns across a large gradient in D_{break} . To meet this goal, I grew 20 grass species, which included both C_3 and C_4 species, in order to look for consistency in the patterns across a range of species and functional groups (species listed in Table 4.1).

Rhizomes were collected from Konza Prairie Biological Station (KPBS, Manhattan, Kansas, USA) during May and June 2010, as grass tillers emerged from the soil and could be identified. Rhizomes were immediately transplanted to pots constructed of PVC pipe (5 cm outside diameter by 40 cm long) filled with local soil. Plants were grown at full sunlight and watered daily until at least 5 mature leaves were fully expanded, but before flowering was initiated. Since rhizomes were collected from May through June, plants did not

synchronously reach this measurement stage, and so sampling was staggered throughout June to early August.

D Response Curves

Plants were watered the morning before gas exchange measurements were made to ensure soil was at pot-holding capacity during measurements. Response curves were determined by measuring the transpiration rate of the entire aboveground portion of each plant at a range of D values. Transpiration (E) was measured using a custom chamber that enclosed the entire plant. The Arabidopsis Whole Plant Chamber for the Li-Cor 6400 (LiCor Biosciences, Inc. Lincoln, Nebraska, USA) was used to couple the PVC-pot to an acrylic chamber via a custom-made compression fitting and the soil surface was sealed with plumber's putty to ensure soil evaporation was excluded from measurements of E . The chamber was constructed of cast acrylic with a low adsorption capacity for water (product 8486K351, McMaster-Carr, Chicago, Illinois, USA). A fan (model SanAce40 9GV0412K301, Sanyo Denki, Tokyo, Japan) was installed inside the chamber to mix the air and minimize boundary layer conductance of the leaves, wind speed within the chamber was $\sim 4.8 \text{ m s}^{-1}$. A fine wire thermocouple was also installed in the chamber that could be secured to the leaf so that D could be calculated from leaf temperature.

E was calculated based on the concentration differential of H_2O for air entering and leaving the chamber. This differential was then multiplied by the flow rate through the chamber and normalized by leaf area for final determination of E ($\text{mmol m}^{-2} \text{ s}^{-1}$). The flow rate through the chamber was measured by the pressure differential (model 68075, Cole-Parmer Instrument Company, Vernon Hills, Illinois, USA) across a 1-m piece of stainless steel tubing (0.16 cm internal diameter). The pressure differential was calibrated for flow rate to a mass flow meter (Type 1640, MKS Instruments, Inc., Andover, Massachusetts, USA). The CO_2 and H_2O concentration differential across the chamber was measured with a LiCor 6262 (LiCor Biosciences, Inc., Lincoln, Nebraska, USA) in differential mode. The inlet air was plumbed through the reference cell and the outlet air passed through the sample cell. The source air was from a tank of dry air with a CO_2 concentration of 394 ppm. D of chamber air was adjusted by changing the flow rate of source air through the chamber

(Gholipoor *et al.* 2010). The plant inside the chamber was illuminated with a LED light source (180W LED light, Advanced LED Grow Lights, Bentonville, Arkansas, USA) and was kept at $\sim 1000 \mu\text{mol m}^{-2} \text{s}^{-1}$. Following measurements all leaves were scanned (at 600 dpi, Epson Perfection V500, Epson America Inc., Long Beach, California, USA) and leaf area measured (Rasband ImageJ, 1997-2011) to normalize gas exchange by leaf area in the chamber.

Hydraulic Conductivity

The hydraulic conductivity of grass leaves was measured immediately following determination of the *D* response curves using the steady-state High Pressure Flow Method (HPFM) described by Yang and Tyree (1994). Briefly, the flow rate through the leaves were determined by measuring the pressure differential across a high-resistance piece of tubing (PEEK tubing with internal diameters of 0.127, 0.178, 0.254 and 0.508 mm), upstream from the leaf being measured. A range of hydraulic resistors were calibrated to accommodate a range of leaf conductance values so that the pressure differential across the resistor could be maintained between 5-30 kPa, and the pressure of water entering the leaf was kept between 15-30 kPa.

Hydraulic conductivity of the whole leaf (k_{leaf}) was measured by cutting the leaf near the ligule under water using a razor blade and then placing the cut end immediately inside a custom-made hydraulic chamber. The path of water flow for this measurement was through the entire leaf, including both xylem and extra-xylery components. The leaf was kept submerged during the measurement and was illuminated to $\sim 1000 \mu\text{mol m}^{-2} \text{s}^{-1}$ with a fiber optic light source (FL-150, Meiji Techno Company, Saitama, Japan). Once flow through the leaf stabilized, the pressure differential across the resistor and the pressure of water entering the leaf were recorded. Following the measurement of k_{leaf} another transverse cut was made across the leaf to remove most of the distal portion of the leaf and measure axial hydraulic conductivity through the xylem (k_{xylem}). The leaf segment used for this measurement was ~ 3 cm long and the path of water movement was primarily through the xylem. Flow through this leaf section was allowed to stabilize and the pressures across the resistor and of water entering the leaf were again recorded. Flow rate was divided by

the pressure of water entering the leaf and then normalized by leaf area to calculate leaf specific hydraulic conductance of the leaf (K_{leaf}) and xylem (K_{xylem}). The hydraulic conductance outside the xylem (K_{ox}) was calculated by subtracting the inverse of K_{xylem} (which is equal to the xylem resistance) from the inverse of K_{leaf} . Finally, in order to calculate the proportional contribution of each plant component to K_{plant} , all conductances were converted to resistance. I present both conductance and resistance values in the results to discuss plant hydraulic architecture because while conductance values are somewhat more intuitive, resistances are necessary to calculate the proportional contribution of each plant component to the movement of water through the whole plant.

Following the measurement of hydraulic conductivity through the leaf, root hydraulic conductivity (k_{root}) was measured on the entire root system in the same manner. While holding the remaining plant and pot under water, the tiller was cut ~ 3 cm above the soil surface using a razor blade and the cut end was immediately placed in the hydraulic chamber and the HPFM was used to determine the hydraulic conductance of the root system as described above. Following this measurement the root system was rinsed thoroughly in the water bath and then rinsed under a faucet to remove all the soil. The root system was scanned for determination of root length using WinRHIZO software (Regent Instruments Inc., Quebec City, Quebec, Canada). Finally, all leaf and root tissue was dried at 60°C for ~ 48 hours and then weighed (± 0.0001 g, Pioneer PA214, Ohaus Corporation, Pine Brook, New Jersey, USA). All conductivity measurements were normalized to a water temperature of 20°C.

Statistical Analyses

All statistical analyses were carried out in the R open source statistical software package (R Development Core Team, 2008). Data were checked for normality and any outliers removed. Two-sample t-test was used for comparisons between functional groups (C₃ and C₄). Linear regression was performed using the 'lm' function and segmented regression for the determination of D_{break} was performed using the 'segmented' function in the 'segmented' library package.

Results

The proportion of whole plant resistance in each of the three main plant compartments (roots, xylem, outside the xylem) varied greatly among the grass species selected (Table 4.1). In general, the hydraulic resistance in the roots represented the smallest proportion of whole plant resistance and averaged 25% of total plant resistance. The resistance inside the xylem as water moved axially through the leaf represented the greatest resistance in leaves, and was on average 43% of plant resistance. The proportion of resistance in the xylem ranged, however, from 5% to 75% of whole plant resistance. r_{ox} represented 36% of whole plant resistance, but also showed great variability, ranging from 7-78% of r_{plant} . The only significant difference between functional groups was in the proportion of r_{ox} ($p = 0.047$) as C_4 had a lower proportion of their resistance outside the xylem (mean = 0.18) compared to C_3 species (mean = 0.44). The proportion of resistance in the xylem was significantly different between C_3 and C_4 species at the $p < 0.1$ level. K_{plant} varied across the species but no significant differences were found between the C_3 and C_4 species measured here ($p = 0.62$).

r_{leaf} scaled closely with the individual components of leaf resistance (Figure 4.2). r_{xylem} scaled most closely with r_{leaf} (Figure 4.2A) with an $r^2 = 0.85$ and a slope of 0.8, which suggests that across these species the average resistance in the xylem was 80% of total leaf resistance. r_{ox} also scaled with r_{leaf} (Figure 4.2B) but not as closely as r_{xylem} . Interestingly, r_{root} did not scale with r_{leaf} across the species studied, which suggests different roles for these components in plant responses to changes in water availability.

Figure 4.1 shows a typical D response curve with our custom chamber. There is an initial linear increase in E as D increases (ie. drier air) and a corresponding decrease in g_s . The initial decrease in g_s is quite large as D increases, but tapers off when E reaches its maximum value and then stabilizes. E stabilized for most species in this study, but there were several examples where g_s continued to decrease, reducing E with subsequent increases in D . I quantified three parameters from these D response curves; stomatal sensitivity to D , the minimum g_s , and the transpiration breakpoint (D_{break}).

The sensitivity of g_s to D was tightly correlated with the magnitude of g_s at $D = 1.0$ kPa (Figure 4.3A). The variability of g_s was large when D was low, but as D increased the g_s

of all the species converged to a similar value, and the range of values decreased from 0.804 to 0.147 mol m⁻² s⁻¹ (Figure 4.3B). g_{min}/g_{ref} was used as an estimate of the magnitude that g_s decreased in response to D and was closely related with the proportion of plant resistance in the xylem (Figure 4.4). Plants with a greater proportion of resistance in the xylem had to close their stomata to a larger degree than when plants had lower resistance in the xylem.

D_{break} varied from 1.04 to 2.7 across the range of species measured (Table 4.1), but did not differ significantly between C₃ and C₄ species ($p = 0.47$). The best predictor of D_{break} was the hydraulic conductivity of the root system (Figure 4.5), where 79% of the variability was explained. K_{xylem} and g_s were also significant in predicting D_{break} , but explained much less of the variability (8.4 and 17.7%, respectively) than K_{root} (Table 4.2). Plants with lower rates of g_s tended to have a higher D_{break} (Table 4.2, 'Estimated Value'), but plants with high K_{xylem} led to D_{break} at higher pressures (Table 4.2, 'Estimated Value'). K_{ox} was not significant in predicting D_{break} ($p = 0.71$).

I investigated the relationship between K_{root} with characteristics of the root system (Table 4.2), but found no correlation between root morphological characteristics (root length, root mass) and any tissue characteristics (root tissue density, specific root length). Additionally, there was no relationship between the K_{root} and the root:shoot ratio of the plants studied in this experiment.

Discussion

The partitioning of whole plant hydraulic conductance between different plant tissues varies widely in grasses and correlates with the stomatal response to D . Across all species measured the greatest proportion of hydraulic resistance was in the xylem (43%) followed by the resistance outside the xylem (32%) and then the roots (25%). Furthermore, the variability in the proportion of r_{xylem} was correlated with the magnitude of stomatal closure in response to increasing D . When the majority of plant resistance is within the xylem, then at a steady-state flux the largest pressure gradient would also occur in this tissue type. This would leave a smaller pressure gradient from the vascular bundle to the epidermis and result in smaller changes stomatal conductance as D increased.

Finally, high leaf-specific hydraulic conductance in the root system resulted in plants reaching D_{break} at higher vapor pressure deficits. It is unclear, however, whether K_{root} is directly correlated with D_{break} , or rather, if K_{root} may scale with other leaf properties or biochemical processes not measured in this study. Whatever the mechanism, variability in D_{break} is correlated with different water-use strategies among crop species (Sinclair *et al.* 2007, Gholipour *et al.* 2010) as plants with lower D_{break} values tend to conserve water. This type of conservation strategy has been implicated in the success of some drought tolerant grasses (Fernandez and Reynolds 2000).

Previous work has shown that a significant proportion of the resistance in leaves is in the xylem (Sack *et al.* 2004), but that large variability occurs between species (Sack *et al.* 2005). The proportion of resistance in the leaf xylem in the grasses I measured, ranged from 5-73%, which is similar to the range found across a range of shade-tolerant species in a tropical rainforest (Sack *et al.* 2005). In this study of shade-tolerant leaves, Sack *et al.* (2005) found that shade tolerant species had a lower proportion of resistance in the leaf xylem, which they speculated resulted from a lower demand for water of shade-tolerant species when coupled with the cost of building highly conductive xylem (McCulloh *et al.* 2003). The majority of the species I studied were not shade-tolerant; however, I did find that C_4 species had a greater proportion of resistance in their xylem (54%) compared to C_3 species (32%). The lower demand for water in C_4 plants results from their ability to operate at very low internal CO_2 concentrations (Sage and Monson 1999), which may allow them to reduce construction costs associated with the xylem vasculature.

Although the proportion of resistance in the leaves varies greatly between xylery and extra-xylery resistances, both scale closely with whole leaf hydraulic resistance. This agrees with previous work on eudicot leaves (Sack *et al.* 2005, Sack and Frole 2006). The scaling relationship between leaf and xylem resistances is very strong ($r^2 = 0.85$), but there is more variability in the scaling between leaf and extra-xylery resistances. It was surprising to find that the resistance of the root system did not correlate with leaf resistances, which could lead to large differences in plant function despite similarities in leaf properties.

As previously reported, the sensitivity of g_s to D was correlated with the magnitude of g_s at low D (in this case 1.0 kPa). The slope of the relationship between g_{ref} and stomatal

sensitivity has been shown to be ~ 0.6 across a range of species and conditions (Oren *et al.* 1999, Addington *et al.* 2004). The slope in our study is lower (0.52) than the predicted slope, but is somewhat intermediate between the results of Maherali *et al.* (2003) that were measured on C₃ (slope = 0.59) and C₄ (slope = 0.36) grasses. Our regression of stomatal sensitivity with g_{ref} included both C₃ and C₄ species, and although no significant differences were present between C₃ and C₄ plants, the presence of species representing both functional groups could have contributed to our lower slope. Oren *et al.* (1999) suggested that this slope would be lower than 0.6 if plants were responding to some signal other than leaf water potential or if boundary layer conductance contributed to the resistance of water flux from leaves. Although I used a high fan speed in our chamber to minimize boundary layer conductance it is still possible, especially for the plants with greater leaf area, that boundary layer conductance influenced our measurements and contributed to our slope < 0.6 .

The magnitude of g_s reduction in response to D also related to how the hydraulic resistances were partitioned between xylery and extra-xylery tissues. The proportion of resistance in the xylem correlated well with the percent reduction in g_s when D increased from 1.0 kPa until E stabilized (Figure 4.4). If I use an electrical analog approach and assume the hydraulic resistance of root-xylem-mesophyll are in series, then I can model the changes in plant water potential along the hydraulic pathway from soil to leaf. When the proportion of whole plant resistance is greatest in the xylem, then the largest drop in water potential (Ψ) for a given rate of E will be from root to leaf ($\Delta\Psi_{root-leaf}$). Conversely, the water potential gradient from leaf to evaporative site will be relatively small ($\Delta\Psi_{leaf-e}$). Furthermore, as E increases the change in ($\Delta\Psi_{leaf-e}$) will be smaller in a plant with proportionately high r_x . Changes in g_s may be responding to Ψ of leaf cells (Buckley 2005) or the humidity inside the stomatal cavity (Peak and Mott 2011). Whatever the mechanism, smaller changes in $\Delta\Psi_{leaf-e}$ should manifest as smaller reductions of g_s in response to increasing D . This result is meaningful because smaller reductions in g_s will result in the maintenance of higher internal CO₂ concentrations.

The best predictor of the D_{break} was the hydraulic conductivity of the root system; plants with higher rates of leaf-specific conductance through the root system maintained

increases in E to higher values of D . Although r_{root} represented the lowest proportion of resistance to water movement through the plant (25% on average), it still was the best predictor of the point when transpiration reached its maximum rate. K_{xylem} and g_s were also significantly correlated with D_{break} , although they only explained 17% and 8% of the variability, respectively (Table 4.2). Sinclair *et al.* (2008) showed that D_{break} was related to low hydraulic conductance in the leaves of several genotypes of soybean. Using aquaporin inhibitors to reduce leaf hydraulic conductance, Sadok and Sinclair (2010) found some genotypes did not fit their theoretical framework and suggested that the D_{break} could be related to resistances upstream of the leaf. Since the aquaporin inhibitors reduced conductance outside the xylem (r_{ox} in our study) the greater resistance could have occurred in the xylem of the leaves or, as they suggest, in the root system. Our results suggest that both resistance in the xylem and the root system can affect the response of plants to increasing D . Further work is needed to determine whether r_{root} directly affects D_{break} , or whether it simply scales with other plant properties that are responsible for the response of g_s to changing D .

Leaf-specific hydraulic conductance of the root system did not correlate with any of the measured root characteristics (Table 4.2). Root length, specific root length, and the root:shoot ratio were all non-significant in explaining K_{root} , which suggests it was either anatomical differences that don't correlate with root vascular morphology or biochemical processes that caused the variability in K_{root} . The regulation of aquaporin channels plays a significant role in the uptake of water through roots (Bramley *et al.* 2009, Aroca *et al.* 2012) as does the predominate pathway the water takes through the root (apoplastic or symplastic, Steudle and Peterson 1998), both of which could have varied significantly between the species studied here. Although the mechanism behind differences in K_{root} was not identified, the importance of K_{root} on whole plant water use is clear and further research understanding how roots control whole-plant water use is needed.

Conclusions

Our results show large species-level variability in the partitioning of hydraulic resistances between roots, leaf xylem, and extra-xylery tissues. High resistance in the root system limits the increase in E as demand for water in the atmosphere increases, and may contribute to water conservation strategies in plants. A proportionately high resistance in the leaf xylem limits the magnitude of the stomatal response to D thereby reducing the impact of high D on carbon assimilation. The importance of whole-plant hydraulic conductance on plant growth has been well documented previously, but here I have highlighted the importance of measuring the hydraulic architecture of individual plant tissues providing new insights into how plants dynamically respond to short-term environmental change.

Literature Cited

- Addington R.N., Mitchell R.J., Oren R., and Donovan L.A. 2004. Stomatal sensitivity to vapor pressure deficit and its relationship to hydraulic conductance in *Pinus palustris*. *Tree Physiology* 24, 561-569.
- Aroca R., Porcel R., and Ruiz-Lozano, J.M. 2012. Regulation of root water uptake under abiotic stress conditions. *Journal of Experimental Botany* 63, 43-57.
- Bramley H., Turner N.C., Turner, D.W., and Tyerman S.D. 2009. Roles of Morphology, Anatomy, and Aquaporins in Determining Contrasting Hydraulic Behavior of Roots. *Plant Physiology* 150, 348-364.
- Brodribb T. J., Holbrook N. M., and Gutierrez M.V. 2002. Hydraulic and photosynthetic coordination in seasonally dry tropical forest trees. *Plant, Cell and Environment* 25, 1435-1444.
- Brodribb T.J., and Jordan G.J. 2008. Internal coordination between hydraulics and stomatal control in leaves. *Plant, Cell and Environment* 31, 1557-1564.
- Buckley T.N. 2005. The control of stomata by water balance. *New Phytologist* 168, 275-291.
- Buckley T.N., Mott K.A., and Farquhar G.D. 2003. A hydromechanical and biochemical model of stomatal conductance. *Plant, Cell and Environment* 26, 1767-1785.
- Bunce J.A. 2006. How do leaf hydraulics limit stomatal conductance at high water vapour pressure deficits?. *Plant, Cell and Environment* 29, 115-120.
- Cochard H., Nardini A., and Coll L. 2004. Hydraulic architecture of leaf blades: where is the main resistance? *Plant, Cell and Environment* 27, 1257-1267.

- Comstock J.P. 2002. Hydraulic and chemical signalling in the control of stomatal conductance and transpiration. *Journal of Experimental Botany* 53, 195-200.
- Fernandez R., and Reynolds J. 2000. Potential growth and drought tolerance of eight desert grasses: lack of a trade-off? *Oecologia* 123, 90-98.
- Gholipoor M., Prasad P.V.V., Mutava R., and Sinclair T.R. 2010. Genetic variability of transpiration response to vapor pressure deficit among sorghum genotypes. *Field Crops Research* 119, 85-90.
- Maherali H., Johnson H.B., and Jackson R.B. 2003. Stomatal sensitivity to vapour pressure difference over a subambient to elevated CO₂ gradient in a C-3/C-4 grassland. *Plant, Cell and Environment* 26, 1297-1306.
- McCulloh K., Sperry J., and Adler F. 2003. Water transport in plants obeys Murray's law. *Nature* 421, 939-942.
- Mott K.A. 2007. Leaf hydraulic conductivity and stomatal responses to humidity in amphistomatous leaves. *Plant, Cell and Environment* 30, 1444-1449.
- Oren R., Sperry J.S., Katul G.G., Pataki D.E., Ewers B.E. Phillips N., and Schafer K.V.R. 1999. Survey and synthesis of intra- and interspecific variation in stomatal sensitivity to vapour pressure deficit. *Plant, Cell and Environment* 22, 1515-1526.
- Peak D., and Mott K.A. 2011. A new, vapour-phase mechanism for stomatal responses to humidity and temperature. *Plant, Cell and Environment* 34, 162-178.
- R Development Core Team, 2008. R: A language and environment for statistical computing. R Foundation for Statistical Computing, Vienna, Austria. ISBN 3-900051-07-0, URL <http://www.R-project.org>.
- Rasband W.S., ImageJ, U. S. National Institutes of Health, Bethesda, Maryland, USA, URL <http://imagej.nih.gov/ij/>, 1997-2011.
- Sack L., and Frole K. 2006. Leaf structural diversity is related to hydraulic capacity in tropical rain forest trees. *Ecology* 87, 483-491.
- Sack, L., Streeter, C.M., and Holbrook, N. M. 2004. Hydraulic analysis of water flow through leaves of sugar maple and red oak. *Plant Physiology* 134, 1824-1833.
- Sack L., Tyree M.T., and Holbrook N. M. 2005. Leaf hydraulic architecture correlates with regeneration irradiance in tropical rainforest trees. *New Phytologist* 167, 403-413.
- Sadok W., and Sinclair T.R. 2010. Genetic variability of transpiration response of soybean [*Glycine max* (L.) Merr] shoots to leaf hydraulic conductance inhibitor AgNO₃. *Crop Science* 50, 1423-1430.
- Sage R.F., and Monson R.K. 1999. C₄ Plant Biology, Academic Press. San Diego, CA, USA.

- Saliendra N., Sperry J., and Comstock J. 1995. Influence of leaf water status on stomatal response to humidity, hydraulic conductance, and soil drought in *Betula occidentalis*. *Planta* 196, 357-366.
- Sinclair T.R., Hammer G.L., and van Oosterom E.J. 2005. Potential yield and water-use efficiency benefits in sorghum from limited maximum transpiration rate. *Functional Plant Biology* 32, 945-952.
- Sinclair T.R., Fiscus E., Wherley B., Durham M., and Rufty T. 2007. Atmospheric vapor pressure deficit is critical in predicting growth response of “cool-season” grass *Festuca arundinacea* to temperature change. *Planta* 227, 273-276.
- Sinclair T.R., Zwieniecki M.A., and Holbrook N.M. 2008. Low leaf hydraulic conductance associated with drought tolerance in soybean. *Physiologia Plantarum* 132, 446-451.
- Steudle E., and Peterson C. 1998. How does water get through roots? *Journal of Experimental Botany* 49, 775-788.
- Wherley B.G., and Sinclair T.R. 2009. Differential sensitivity of C(3) and C(4) turfgrass species to increasing atmospheric vapor pressure deficit. *Environmental and Experimental Botany* 67, 372-376.
- Wullschleger S., Gunderson C.A., Hanson P.J., Wilson K.B., and Norby R.J. 2002. Sensitivity of stomatal and canopy conductance to elevated CO₂ concentration - interacting variables and perspectives of scale. *New Phytologist* 153, 485-496.
- Yang S., and Tyree M.T. 1994. Hydraulic architecture of *Acer saccharum* and *A. rubrum*: comparison of branches to whole trees and the contribution of leaves to hydraulic resistance. *Journal of Experimental Botany* 45, 179-186.
- Zwieniecki M. A., Melcher P.J., Boyce, C.K., Sack L., and Holbrook N.M. 2002. Hydraulic architecture of leaf venation in *Laurus nobilis* L. *Plant, Cell and Environment* 25, 1445-1450.

Tables and Figures

Table 4.1 The 20 species selected for our study are shown, grouped by their photosynthetic pathway. The vapor pressure deficit breakpoint (D_{break}) for each species is listed, multiple values are listed if replicates were measured. The hydraulic conductance of the whole plant along with the partitioning of plant resistances by plant component are also shown. A two sample t-test was carried out between C₃ and C₄ species and significant differences at the $p < 0.05$ and $p < 0.1$ level

are indicated with '*' and '**', respectively. 'nd' indicates these values could not be determined for that species.

	Species	D_{break} (kPa)	K_{plant}	r_{ox} / r_{plant}	r_{xylem} / r_{plant}	r_{root} / r_{plant}
C₃ species	<i>Agrostis hyemalis</i> Walter	1.7, 1.4	2.56	0.55	0.33	0.12
	<i>Bromus inermis</i> Leyss.	1.3, 1.3	1.82	0.18	0.34	0.48
	<i>Dactylis glomerata</i> L.	nd	1.06	0.07	0.65	0.28
	<i>Dichanthelium oligosanthes</i> Schult.	1.3	1.09	0.09	0.57	0.33
	<i>Festuca subverticillata</i> Pers.	nd	1.91	0.60	0.05	0.35
	<i>Hordeum pusillum</i> Nutt.	2.5	0.44	0.61	0.37	0.02
	<i>Koeleria macrantha</i> Ledeb.	2.0	4.49	0.64	0.20	0.15
	<i>Poa pratensis</i> L.	2.8	8.57	0.78	0.06	0.16
	C₃ mean	1.79	2.74	0.44*	0.32**	0.24
C₄ species	<i>Andropogon gerardii</i> Vitman	2.7	nd	nd	nd	nd
	<i>Bouteloua dactyloides</i> Nutt.	2.3	9.60	0.16	0.64	0.20
	<i>Chloris verticillata</i> Nutt.	nd	5.71	0.10	0.69	0.21
	<i>Digitaria californica</i> Benth.	1.6	nd	nd	nd	nd
	<i>Panicum virgatum</i> L.	1.6	4.31	0.21	0.11	0.67
	<i>Pascopyrum smithii</i> Rydb.	1.4, 1.5	1.46	0.21	0.73	0.05
	<i>Setaria pumila</i> Poir.	1.9	2.47	0.20	0.63	0.17
	<i>Spartina pectinata</i> Bosc.	1.6, 1.5	3.12	0.15	0.57	0.28
	<i>Sporobolus cryptandrus</i> Torr.	1.04	nd	nd	nd	nd
	<i>Sporobolus heterolepis</i> A. Gray	1.4	1.33	0.23	0.21	0.55
	<i>Tripsacum dactyloides</i> L.	1.6	2.56	0.20	0.71	0.09
	C₄ mean	1.68	3.82	0.18*	0.54**	0.28
Overall mean	1.72	3.33	0.31	0.43	0.26	

Table 4.2 Results from multiple linear regression analyses and the percentage of the Sums of Squares (SS) explained by the significant variables. 'ns' indicates non-significant variables at the $p < 0.1$ level, and 'nd' indicates these values could not be determined. K_{root} , g_s , and K_{xylem} are all significant in predicting the vapor pressure deficit breakpoint (D_{break}). K_{root} was not correlated with any of the root system characteristics measured in this study.

Dependant variable	independent variable	Estimated value	P-value	percentage of SS explained
D_{break}	K_{root}	0.02	<0.005	64.9
	g_s	-1.57	<0.005	17.7
	K_{xylem}	0.01	0.006	8.4
	K_{ox}	ns	0.71	nd
	drought tolerance	ns	0.602	nd
	functional type	ns	0.785	nd
K_{root}	root length	ns	0.56	nd
	specific root length	ns	0.83	nd
	root density	ns	0.78	nd

Figure 4.1 Vapor pressure response curve of *Panicum virgatum* shown as an example. Measurements were started with a low vapor pressure deficit (D) and then increased in discrete increments, waiting for transpiration (E) and photosynthesis (A) to stabilize at each level of D . The breakpoint for E and A were calculated using a segmented regression analysis in R .

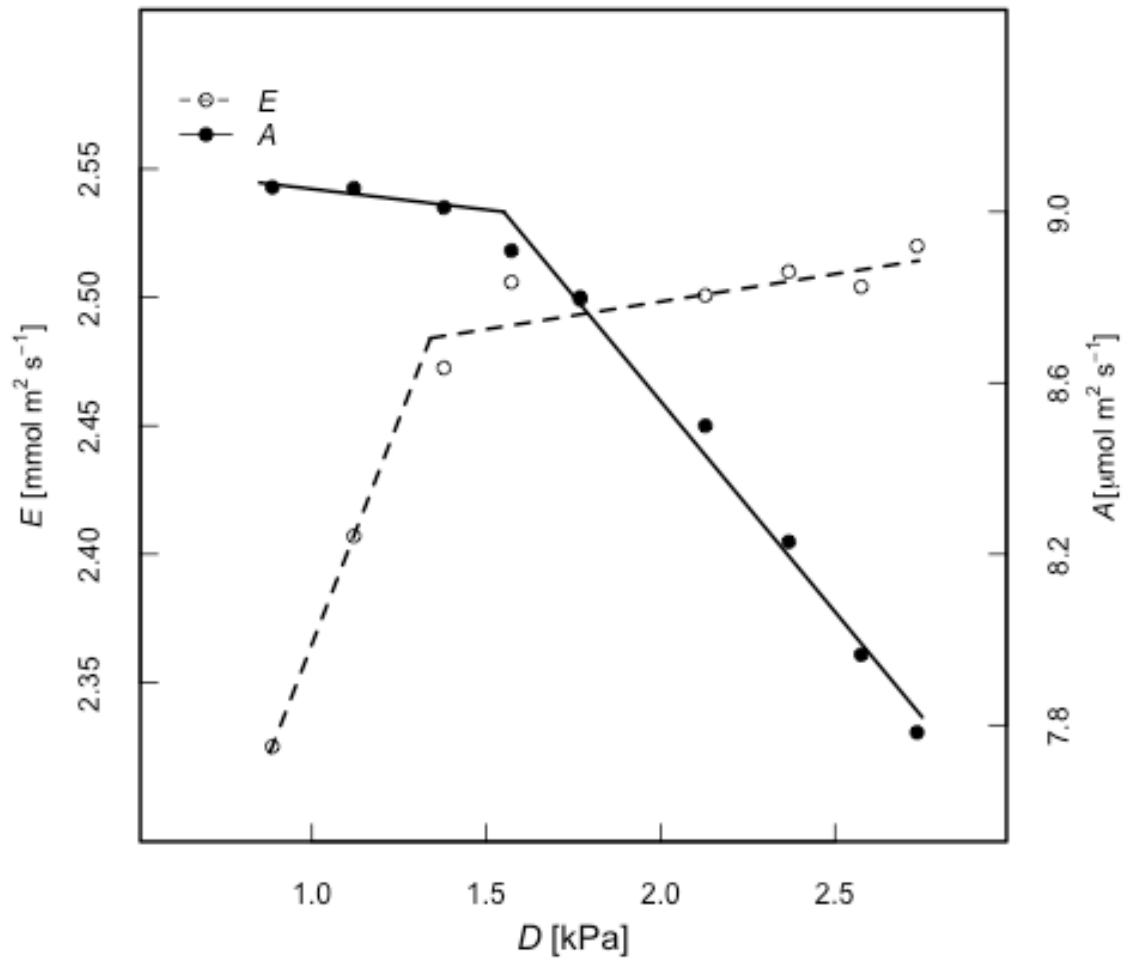


Figure 4.2 The resistance of the xylem (r_x) and extra-xylery (r_{ox}) components scale with whole-leaf resistance (r_{leaf}). r_x scaled most closely with r_{leaf} (panel A). r_{ox} did not scale as closely with r_{leaf} (panel B) but was still significantly correlated ($p = 0.02$). Finally, resistance of the root system was not significantly correlated with r_{leaf} (panel C, $p = 0.262$).

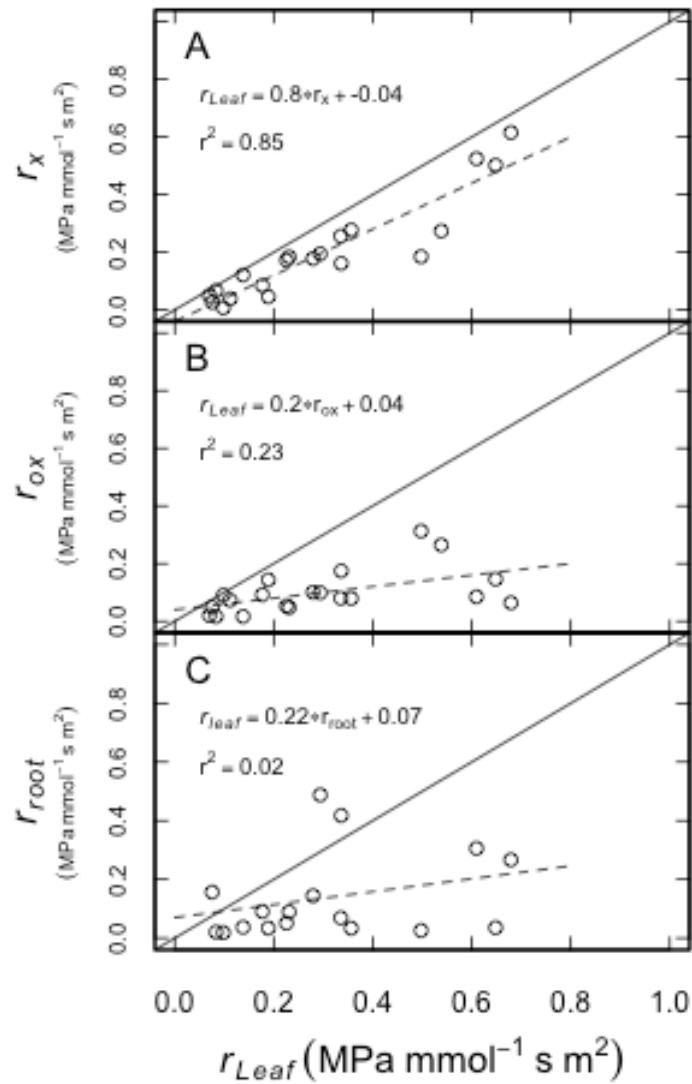


Figure 4.3 The sensitivity of stomatal conductance in response to changing D was related to the magnitude of g_s at $D = 1.0$ kPa (g_{ref} , panel A). g_{ref} was calculated from the regression of g_s and $\ln(D)$. g_s of the different species converged to similar values as D was increased to the point that transpiration rate stabilized (g_{min} , panel B). At a vapor pressure deficit of 1.0 kPa the coefficient of variation was 0.59, but decreased to 0.47 at high values of D .

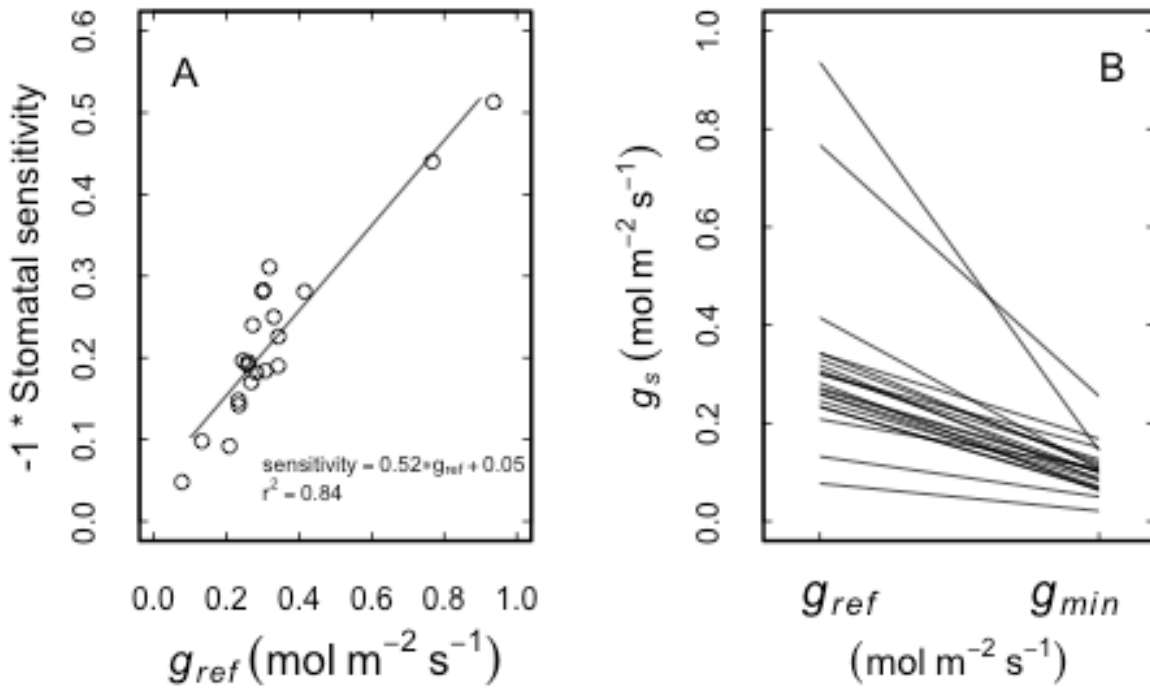


Figure 4.4 The minimum g_s calculated from a non-linear regression were related to the proportion of plant resistance that occurred in the xylem. When a greater proportion of resistance occurred in the xylem, g_s did not decrease as much from g_{ref} compared to when xylem resistance was a small proportion of whole plant resistance.

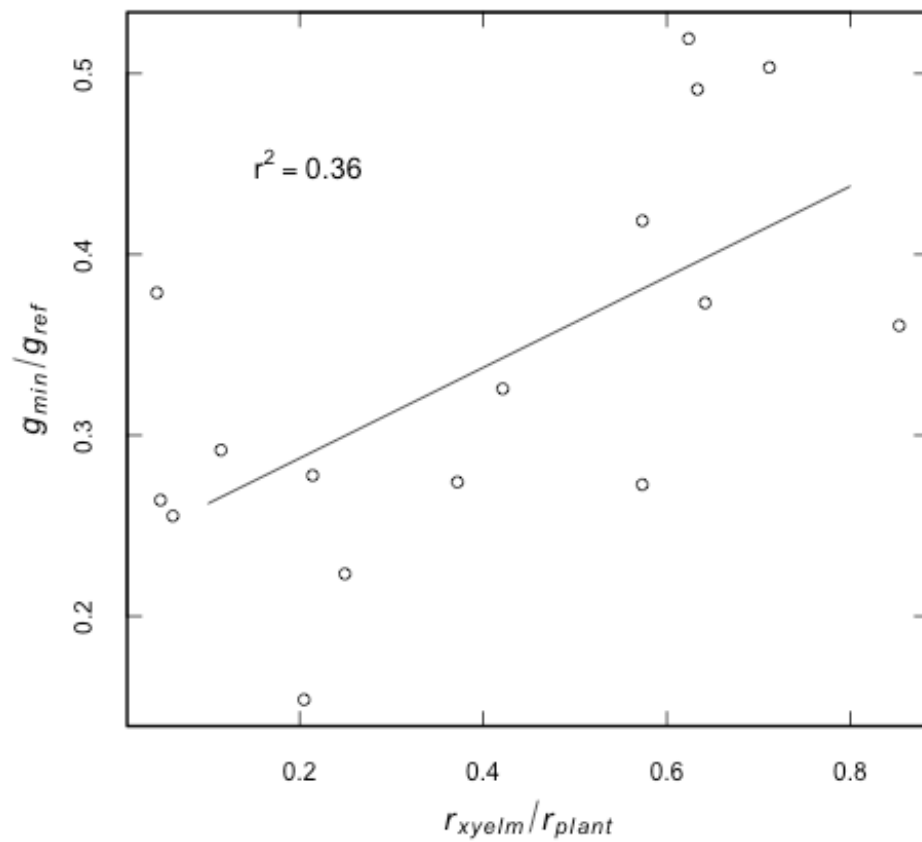
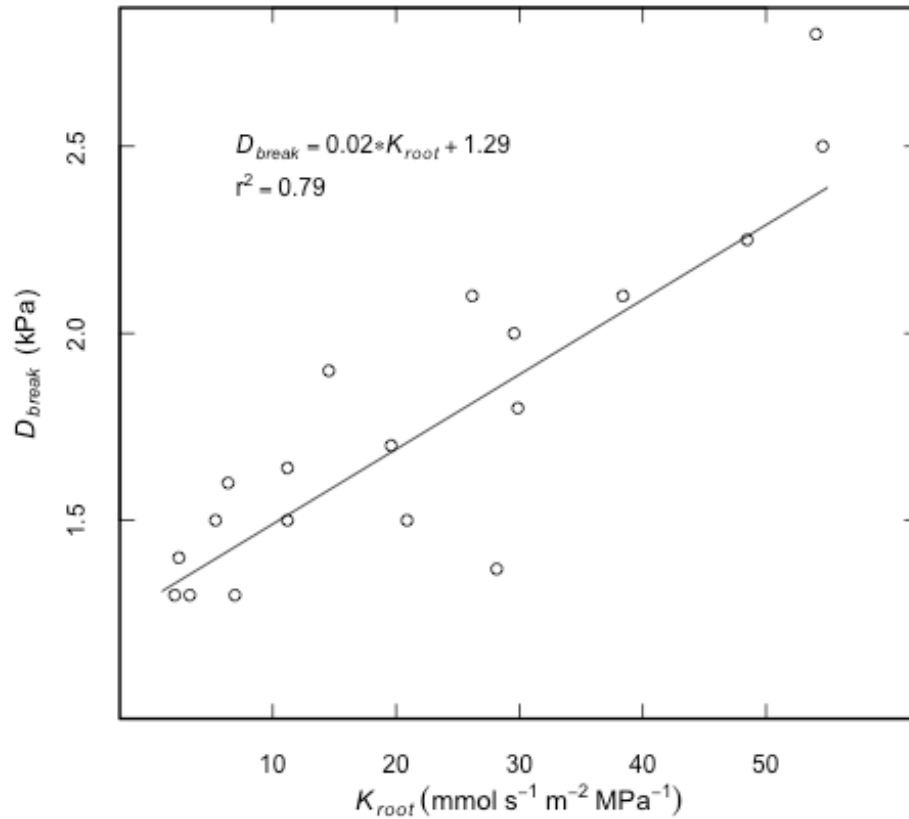


Figure 4.5 Relationship between the hydraulic conductance of the root system and D_{break} . The breakpoint between D and E was tightly correlated with the hydraulic conductivity of the root system such that plants with lower K_{root} reached the asymptote of E at lower values of D .



Chapter 5 - A trade-off between drought tolerance and growth characteristics at the leaf-level in grasses

Abstract

A central tenant in plant physiology is the trade-off between stress tolerance and growth, but support for this theory in relation to drought tolerance of grasses has not been found. Tests for a trade-off between drought tolerance and growth have not been assessed on the basis of leaf-level drought tolerance of the leaf hydraulic system. Here, I quantified leaf-level drought tolerance as the leaf water potential at which plants lost 80% of their maximum leaf hydraulic conductance (K_{leaf}), expressed as Ψ_{80K} . This measure of drought tolerance was compared with various measures of growth rate, including: stomatal conductance, photosynthesis, and whole plant biomass production. I found that when K_{leaf} was expressed on a leaf area basis there was no clear trade-off between drought tolerance and maximum rates of K_{leaf} ($p=0.19$). When leaf hydraulic conductance was expressed on a mass basis (K_{mass}), however, a trade-off became apparent; drought tolerant leaves had the lowest values of K_{mass} . There was a tight correlation between Ψ_{80K} and stomatal conductance expressed on a mass basis, which contradicts previous results on leaves from eudichots and suggests there is not a trade-off between leaf level drought tolerance and rates of gas exchange across a range of grass species. Plants that are found primarily in arid environments always had relatively high values of Ψ_{80K} , but plants from areas that receive larger amounts of precipitation had a large range of Ψ_{80K} values. This suggests that having drought tolerance leaves may be a requirement for success as a perennial grass in arid environments.

Introduction

Grasses are the dominant growth-form in ecosystems that span a wide range of water availability from desert grasslands that receive <300 mm of precipitation to tropical grassland/savanna's that can receive ~1500 mm (Staver *et al.* 2011), yet very little is known about how hydraulic architecture allows this functional group to be successful across such a wide range of conditions. In xeric environments, drought avoidance strategies require short life-cycles while water is available but drought tolerant grasses (typically perennial C₄ grasses), however, maintain growth and an active leaf canopy throughout drought periods. Conversely, as precipitation amount increases across space, drought tolerance is not as important, but competition for light and other resources becomes the driving force in shaping grassland communities. Successful growth strategies across a precipitation gradient impart different requirements and constraints on the plant hydraulic system. Understanding the relationship between hydraulic architecture different growth strategies is important in grasses, but very little data exists on the inter-species variability of these traits.

A central tenet in plant ecology is the trade-off between rapid growth and the ability to withstand stress (Chapin 1980). In the context of drought tolerance this theory would predict that species with rapid growth would be uncommon in water-limited ecosystems. Research at the whole-plant level suggests that a drought tolerance trade-off may not exist in grasses (Fernandez and Reynolds 2000); when xeric grasses were grown at different levels of soil moisture, no trade-off between growth rate and drought tolerance was found as all species had the same reduced growth under drought. Similarly, no trade-off in leaf-level drought tolerance traits and aboveground biomass was found during a drought experiment across four genotypes of grasses (Holloway-Phillips and Brodribb 2011a). Low rates of gas exchange may be a water conservation strategy in many grasses, reinforcing the growth-rate/stress tolerance framework (Baruch and Fernandez 1993, Baruch *et al.* 1985).

A corollary to the species-level growth/stress trade-off for drought tolerance also exists to describe the trade-offs within the vascular system, referred to as the safety vs. efficiency trade-off (Tyree and Zimmerman 2002). Vessel elements with high transport

capacity ('efficiency') are more prone to embolisms induced by cavitation ('safety') under water stress (Hacke *et al.* 2006). Vessels can overcome this trade-off by increasing the number of low conducting elements, although this may be uncommon due to the high cost of xylem construction (McCulloh *et al.* 2003). This trade-off in the vasculature of plants has been shown in the woody tissue of trees and shrubs (Pockman and Sperry 2000, Maherali *et al.* 2004, Jacobsen *et al.* 2007). When compared across different plant organs (stems vs. leaves) and using different measures of efficiency (e.g. rates of gas exchange rather than hydraulic conductance) the trade-off is less clear. Although scaling the safety vs. efficiency tradeoffs across plant organs and measurement types can obscure the trade-off within the xylem (Meinzer *et al.* 2010) these metrics are still useful in understanding overall plant function.

To date, studies comparing drought tolerance and growth among grass species have focused on species with limited geographic and precipitation ranges. The objective of this study was to investigate if there is a trade-off between safety vs. efficiency in grasses from a broad geographic and climatic range. I hypothesized that: 1) there would be a safety vs. efficiency trade-off on the leaf level between hydraulic conductance and drought tolerance; 2) this trade-off would be stronger when comparisons were made on a whole plant level, and 3) leaf level drought tolerance traits would be related to species distributions based on Mean Annual Precipitation.

Materials and Methods

I selected C₄ perennial grass species that dominate a diverse range of grassland ecosystems (Table 5.1). Seeds were obtained through the Germplasm Resources Information Network (GRIN, www.ars-grin.gov). Seeds were germinated in commercial potting soil and grown for ~ 4 weeks at which point 30-35 plants per species were transplanted into native soil collected from the Konza Prairie Biological Station (KPBS, Manhattan, Kansas, USA) in 1.25 L containers ("Short One" Treepots, Stuewe and Sons, Inc., Tangent, Oregon, USA). Plants were grown in a growth chamber (Convion PGV 36, Convion Environments Limited, Winnipeg, Manitoba, Canada) with a 16 hour photoperiod (PAR~1200 $\mu\text{mol m}^{-2} \text{s}^{-1}$) and daytime/nighttime temperatures held at 25/22°C,

respectively. Plants were watered daily and fertilized weekly with a Hoagland's solution until the initiation of the drought treatment.

Pressure-volume curves were measured on 5 individuals per species to determine leaf cellular and structural characteristics (Tyree and Hammel 1972). Briefly, plants were watered to pot-holding capacity and then placed in a dark chamber overnight to allow the leaves to fully hydrate. The following morning the most recently matured leaf was wrapped in parafilm and cut near the ligule so that ~75% of the leaf was used for the pressure-volume curves. The leaf and parafilm were weighed immediately on a micro-balance (± 0.1 mg, Ohaus Pioneer, Ohaus Corporation, Parsippany, New Jersey, USA.) and then placed in a Scholander-style pressure chamber (PMS Instruments, Albany, Oregon, USA) and pressurized until water was extruded from the cut surface of the leaf. The leaf was removed from the pressure chamber, dried, and re-weighed. This procedure was repeated by increasing the pressure in ~ 0.2 MPa increments until a pressure of ~ 3.0 MPa was reached. When the pressure-volume curve was completed the leaf was rehydrated and then scanned (at 600 dpi, Epson Perfection V500, Epson America Inc., Long Beach, California, USA) to measure leaf area using imageJ (Rasband, 1997-2011, U. S. National Institutes of Health, Bethesda, Maryland, USA, <http://rsb.info.nih.gov/ij/>), dried for 24 hours at 60°C and weighed.

To initiate drought treatments, water was withheld from the remaining plants and measurements were made every 1-2 days to monitor plant responses to drought. During each measurement period, 4-5 plants were measured for each species. Stomatal conductance (g_s), photosynthesis (A), leaf hydraulic conductance (K_{leaf}), leaf and soil water potential (Ψ_{leaf} and Ψ_{soil} , respectively), and leaf relative water content were measured during each sampling period. After this suite of measurements was made on an individual plant, it was re-watered for 4 days and the percentage of leaf mortality recorded.

Rates of gas exchange were measured using a Li-6400 gas exchange system (Li-Cor, Inc., Lincoln, Nebraska, USA) and the conditions inside the chamber were set to match conditions in the growth chamber (50% relative humidity, PAR = $1500 \mu\text{mol m}^{-2} \text{s}^{-1}$, CO_2 concentration = $400 \mu\text{mol mol}^{-1}$). Measurements were made at the center of each leaf to minimize the effect of acropetal changes in gas exchange rates (Ocheltree *et al.* 2012).

Rates of gas exchange were monitored until they stabilized (~2-8 minutes) and 1 point was logged.

Following gas exchange measurements, leaf hydraulic conductance was measured on the same leaf using the rehydration kinetics method (Holloway-Phillips and Brodribb 2011b). Briefly, the distal 1/3 of the leaf was cut with a razor blade, sealed in a plastic bag, and placed in the dark for ~1 hr to allow leaf water potential to equilibrate within the leaf. The water potential of this leaf segment was determined and used as a measure of mid-day leaf water potential (Ψ_{mid}) and as the initial leaf water potential (Ψ_0) in the calculation of K_{leaf} (Eqn. 5.1). The basal portion of the remaining leaf was submerged in filtered and de-ionized water and re-cut near the base of the leaf. The apical portion of the leaf segment was kept out of the water so that rehydration of the leaf could only occur through the exposed xylem at the cut surface. Leaves were allowed to rehydrate for 60-300 sec depending on the species and hydration status of the plant and then the leaf was cut again ~30 mm from the basal section submerged in the water bath. This leaf section was then sealed in a plastic bag in the dark and allowed to equilibrate for ~1 hr and then leaf water potential was measured and used as the rehydrated leaf water potential (Ψ_f) in Eqn. 5.1. K_{leaf} was calculated using the leaf water potentials and leaf capacitance (calculated from the pressure-volume curve):

$$K_{leaf} = \frac{C_{leaf} \ln \left[\frac{\Psi_0}{\Psi_f} \right]}{t} \quad \text{Eqn. 5.1}$$

where C_{leaf} is bulk leaf capacitance normalized by leaf area, t is the duration of rehydration, and Ψ_0 and Ψ_f are the leaf water potentials before and after rehydration, respectively. Leaf Dry Matter Content (LDMC) was also calculated as leaf dry weight divided by fully hydrated leaf weight.

After gas exchange and K_{leaf} measurements, the plant was placed inside a black plastic bag to allow leaf water potential to equilibrate with the soil water for 4-6 hours. Water potential was measured on a leaf, which I assumed to be in equilibrium with the soil and so this measurement was used as an estimate of soil water potential (Ψ_{soil}).

Climate envelopes for temperature and precipitation were determined for the geographic range of each species in the study. The global occurrence of each species was

harvested from the Global Biodiversity Information Facility (GBIF, www.gbif.org). The Mean Annual Precipitation (MAP) for each geographic location was determined, and then the median, 10th, and 90th percentile was calculated for each species.

All statistical analyses were performed using R. Data was checked for normality and any outliers removed. Vulnerability curves were calculated by fitting a general logistic equation to the data in the form:

$$y = X_{sat} \left[1 - \frac{1}{1 + e^{\alpha(x-\beta)}} \right] \quad \text{Eqn. 5.2}$$

where y was either K_{leaf} , g_s , or A and x was $-\Psi_{leaf}$. X_{sat} is the maximum K_{leaf} , g_s , or A calculated as the average value for all measurements made on leaves when the soil was fully hydrated, and α and β were constants fit using the ‘nls’ function in R (R Development Core Team 2008, open-source statistical software package). The point at which y decreased by 80% from maximum was calculated from these curves and presented as $\Psi80_K$, $\Psi80_g$ and $\Psi80_A$. Quantile regressions were calculated using the ‘quantreg’ library in R. Unless stated otherwise, significance was determined at the $p < 0.05$ level.

Results

Vulnerability curves for two species with contrasting responses to drought are shown in Figure 5.1. The reduction of K_{leaf} was slower in response to declining Ψ_{leaf} for *Sorghastrum nutans* L. Nash (red symbols and line) compared to *Spartina pectinata* Bosc. Ex Link (black symbols). The point at which K_{leaf} was reduced by 80% ($\Psi80_K$) from well-watered conditions was -2.73 and -6.45 MPa for *Spartina pectinata* and *Sorghastrum nutans*, respectively, which were the two extreme values for the set of species I measured. The $\Psi80_K$ values for all species are shown in Table 5.1.

The range of values for when g_s and A were reduced by 80% from well-watered conditions were much narrower than for K_{leaf} (Figure 5.2). $\Psi80$ for g_s and A were nearly identical due to the tight correlation between these variables ($r^2 = 0.96$, data not shown). As a result of the convergence in g_s among the species in response to drought, species with greater ability to withstand cavitation tended to operate with a larger safety margin between $\Psi80_K$ and $\Psi80_g$ (or $\Psi80_A$) shown in Figure 5.2.

I did not find a trade-off between leaf specific hydraulic conductance and any drought tolerance trait (Figure 5.3). At the leaf-level, no correlation existed between K_{sat} and Ψ_{80K} (Figure 5.3A), but the lack of a relationship was driven primarily by one species. If *S. nutans* was removed from the analysis the correlation between K_{leaf} and Ψ_{80K} increased to $r^2=0.97$. There does appear to be a lower boundary in this relationship, as there are no species with both high K_{leaf} and high Ψ_{80K} . Plants with higher Ψ_{80K} values did not necessarily have higher Ψ_{80mort} values (Figure 5.3B), indicating that some species could have complete loss of K_{leaf} but still rehydrate when soil moisture became available. There was a weak negative correlation between K_{leaf} and g_s (Figure 5.3C), but this relationship also appears to have a threshold, as species with low K_{leaf} exhibited a range of g_s values, but high K_{leaf} species always had low g_s . The dotted line in Figure 5.3C represents a regression through the 90% quantile highlighting the boundary between K_{leaf} and g_s .

When hydraulic conductance was calculated on a mass basis (K_{mass}), rather than a leaf area basis, a significant correlation between Ψ_{80K} and K_{leaf} was present (Figure 5.4, $p = 0.029$). This suggests that a safety vs. efficiency trade-off exists when I consider the mass of plant tissue that must be supplied with water rather than just the area of the leaf surface. There was also a strong relationship between drought tolerance and stomatal conductance calculated on a mass basis (g_{mass} , Figure 5.5A), but these variables are positively correlated suggesting no trade-off between drought tolerance and leaf level gas exchange. There was a weak non-linear relationship between leaf-level drought tolerance and whole plant growth rate (Figure 5.5B). This relationship was driven, however, by one drought intolerant species with an extremely high growth rate, most of the species had lower growth rates despite a range of Ψ_{80K} values.

Ψ_{80K} of leaves from the species I studied were generally related to the historical amount of precipitation received from the species' home range. Grasses with low Ψ_{80K} were not commonly found in systems with low precipitation, but species with high Ψ_{80K} were found across a wide range precipitation amounts.

Discussion

As the safety vs. efficiency theory would predict, our data shows a trade-off between leaf-level hydraulic efficiency and drought tolerance from common grass species occurring across a rainfall gradient. Grass species with high leaf-specific hydraulic conductance normalized by leaf mass (rather than leaf area as is typical) lost 80% of their ability to conduct water at higher leaf water potentials than species with lower leaf-specific hydraulic conductance. There was not, however, a trade-off between Ψ_{80K} and leaf-level gas exchange; the most drought tolerant species in our study also had the highest rates of gas exchange on a mass basis. Furthermore, the species with the lowest K_{leaf} also had some of the highest rates of gas exchange in this study. Typically, the hydraulic conductance of the leaf and stem are positively correlated with gas-exchange rates, but our results, over a broad range of grass species, suggest that this relationship may be decoupled in grasses.

Based on the established understanding of cavitation and hydraulic conductance from woody species (Maherali *et al.* 2004, Wheeler *et al.* 2005, Hacke *et al.* 2006), one would expect a trade-off between conductance and cavitation resistance. Air-seeding occurs through the membrane of the bordered pits of xylem (Hacke *et al.* 2006) and is related to the size of the openings as large pores are more prone to cavitation. Small pores, however, reduce hydraulic conductance through these pits as water moves through the vascular system. This trade-off has been identified in stems of woody plants both within individual species (Jacobsen *et al.* 2007), and a weak correlation was found across a wide range of woody plants (Maherali *et al.* 2004). In contrast, this trade-off was not identified in the leaves of woody species (Blackman *et al.* 2010) and the authors suggested that this trade-off shouldn't be expected in leaves because K_{leaf} and Ψ_{80K} are the result of different process. Ψ_{80K} in leaves is related to the structure of individual vessel elements (Wheeler *et al.* 2005, Hacke *et al.* 2006, Blackman *et al.* 2010) where K_{leaf} is more closely related to vein density (Sack and Frole 2006, Scoffoni *et al.* 2011), mesophyll hydraulic architecture (Brodribb *et al.* 2007, Ocheltree *et al.* 2012) and aquaporin regulation (Cochard *et al.* 2007). When I normalized hydraulic conductance by leaf-area our results agree with Blackman *et al.* (2010, Figure 5.3A), but when I normalized conductance by leaf mass rather than leaf-area, a strong trade-off between safety and efficiency was present (Figure

5.4). Using leaf mass may re-couple K_{leaf} and Ψ_{80K} because conductance on a mass basis should account for vein density and structural characteristics of the mesophyll, processes that would ultimately impact K_{mass} in the leaf.

As hypothesized, a trade-off was present between the species that maintain low Ψ_{80K} and hydraulic conductance on a mass basis (Figure 5.5). Drought tolerance in leaves is related to vascular density (Scoffoni *et al.* 2011) and thick-walled vessels (Blackman *et al.* 2010); both anatomical traits that are costly to build (McCulloh *et al.* 2003). Leaf dry matter content was related to both growth rates and Ψ_{80K} , which suggests that there was more investment in cell walls in the slow-growing/drought tolerant grass species. This investment into drought tolerant leaves would slow overall plant growth rates, so even though leaf-level gas exchange was high in drought tolerant grasses (Figure 5.4), this was decoupled from whole plant growth.

It has been suggested that a trade-off between drought tolerance and growth rate in grasses does not exist (Fernandez and Reynolds 2000). The authors grew plants at different levels of soil moisture, rather than exposing them to a single drought event, and found the growth of all species was reduced by similar magnitudes when soil moisture was limited and no relationship between drought tolerance and growth could be identified. Growing plants at different levels of soil moisture may produce different results than exposing plants to a severe drought. In our experiment I investigated the lower Ψ_{leaf} boundary at which grasses could maintain function, which is different than looking for changes in growth potential. Previous studies investigating the drought tolerance of grasses have suggested that small plants are more drought tolerant because the lower demand for resources allows individuals to conserve resources, resulting in a longer growth period (Baruch *et al.* 1985, Baruch and Fernandez 1993, Fernandez and Reynolds 2000). Although I did not present a measure of plant size, I did not find a clear trade-off between drought tolerance and growth rates or leaf-level gas exchange. These results do not support the idea that these species are conserving resources more than drought intolerant species.

I also found a threshold relationship between hydraulic conductance and rates of gas-exchange, as grasses with low hydraulic conductance, typical of drier sites (Figure 5.4),

had the highest rates of gas exchange. This contradicts other studies that have shown positive correlations between K_{leaf} and A (Brodribb *et al.* 2007, Maherali *et al.* 2008). These contrasting results may be related to the geographic distribution of the plants selected. I selected species with a broad geographic and drought tolerance range and so our negative correlation between K_{leaf} and gas exchange may reflect differences in growth strategies that were not captured in previous studies. Maherali *et al.* (2008) investigated the genetic linkage between conductance and gas-exchange in a single annual grass species using recombinant inbred-lines. Brodribb *et al.* (2007) found a positive correlation both within and between functional groups (ferns, conifers, deciduous angiosperms), but grasses and other species adapted to arid environments were not included. In general, a positive relationship between K_{leaf} and A is expected because an efficient supply of water is needed to supply the large cell volume required and high g_s required for high rates A . This relationship may become decoupled in arid ecosystems where the need for cavitation resistance xylem (often associated with low K_{leaf} , Figure 5.3A) is contrasted by the need for high rates of gas exchange (Reich *et al.* 1999, Maherali and DeLucia 2000, Pinol and Sala 2000). An interesting example to consider is *S. nutans*, which has the ability to maintain K_{leaf} even at low values of Ψ_{leaf} , but is not typically found in arid ecosystems (Figure 5.6). This response may reflect the comparatively low rates of gas exchange in this species. I speculate that grasses from arid environments have, in general, lower hydraulic conductance as consequences of building drought tolerant vasculature but also have high rates of gas exchange in order to meet high evaporative demand and to have high growth rates to respond to short growing season in these pulse-dominated systems.

Leaf-level drought tolerance does appear to be a requirement to grow in drier climates (Figure 5.6) as the grasses from arid systems all had low Ψ_{80K} in low precipitation ecosystems. This does not mean plants with low leaf-level drought tolerance aren't present in arid systems, but to be a dominant grass in these systems may require this trait. Leaf-level drought tolerance has also been shown to be important in plant distributions in the tropics (Engelbrecht *et al.* 2007, Baltzer *et al.* 2008). Interestingly, species with high Ψ_{80K} values could still be successful in more mesic systems if they had high leaf hydraulic conductance, which may be related to the shift to competition for light as precipitation

increased (Burke *et al.* 1998). *S. nutans* had high leaf-level drought tolerance but is not found in as dry as habitats, which may be related to its lower leaf-level gas exchange rates. Other biotic or abiotic factors may also limit the ability of plants to grow in arid environments such as; defense to herbivory, heat tolerance, or nutrient uptake dynamics. It would be useful to incorporate these other factors into the hydraulic framework established here to better understand the control of grass distributions.

Conclusions

I have shown that dominant grasses in arid ecosystems must have the ability to maintain leaf hydraulic conductance at low leaf-water potentials. Contrary to expectations, drought tolerant leaves do not sacrifice leaf-level rates of gas exchange. There may be a trade-off at the plant growth level, although this is not strongly supported by our data. Plants with leaf-level drought tolerance traits, however, are also found commonly in grasslands that receive greater amounts of precipitation. This suggests that leaf-level drought tolerance is necessary to be successful in arid ecosystems, but there are other constraints to growth and success in these systems that drought tolerance alone may not explain. The typical positive relationship between hydraulic conductance and gas exchange found in some grasses may be decoupled in arid ecosystems, which may be one mechanism that leads to the success of some grasses in these systems.

Literature Cited

- Baltzer J.L., Davis S.J., Bunyavejchewin S., and Noor N.S.M. 2008. The role of desiccation tolerance in determining tree species distributions along the Malay–Thai Peninsula. *Functional Ecology* 22, 221-231.
- Baruch Z. and Fernandez D. 1993. Water relations of native and introduced C-4 grasses in a neotropical savanna. *Oecologia* 96, 179-185.
- Baruch Z., Ludlow M.M., and Davis R. 1985. Photosynthetic responses of native and introduced C4 grasses from Venezuelan savannas. *Oecologia* 67, 388-393.

- Blackman C.J., Brodribb T.J., and Jordan, G.J. 2010. Leaf hydraulic vulnerability is related to conduit dimensions and drought resistance across a diverse range of woody angiosperms. *New Phytologist* 188, 1113-1123.
- Brodribb T.J., Feild T.S., and Jordan G.J. 2007. Leaf maximum photosynthetic rate and venation are linked by hydraulics. *Plant Physiology* 144, 1890-1898.
- Burke I., Lauenroth W.K., Vinton M.A., Hook P.B., Kelly R.H., Epstein H.E., Agular M.R., Robles M.D., Aguilera M.O., Muprhy K.L., and Gill R.A., 1998. Plant-soil interactions in temperate grasslands RID A-1420-2009. *Biogeochemistry* 42, 121-143.
- Chapin F.S. 1980. The mineral-nutrition of wild plants. *Annual Review of Ecology and Systematics* 11, 233-260.
- Cochard H., Venisse J.S, Barigah T.S., Brunel N., Herette S., Guilliot A., Tyree M.T., and Sakr S. 2007. Putative role of aquaporins in variable hydraulic conductance of leaves in response to light. *Plant Physiology* 143, 122-133.
- Engelbrecht B.M.J., Comita L.S., Condit R., Kursar T.A., Tyree M.T., Turner B.L., and Hubbell S.P. 2007. Drought sensitivity shapes species distribution patterns in tropical forests. *Nature* 447, 80-82.
- Fernandez R. and Reynolds J. 2000. Potential growth and drought tolerance of eight desert grasses: lack of a trade-off? *Oecologia* 123, 90-98.
- Hacke U.G., Sperry J.S., Wheeler J.K., and Castro L. 2006. Scaling of angiosperm xylem structure with safety and efficiency. *Tree Physiology* 26, 689-701.
- Holloway-Phillips M.M., and Brodribb T.J. 2011. Minimum hydraulic safety leads to maximum water-use efficiency in a forage grass. *Plant, Cell and Environment* 34, 302-313.
- Holloway-Phillips M.M., and Brodribb T.J. 2011. Contrasting hydraulic regulation in closely related forage grasses: implications for plant water use. *Functional Plant Biology* 38, 594-605.
- Jacobsen A.L., Pratt R.B., Davis S.D., and Ewers F.W. 2007. Cavitation resistance and seasonal hydraulics differ among three arid Californian plant communities. *Plant, Cell and Environment* 30, 1599-1609.
- Maherali H., and DeLucia E.H. 2000. Xylem conductivity and vulnerability to cavitation of ponderosa pine growing in contrasting climates. *Tree Physiology* 20, 859-867.
- Maherali H., Pockman W.T., and Jackson R.B. 2004. Adaptive variation in the vulnerability of woody plants to xylem cavitation. *Ecology* 85, 2184-2199.

- Maherali H., Sherrard M.E., Clifford M.H., Latta R.G. 2008. Leaf hydraulic conductivity and photosynthesis are genetically correlated in an annual grass. *New Phytologist* 180, 240-247.
- McCulloh K., Sperry J.S., and Adler F. 2003. Water transport in plants obeys Murray's law. *Nature* 421, 939-942.
- Meinzer F.C., McCulloh K.A., Lachenbruch B., Woodruff D.R., and Johnson D.M. 2010. The blind men and the elephant: the impact of context and scale in evaluating conflicts between plant hydraulic safety and efficiency. *Oecologia* 164, 287-296.
- Ocheltree T.W., Nippert J.B., and Prasad P.V.V. 2012. Changes in stomatal conductance along grass blades reflects changes in leaf structure. *Plant, Cell and Environment* 35, 1040-1049.
- Pockman W. and Sperry J.S. 2000. Vulnerability to xylem cavitation and the distribution of Sonoran desert vegetation. *American Journal of Botany* 87, 1287-1299.
- Pinol J., and Sala A. 2000. Ecological implications of xylem embolism for several Pinaceae in the Pacific Northern USA. *Functional Ecology* 14, 538-545.
- R Development Core Team. 2008. R: A language and environment for statistical computing. R Foundation for Statistical Computing, Vienna, Austria. ISBN 3-900051-07-0, URL <http://www.R-project.org>.
- Rasband W.S., ImageJ, U. S. National Institutes of Health, Bethesda, Maryland, USA, URL <http://imagej.nih.gov/ij/>, 1997-2011.
- Reich P.B., Ellsworth D.S., Walters M.B., Vose J.M., Gersham C., Volin J.C., and Bowman W.D. 1999. Generality of leaf trait relationships: a test across biomes. *Ecology* 80, 1955-1969.
- Sack L. and Frole K. 2006. Leaf structural diversity is related to hydraulic capacity in tropical rain forest trees. *Ecology* 87, 483-491.
- Scoffoni C., Rawls M., McKown A., Cochard H., and Sack L. 2011. Decline of leaf hydraulic conductance with dehydration: relationship to leaf size and venation architecture. *Plant Physiology* 156, 832-843.
- Staver A.C., Archibald S., and Levin S.A. 2011. The global extent and determinants of savanna and forest as alternative biome states. *Science* 334, 230-232.
- Tyree M.T. and Hammel H. 1972. The measurement of the turgor pressure and the water relations of plants by the pressure-bomb technique. *Journal of Experimental Botany* 23, 267-282.

Tyree M.T., and Zimmerman M.H. 2002. *Xylem Structure and the Ascent of Sap* Second., Berlin: Springer-Verlag.

Wheeler J.K., Sperry J.S., Hacke U.G., and Hoang N. 2005. Inter-vessel pitting and cavitation in woody Rosaceae and other vesselless plants: a basis for a safety versus efficiency trade-off in xylem transport. *Plant, Cell and Environment* 28, 800-812.

Tables and Figures

Table 5.1 Grass species used to test drought tolerance. All plants except *Andropogon gerardii* were grown from seeds obtained through the Germplasm Resources Information Network (GRIN). An insufficient number of *A. gerardii* seeds germinated and so plants were grown from rhizomes collected at Konza Prairie Biological Station, Kansas, USA. The median of the Mean Annual Precipitation (MAP) is also shown for all occurrences of each species in the GBIF database. Leaf-level drought tolerance quantified as the point at which there was an 80% loss in K_{leaf} , g_s , and A (Ψ_{80_K} , Ψ_{80_g} , and Ψ_{80_A} , respectively) are listed as well as K_{leaf} when the soils were at pot-holding capacity (K_{sat}).

Species	accession number	seed source	MAP	Ψ_{80_K}	Ψ_{80_g}	Ψ_{80_A}	K_{sat} (SE)
<i>Andropogon gerardii</i>	rhizome	Kansas, U.S.A.	968	5.80	3.11	2.95	6.75 (0.37)
<i>Bouteloua gracilis</i> Lag. ex Griffiths	PI 648364	New Mexico, U.S.A.	467	6.34	4.26	4.22	18.01 (3.64)
<i>Cenchrus flaccidus</i> (Griseb.) Morrone	PI 434640	Punjab, Pakistan		6.25	3.28	3.50	11.49 (0.92)
<i>Eragrostis lehmanniana</i> Nees	PI 410109	Thabazimbi, South Africa	365	3.47	2.30	2.30	106.4 12.86)
<i>eragrostis nigra</i>	W6 23585	Xizang, China		5.62	3.40	3.07	7.93 (0.51)
<i>Panicum virgatum</i> L.	PI 657661	Oklahoma, U.S.A.	1007	4.28	1.89	2.20	17.25 (0.87)
<i>Schizachyrium scoparium</i>	PI 421553	Kansas, U.S.A.	1021	nd	4.23	3.95	6.54 (0.19)
<i>Sorghastrum nutans</i> (L.) Nash	PI 648380	Kansas, U.S.A.	1007	6.45	2.69	3.10	80.19 (0.73)
<i>Spartina pectinata</i> Bosc. ex Link	W6 30925	Wisconsin, U.S.A.	927	2.73	2.09	2.10	67.41 (0.55)

Figure 5.1 An example of vulnerability curves constructed for leaf level hydraulic conductance. K_{leaf} declined as leaf water potential decreased in all species, but the rate of decline varied greatly. A general logistic curve was fit to the data (Eqn. 5.1) and the point at which K_{leaf} decreased by 80% from K_{sat} was calculated and reported as Ψ_{80K} . Two contrasting species are shown; *Sorghastrum nutans* (red symbols) maintained higher rates of K_{leaf} compared to *Spartina pectinata* (black symbols). Ψ_{80K} for all species are shown in Table 5.1.

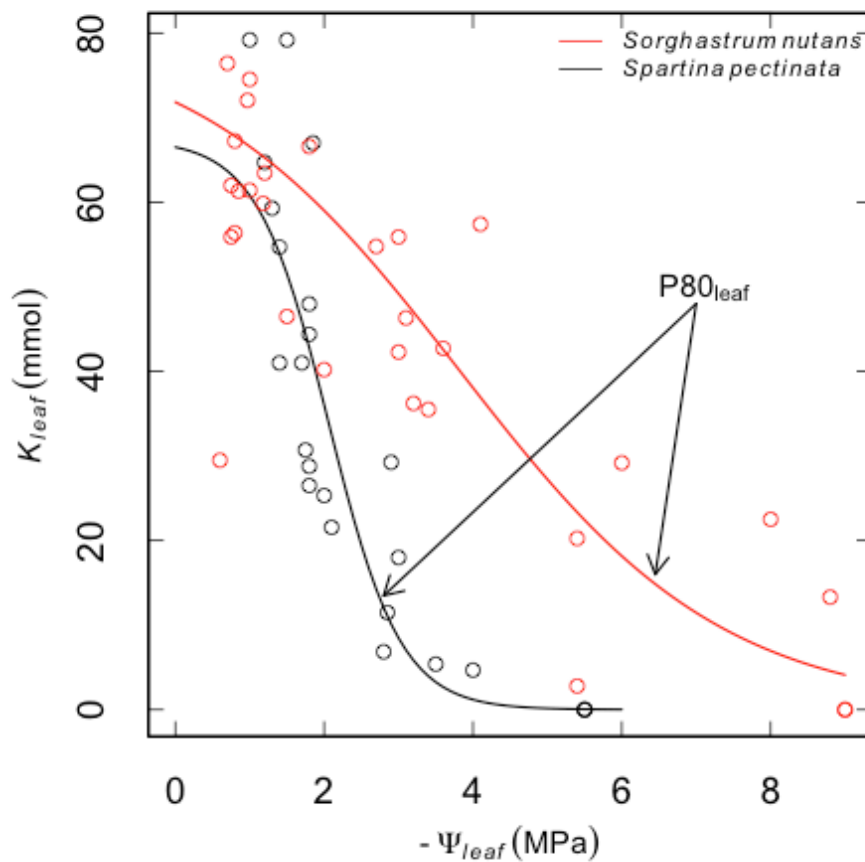


Figure 5.2 The relationship between Ψ_{80} for K_{leaf} and g_s . The dotted line is a 1:1 reference line and the solid line is the linear regression between the two variables with the intercept set to zero. Ψ_{80_g} was always lower than Ψ_{80_K} indicating that the plants studied close their stomata to prevent catastrophic cavitation. The slope of the line was less than one, indicating that plants with greater resistance to cavitation also operated with a larger safety margin.

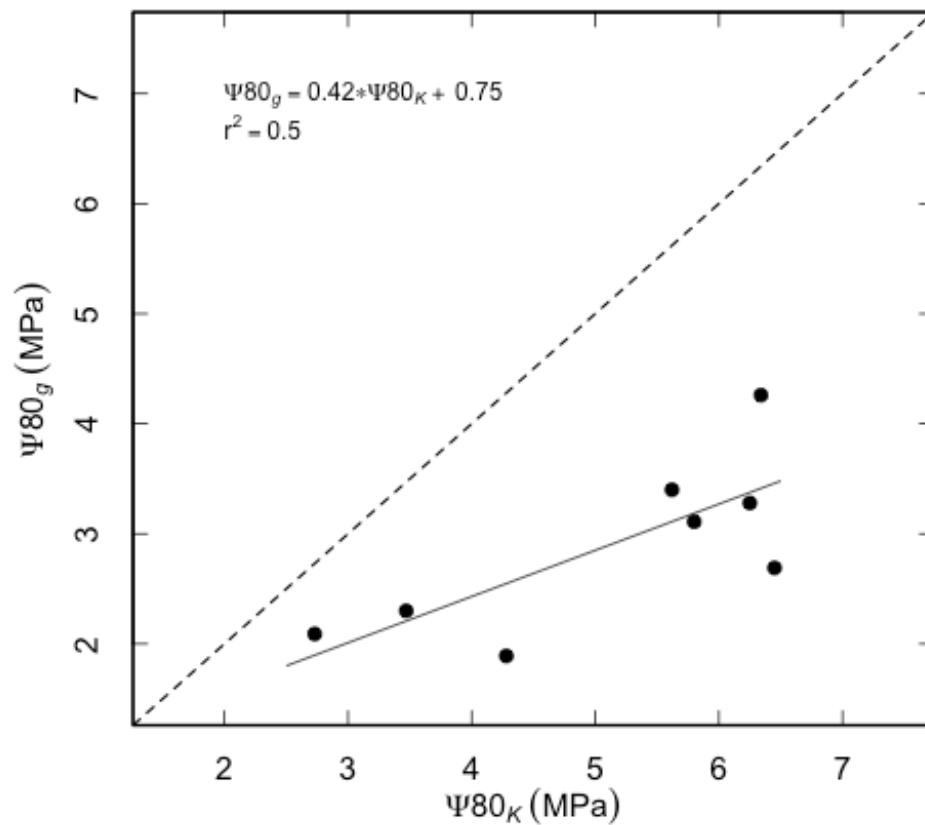


Figure 5.3 The trade-off between hydraulic conductance and drought tolerance. The relationship between K_{leaf} and Ψ_{80K} was not significant unless (panel A) or the point at which 80% leaf mortality after re-watering (Ψ_{80mort} , panel B). Finally, there was a negative correlation between K_{leaf} and g_s (panel C). 'ns' indicates relationships that were non-significant at the $p < 0.05$ level. The dotted line in panel C is a linear regression of the 90% quantile suggesting the relationship between K_{leaf} and g_s has a threshold such that drought intolerant species do not have high stomatal conductance.

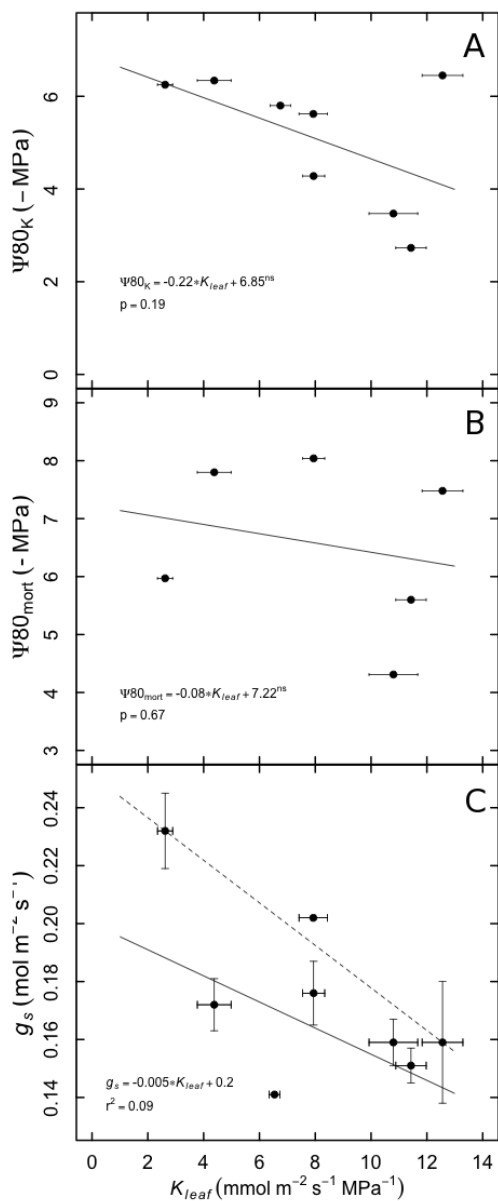


Figure 5.4 The relationship between leaf hydraulic conductance normalized by leaf mass) and leaf-level drought tolerance. Grasses that had an ability to transport water efficiently (high K_{mass}) were not able to maintain K_{leaf} at low leaf water potentials. Normalizing leaf hydraulic conductance by leaf mass accounts for total leaf material that must be supplied with water rather than just the surface area of the leaf.

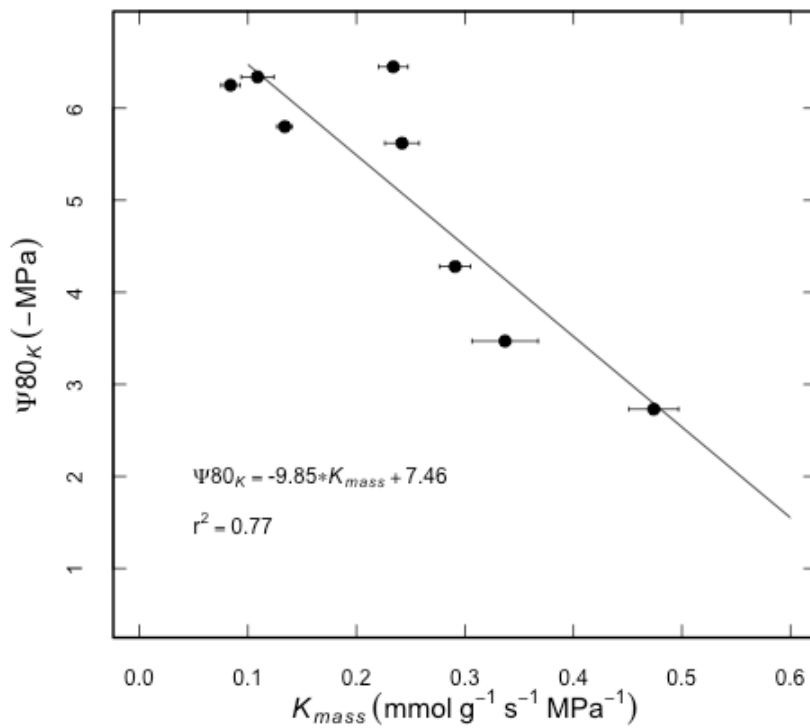


Figure 5.5 Relationship between leaf level drought tolerance (Ψ_{80K}) and plant growth rate calculated on the whole plant level (including both above and below ground growth). There was a strong correlation between Ψ_{80K} and stomatal conductance calculated on mass basis (panel A), but only a weak non-linear relationship between drought tolerance and whole plant growth (panel B).

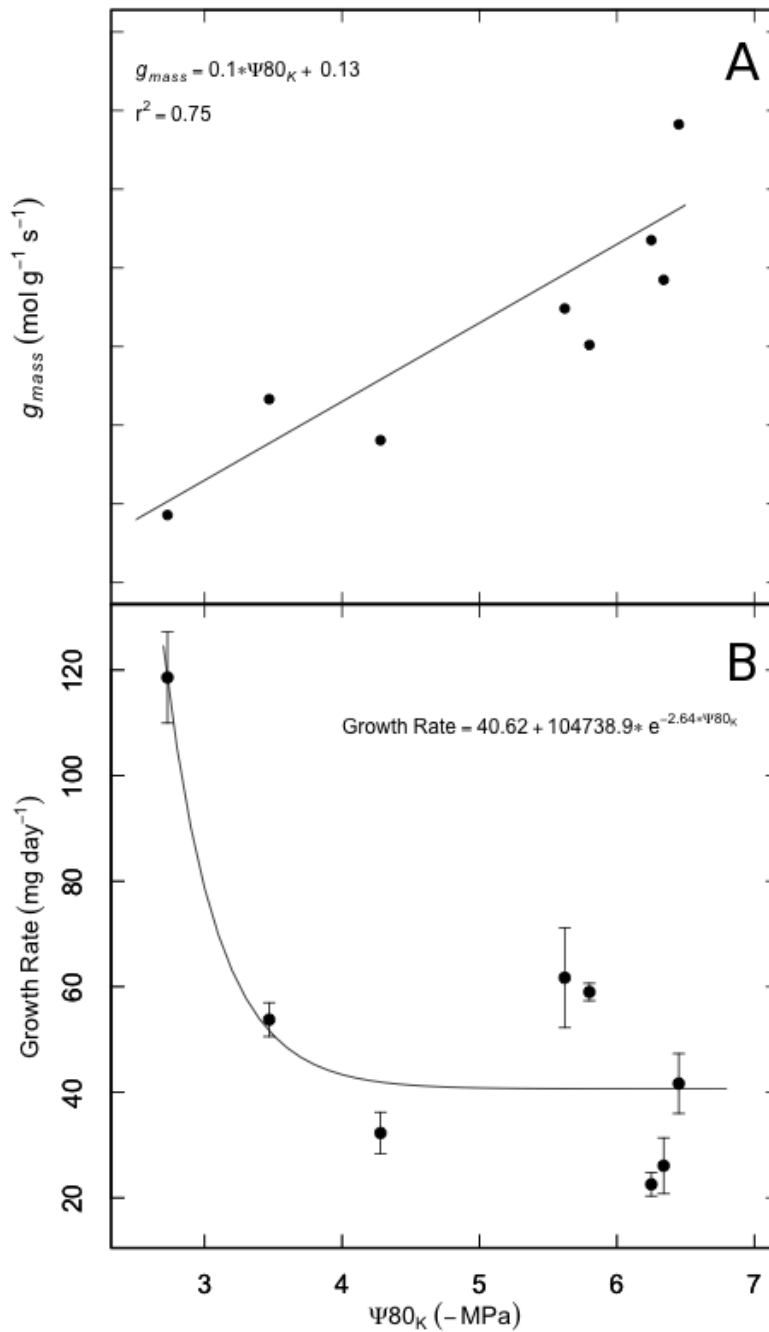
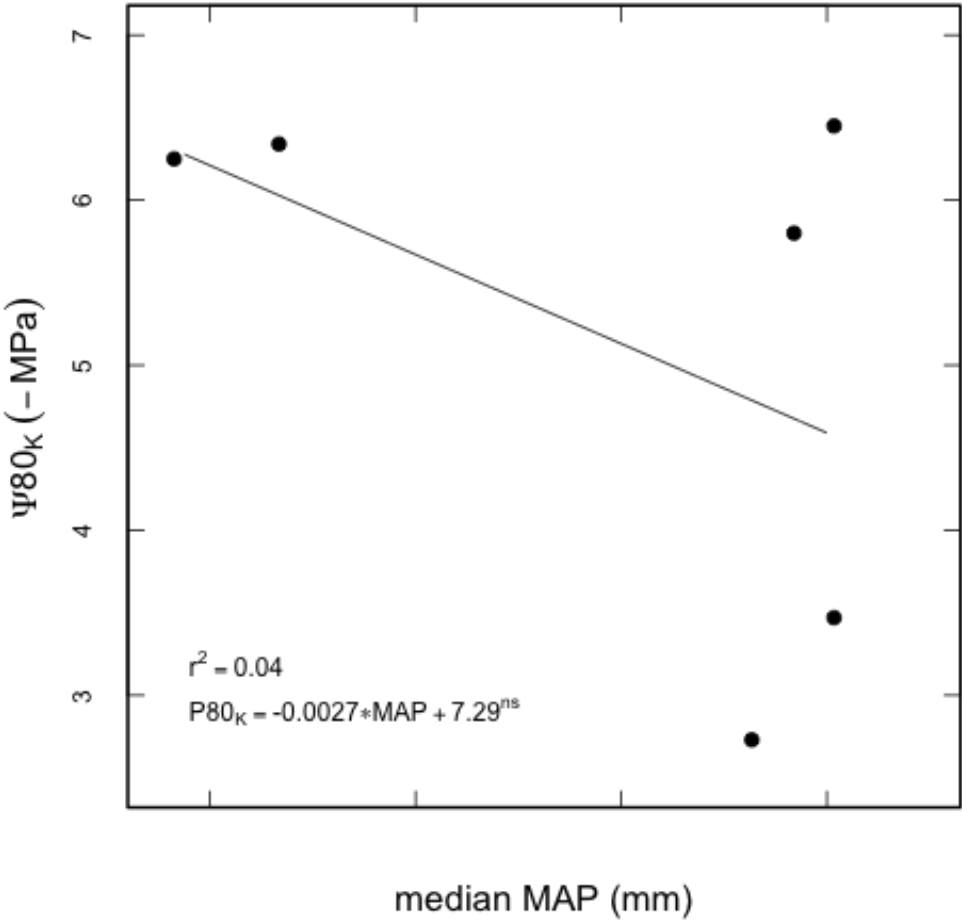


Figure 5.6 The Mean Annual Precipitation for all occurrences of each species correlates with leaf-level drought tolerance. Although the regression analysis was not significant, none of the grasses that were drought intolerant were commonly found in dry ecosystems, (lower left section of the figure).



Chapter 6 - Conclusions

General Discussion

Whole plant resistance is not just the sum of its parts, and so we can no longer think of plant hydraulics as a single quantity. If two plants have the same whole plant hydraulic resistance but different partitioning between roots, xylem, and extra-xylery tissue they can exhibit very different responses to water limitation. The body of work presented here highlights the importance of understanding the partitioning of hydraulic resistances and begins to reveal some of the relationships between hydraulic architecture and plant strategies in grasses.

Much of what we know about plant hydraulic architecture comes from studies that consider the characteristics of a single organ. Drought tolerance in woody plants has focused on the cavitation resistance of stems with very little research focusing on leaf-level drought characteristics. Due to the difficulty of measuring root systems, information on the drought tolerance or hydraulic capacity of roots remains uncertain. The research presented here suggests that understanding the relationship between axial transport through the xylem and extra-xylery transport will shed new light onto plant hydraulics. A recent review calls for a better understanding of cavitation resistance between plant organs (Meinzer *et al.* 2010), but this should be coupled with a better understanding of maximum hydraulic conductance of different plant organs as this can also have a large impact on plant performance as spatial and temporal patterns of soil moisture decline.

Specific Conclusions

Recent work has investigated and debated where the hydraulic 'bottleneck' is within leaves; xylery or extra-xylery resistance. Recent conclusions acknowledge that the resistance within leaves is highly variable, but when averaged across a range of species they were roughly equivalent. The functional significance of these two leaf resistances, however, has not been investigated in relation to drought and water-use strategies. The work here also suggests that the partitioning of these resistances varies greatly across

genotypes (Chapter 3) and species (Chapter 4). More importantly, the functional significance of these resistances has been identified in relation to changes in stomatal conductance as soils dry and evaporative demand increases. The resistance outside the xylem correlates with stomatal conductance when soil moisture is readily available, which could result in a more conservative water-use strategy in cropping systems where competition for water may be less important in a monoculture stand. Having a proportionately large resistance outside the xylem in leaves is also related to stomatal conductance that is more sensitive to changes in vapor pressure deficit. Therefore, I conclude that having large resistance outside the xylem in leaves leads to more conservative water use, both in regards to water use from the soil and limiting water loss through transpiration. Conserving water in cropping systems is often a consideration in crop breeding programs, especially for dryland cropping systems. Crops that can conserve water through the dry season often have higher levels of productivity and yield (Sinclair *et al.* 2007). In natural grasslands, water conservation has also been suggested as a growth strategy (Fernandez and Reynolds 2000). In this work I studied the proportion of xylem and extra-xylery resistances within a species and across species found at Konza Prairie Biological Station, it would also be useful to look for this trait correlates with successful growth strategies across a larger precipitation gradient. If water conservation is indeed a viable growth strategy in arid systems, the relative abundance of species with high extra-xylery resistance should be greater than in more mesic environments.

Similarly, low root hydraulic conductance is correlated with a more conservative water-use strategy. Transpiration rates increase as the evaporative demand in the atmosphere increases, but most plants have a point at which stomatal conductance controls E at a constant rate despite continued increases in D . Plants with low root conductance tend to reach this breakpoint at lower levels of D , resulting in reduced water use. Combined with the lower water use of plants with greater resistance outside the xylem in leaves, the most water efficient plants should be those with a low root conductance and low conductance outside the xylem.

Comparing our results to data collected on woody species highlights an interesting contrast between grasses and trees. A recent study investigated the linkage between hydraulic conductance and photosynthesis across a range of growth forms, but excluding

grasses and sedges (Brodrribb *et al.* 2007) found that the hydraulic conductance of leaves correlated tightly with maximum photosynthetic rates. High photosynthetic rates require a large amount of cell volume to keep hydrated and necessitates high stomatal conductance to supply the carboxylating enzymes with CO₂. The opposite trend is found in grasses, however, low hydraulic conductance correlated with high rates of stomatal conductance and photosynthesis. The relationship found here (Chapter 5) appears more of a threshold response, where low conducting plants can have either high or low stomatal conductance, but plants with high leaf conductance always have lower rates. This brings up an interesting question, do tree leaves act just like grass leaves, or does the constraint (or benefit) of woody tissue result in different physiology of the leaves of woody plants. The data presented here would need further verification, but does suggest that grasses may operate in a 'riskier' manner compared to trees, using water at a much greater rate per leaf conductance than woody species. This is consistent with eddy-covariance data collected on neighboring grassland/forest pairs across Europe during the 2003 heat wave (Teuling *et al.* 2010). The forested ecosystems had a more conservative water use strategy, lower water use early in the season that were maintained longer into the heat wave. Grasses, on the other hand, had higher rates of water use and kept the high rates up until all water resources were exhausted and then productivity of the plants ceased. These different strategies are likely a result of different leaf-level physiology that has yet to be fully explored, but the contrast of the results presented here compared to published data on woody-species suggests that there may be fundamental differences in leaf-level physiology between these different growth forms.

Future Directions

Conserving water while maintaining growth is vital to successful plant growth in dryland cropping systems and may be important in the success of grasses in xeric environments. High hydraulic resistance outside the xylem can help minimize water loss when soils are saturated, effectively saving the water until later in the growing season. This same trait is also correlated with stomatal sensitivity to vapor pressure deficits, which also leads to plants with the ability to limit water use despite harsh conditions. The

mechanism that limits hydraulic resistance outside the xylem, however, could come at a trade-off with carbon uptake. The internal conductance to CO₂ is important in photosynthetic rates, and if high hydraulic resistance was directly correlated to high resistance to CO₂ diffusion than water conservation could come at a cost to carbon uptake. More work investigating the potential trade-off of high hydraulic resistance outside the xylem is needed to understand the full impact of this trait. One way to do this is to incorporate more detailed parameters of plant hydraulic architecture into simulation models of plant growth, which would be helpful in predicting when water conservation to prolong growth may be more important than high rates of carbon uptake.

Understanding the function of root systems is often described as the biggest 'missing component' to our understanding of plant function. This research highlights the importance of root hydraulic conductivity, as it can control maximum rates of transpiration (E) across a range of species. The strong correlation between root hydraulic conductance and the vapor pressure deficit breakpoint ($r^2=0.79$) suggests that this relationship is general across species, but root morphology and root tissue characteristics had no correlation with root conductance. Looking closer at the controls of root hydraulic conductance will be important to understanding the trade-offs that might exist for particular root hydraulic characteristics. For example, can you have low root hydraulic conductance (to conserve water) but still have high enough rates of nutrient uptake to maintain high growth rates? Combining root hydraulic measurements with root morphology and nutrient uptake studies would be useful in better understanding belowground controls over plant growth.

Leaf-level drought tolerance in grasses is important in controlling plant species distributions, but there are obviously other factors that influence where specific plants are successful. For example, *Sorghastrum nutans* and *Andropogon gerardii* appear drought tolerant based on leaf functional traits but they are not dominant species of desert grasslands, so there must be other factors that limit this species (and others) from realizing their potential niche. Interestingly, all the species with high hydraulic conductivity described in Chapter 5 were rhizomatous species, and so this growth form may have disadvantages in arid environments. Furthermore, nutrient availability and biogeochemical processes differ along precipitation gradients as well, and so other edaphic

factors may also limit the range of grasses. Future work investigating both drought tolerance, growth form, competition for light, and nutrient uptake capacity may help us better understand what controls the patterns of grass species distributions across the landscape.

Literature Cited

- Brodribb T.J., Feild T.S., and Jordan G.J. 2007. Leaf maximum photosynthetic rate and venation are linked by hydraulics. *Plant Physiology* 144, 1890-1898.
- Fernandez R., and Reynolds J. 2000. Potential growth and drought tolerance of eight desert grasses: lack of a trade-off? *Oecologia* 123, 90-98.
- Maherali H., Pockman W.T., and Jackson R.B. 2004. Adaptive variation in the vulnerability of woody plants to xylem cavitation. *Ecology* 85, 2184-2199.
- Meinzer F.C., McCulloh K.A., Lachenbruch B., Woodruff D.R., and Johnson D.M. 2010. The blind men and the elephant: the impact of context and scale in evaluating conflicts between plant hydraulic safety and efficiency. *Oecologia* 164, 287-296.
- Sinclair T.R., Fiscus E., Wherley B., Durham M., and Rufty T. 2007. Atmospheric vapor pressure deficit is critical in predicting growth response of "cool-season" grass *Festuca arundinacea* to temperature change. *Planta* 227, 273-276.
- Teuling A.J., Seneviratne S.I., Stöckli R., Reichstein M., Moors E., Ciais P., Luysaert S., *et al.* 2010. Contrasting response of European forest and grassland energy exchange to heat waves. *Nature Geoscience* 3, 722-727.